UNIVERSITEIT•STELLENBOSCH•UNIVERSITY
jou kennisvennoot • your knowledge partner

PERFORMANCE EVALUATION OF WET-COOLING TOWER FILLS WITH COMPUTATIONAL FLUID DYNAMICS

By

Yngvi Gudmundsson

Thesis presented in partial fulfilment of the requirements for the degree of Master of Science in Engineering (Mechanical) at Stellenbosch University

Supervisor: Prof. Hanno R. C. Reuter

March 2012

Departement Meganiese en Megatroniese Ingenieurswese

Department of Mechanical and Mechatronic Engineering

DECLARATION

By submitting this thesis electronically, I declare that the entirety of the work contained therein is my own, original work, and that I have not previously in its entirety or in part submitted it for obtaining any qualification.

Signature ……..

Date: ……

ABSTRACT

A wet-cooling tower fill performance evaluation model developed by Reuter is derived in Cartesian coordinates for a rectangular cooling tower and compared to cross- and counterflow Merkel, e-NTU and Poppe models. The models are compared by applying them to a range of experimental data measured in the cross- and counterflow wet-cooling tower test facility at Stellenbosch University. The Reuter model is found to effectively give the same results as the Poppe method for cross- and counterflow fill configuration as well as the Merkel and e-NTU method if the assumptions as made by Merkel are implemented. A second order upwind discretization method is applied to the Reuter model for increased accuracy and compared to solution methods generally used to solve cross- and counterflow Merkel and Poppe models. First order methods used to solve the Reuter model and crossflow Merkel and Poppe models are found to need cell sizes four times smaller than the second order method to obtain the same results. The Reuter model is successfully implemented in two- and three-dimensional ANSYS-*Fluent*® CFD models for under- and supersaturated air. Heat and mass transfer in the fill area is simulated with a user defined function that employs a second order upwind method. The two dimensional ANSYS-*Fluent*® model is verified by means of a programmed numerical model for crossflow, counterflow and cross-counterflow.

SAMEVATTING

‘n Natkoeltoring model vir die evaluering van pakkings werkverrigting, wat deur Reuter ontwikkel is, word in Kartesiese koördinate afgelei vir ‘n reghoekige koeltoring en word vergelyk met kruis- en teenvloei Merkel, e-NTU en Poppe modelle. Die verskillende modelle word vergelyk deur hulle op ‘n reeks eksperimentele data toe te pas wat in die kruis- en teenvloei natkoeltoring toetsfasiliteit by die Universiteit van Stellenbosch gemeet is. Dit is bevind dat die Reuter model effektief dieselfde resultate gee as die Poppe model vir kruis- en teenvloei pakkingskonfigurasies sowel as die Merkel en e-NTU metode, indien dieselfde aannames wat deur Merkel gemaak is geïmplementeer word. ‘n Tweede orde “upwind” metode word op die Reuter model toegepas vir hoër akkuraatheid en word vergelyk met oplossingsmetodes wat gewoonlik gebruik word om kruis- en teenvloei Merkel en Poppe modelle op te los. Eerste orde metodes wat gebruik is om die Reuter model en kruisvloei Merkel en Poppe modelle op te los benodig rooster selle wat vier keer kleiner is as vir tweede orde metodes om dieselfde resultaat te verkry. Die Reuter model is suksesvol in twee- en driedimensionele ANSYS-*Fluent*® BVD (“CFD”) modelle geïmplementeer vir on- en oorversadigde lug. Warmte- en massaoordrag in die pakkingsgebied word gesimuleer mbv ‘n gebruiker gedefinieerde funksie (“user defined function”) wat van ‘n tweede orde numeriese metode gebruik maak. Die tweedimensionele ANSYS-*Fluent*® model word m.b.v. ‘n geprogrameerde numeriese model bevestig vir kruis-, teen- en kruis-teenvloei.

ACKNOWLEDGEMENTS

I would like to thank Prof. Hanno Reuter for making this research possible through guidance, support, friendship and patience.

My family and friends for their undying support and patience.

All the good friends that I have made throughout my studies at Stellenbosch University for their friendship and support.

TABLE OF CONTENTS

LIST OF FIGURES

LIST OF TABLES

LIST OF SYMBOLS

A	Area, m^2
a	Surface area per unit volume, m^{-1},
B	coefficient
C	Capacity
c	Specific heat, J/kgK
c_p	Specific heat at constant pressure, J/kgK
G	Mass velocity, kg/sm^2
E	Error, Energy
h	Heat transfer coefficient, W/m^2K, grid refinement ratio
h_d	Mass transfer coefficient, kg/sm^2
i	Enthalpy, J/kg
i_{fg}	Latent heat, J/kg
k	refinement ratio, index, increment number
L	Length, m
Me	Merkel number
m	Mass flow rate, kg/s, number of units
N	Unit number, units
NTU	Number of transfer units
n	Number of units, units
p	Pressure, N/m^2 or Pa
S	Source term
T	Temperature, °C or K
U	Units, or variable
v	Velocity, m/s
W	Work, J
w	Humidity ratio, kg water vapour/ kg dry air
x	Spatial coordinate, m
y	Spatial coordinate, m
z	Spatial coordinate, m

Greek Symbols

α	Transitional coefficient or coefficient
Δ	Differential
β	Merkel assumption coefficient

θ	Angle, °
ρ	Density, kg/m^3
φ	Coefficient
λ	Correction factor

Dimensionless groups

Le_f	Lewis factor
Me	Merkel number

Subscripts

a	Air
counter	Counterflow
cross	Crossflow
e	effectiveness
e-NTU	effectivness-NTU method
f	Liquid or film
fi	Fill
fr	Frontal
G	Mass velocity
i	Step or increment number, inlet, index, enthalpy
j	Index
Me	Merkel theory
m	Mean, mass transfer, or moist
max	Maximum
min	Minimum
o	Outlet or reference at 0 ºC
P	Poppe
q	Heat source
r	residual
s	Saturation or surface
ss	Supersaturated
us	Unsaturated
v	Vapour
w	Humidity ratio, kg water vapour/ kg dry air, Water
wb	Wet-bulb
x	Coordinate
y	Coordinate
z	Coordinate

1 INTRODUCTION

1.1 Wet-cooling towers

1.1.1 Cooling in steam power plants

In steam power plants, steam is generated from a heat source such as coal, gas, nuclear or geothermal. The steam is used to drive a turbine connected to an electricity generator. The steam enters the turbine at high pressure and leaves at a lower pressure. To maximize cycle efficiency the low pressure outlet is maintained at a vacuum state. The vacuum is created by cooling the steam back into liquid form in a condenser. See Figure 1.1 for a schematic representation of a simple steam power plant.

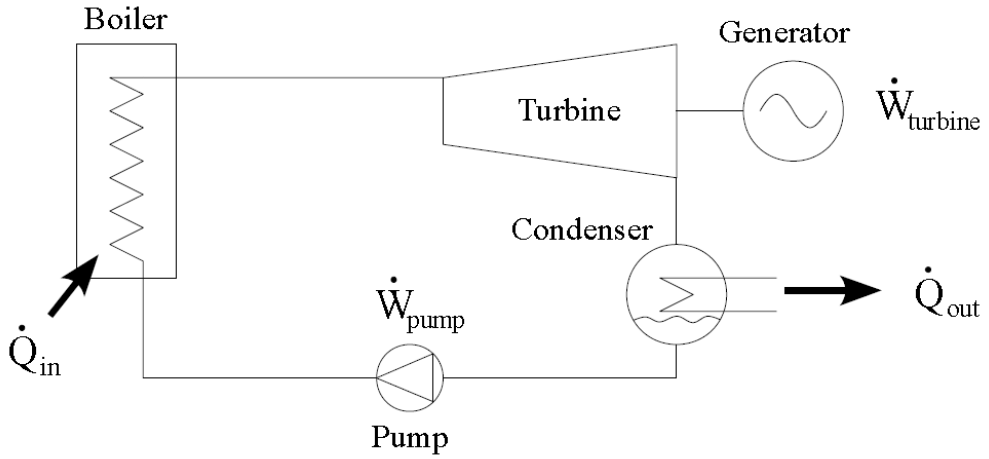

Figure 1.1: Schematic representation of a steam power plant (Rankine cycle)

A common way to provide the cooling is by pumping water from a nearby river lake or sea through the condenser. These cooling sources provide a vast amount of cooling liquid with a low temperature variation. The water is pumped to the power plant, which requires the plant to be as close to the source as possible. Large quantities of cooling water are required which makes distance and elevation from the water source to the plant influence its efficiency. When large quantities of water are extracted from the environment, heated up and returned, the impact on the ecosystem can be significant. Therefore, the increase in temperature is generally restricted by law. Furthermore, power plants often require being close to the heat source (for example coal mine or geothermal field) which eliminates direct cooling as an option.

Wet- or dry-cooling are the alternative choices. In indirect dry-cooling water is in a closed loop and the cooling water from the condenser is pumped through an air cooled heat exchanger. A preferred choice of dry-cooling is often the direct air cooled steam condenser (ACSC). In ACSC's the steam is sent directly to an air

cooled heat exchanger or condenser and cooling water is not needed, the cooling thus takes place only through sensible heat transfer. In wet-cooling, the water goes through a cooling tower where the air and water are in direct contact, providing cooling through heat and mass transfer, that is sensible and latent heat transfer. The research this thesis supplements is focused on the heat and mass transfer in wet-cooling towers.

1.1.2 Description of wet-cooling towers

Wet-cooling towers may be categorized as natural or mechanical draught, which both can be either cross- or counterflow. The function of a cooling tower is to maximize the contact area between the air and water to allow for effective heat and mass transfer. The hot water coming from the condenser is distributed by means of a water distribution system over a fill material (packing) designed to increase the surface area of the water, by creating a water film, small droplets or trickling streams. The water runs through the fill and falls as rain into a water basin at the bottom of the tower where it is collected and pumped back into the condenser. In a counterflow tower the air flows vertically upwards in the fill and the water falls downwards. To get to the fill, the air has to enter horizontally into the sides of the tower and turn 90° upwards while travelling through a rain of water falling from the fill. The air then has to flow through the fill, water distribution system, drift eliminators and out of the tower, see Figure 1.2 and Figure 1.3.

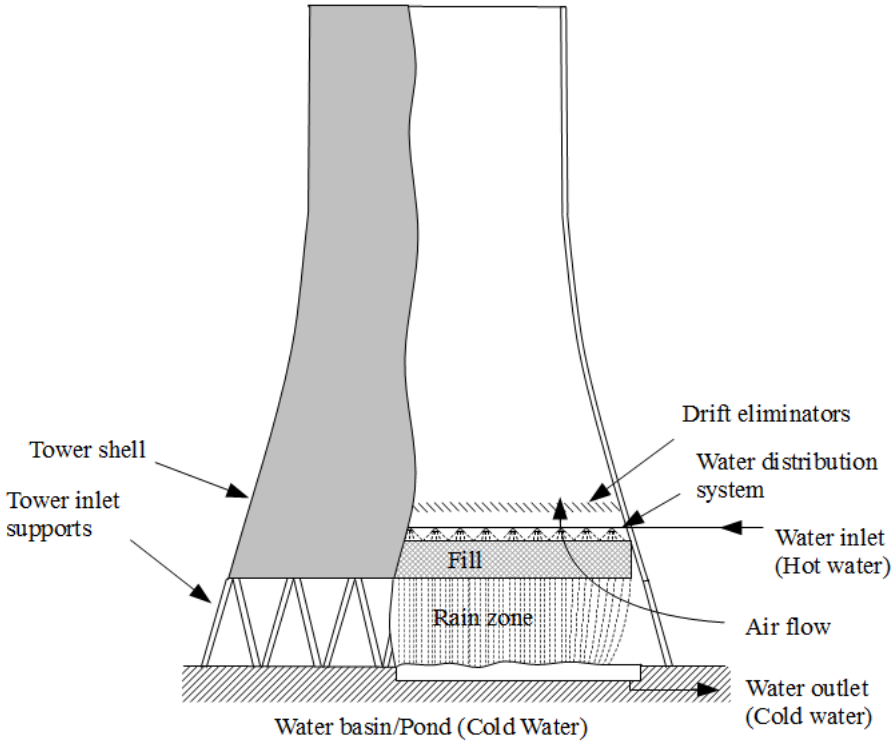

Figure 1.2: Schematic representation of a natural draught counterflow wet-cooling tower (Kröger, 2004)

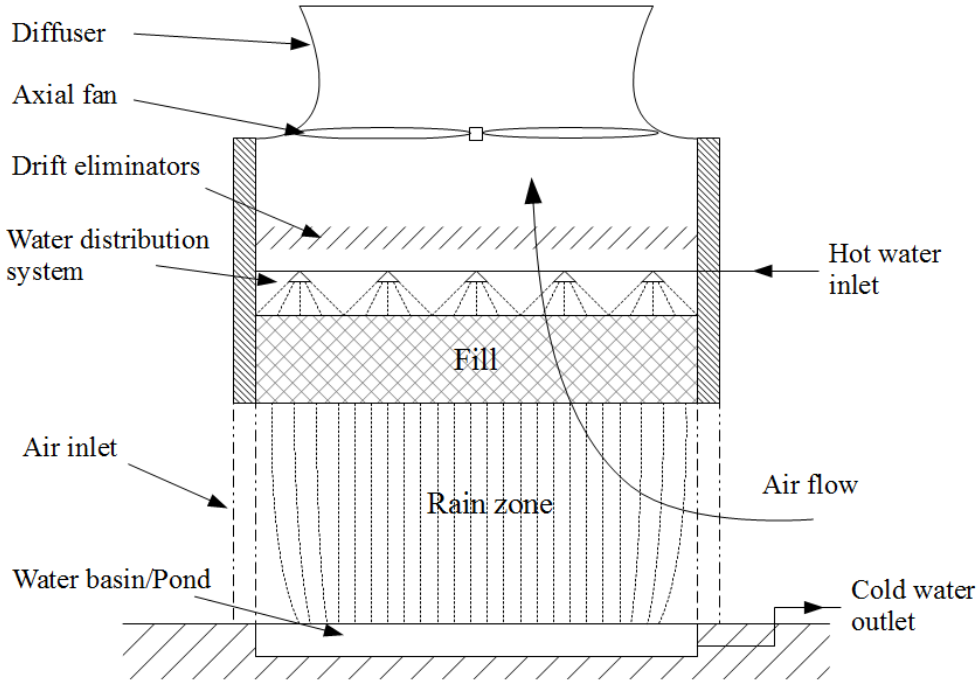

Figure 1.3: Schematic representation of a mechanical draught counterflow wet-cooling tower (Kröger, 2004)

In counterflow towers the height of the inlet is generally the same as the height of the rain zone. The inlet can be several times the fill height to ensure low inlet losses which improves the air inflow to the cooling tower. The water distribution system in counterflow towers consists of an array of spraying nozzles. In crossflow towers the air enters horizontally into the tower and goes directly into the fill as the water falls downwards and there is no rain zone, see Figure 1.4. The air leaves the fill on the other side of the fill and does not need to flow through the water distribution system. Water distribution systems in crossflow towers are therefore, not as restricted in terms of design, which can often allow for a more uniform water distribution over the fill.

In a natural draught cooling tower, the airflow is created by buoyancy as the air warms up and its density decreases. To get a good draught, the elevation between the inlet and outlet is kept as high as possible, often reaching over 100 m. In mechanical draught towers, the airflow is created by fans and the inlet outlet elevation difference is not required. The fans need power and their power consumption decreases the overall power plant cycle efficiency. Natural draught towers are generally not economical unless they are large. Therefore, mechanical draught towers are often the preferred choice for their smaller size.

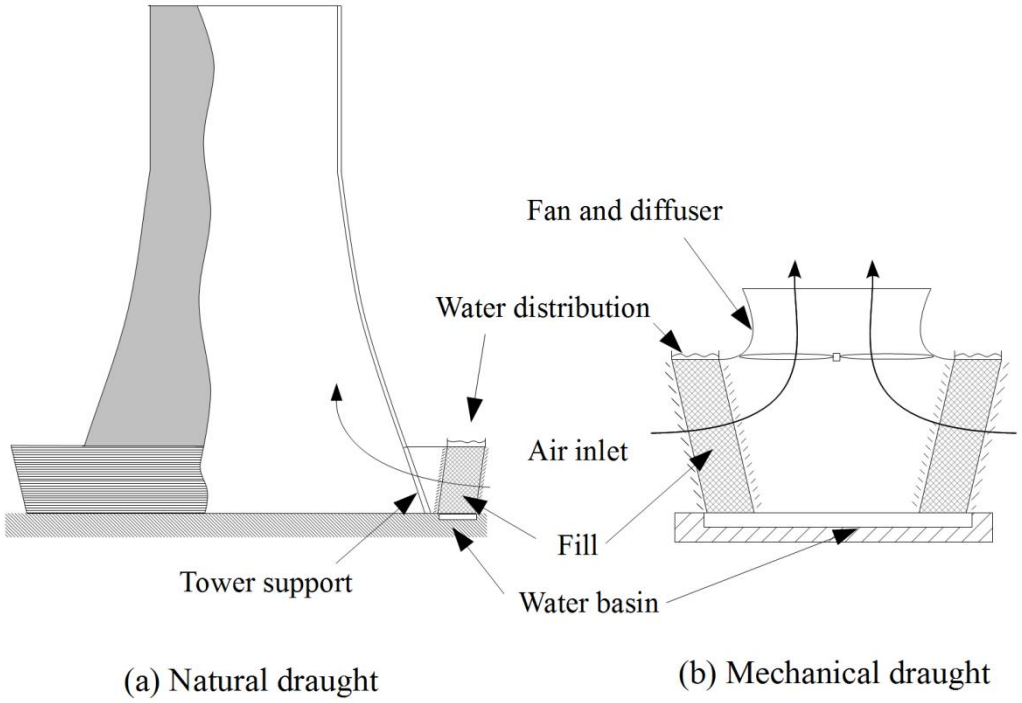

Figure 1.4: Schematic representation of crossflow cooling towers (Kröger, 2004)

When the air becomes saturated with water vapour a mist starts to form and creates a visible plume. The plume is a common sight in most cooling towers and is regarded as visible pollution. When a power plant is situated near or in a populated area, the plume is often not accepted by the local community and can cause hazard on nearby highways. For such cases plume abatement with a hybrid cooling tower can be the preferred choice. In hybrid cooling towers, the hot water is sent through a dry heat exchanger before it is sprayed over the fill. The hot dry air flowing through the dry section mixes with the moist air coming from the fill. By mixing the dry and humid air the capacity of the total air stream to absorb water as vapour is increased and the visibility of the plume can be eliminated. To eliminate the plume, the ratio between the dry and humid air is controlled based on atmospheric conditions, to give maximum cooling and no plume. See Figure 1.5 for a schematic representation of a mechanical draught hybrid cooling tower.

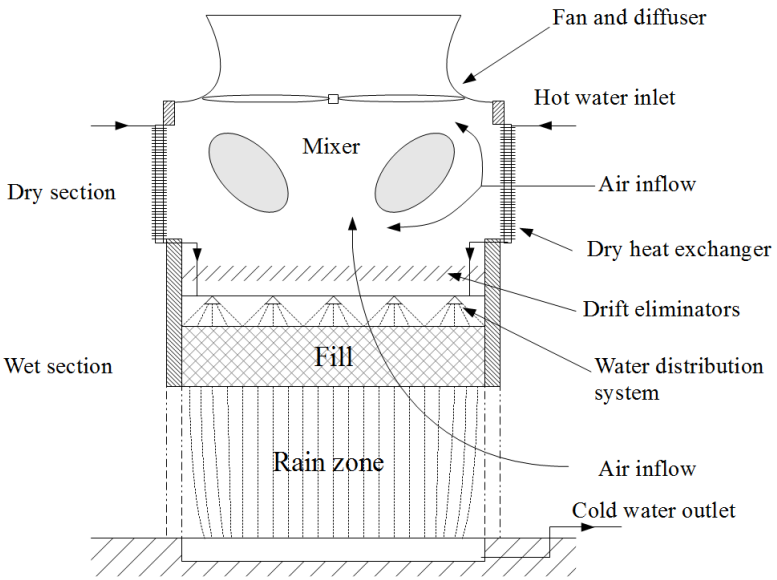

Figure 1.5: Schematic representation of a mechanical draught hybrid cooling tower (Kloppers, 2003)

1.1.3 Water and air flow in wet-cooling towers with different fill types

Air and water flow paths/patterns through the fill depend largely on the fill type used in a cooling tower. There are three general types of fills: splash, film and trickle. Their names all refer to how they are designed to make the water flow through them. Splash fill is designed to break up the water droplets into smaller drops, film fill to create a thin film of water and a trickle fill to create small water streams and droplets. See Figure 1.6 for examples of different fill types (Kröger, 2004)

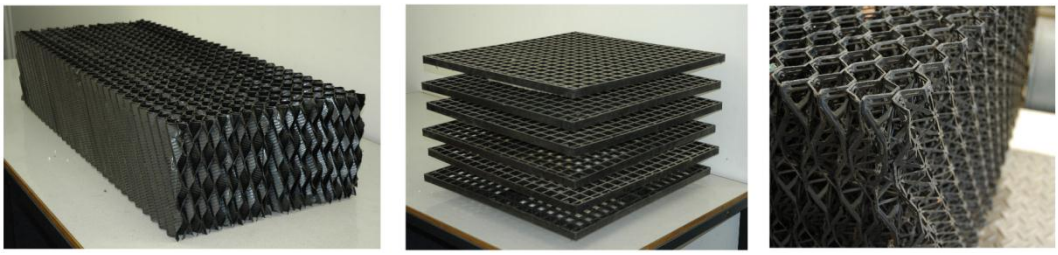

(a) Film (b) Splash (c) Trickle

Figure 1.6: Examples of fill/packing material used in wet-cooling towers

Film fills are made up of sheets packed together and air is channelled to only flow in one direction within the fill. In splash and trickle fill the air flow is not restricted in the same way and air can flow in more than one direction within the fill. In cooling towers with splash or trickle fill the airflow can therefore be oblique or so called cross-counterflow to the water. Figure 1.7 shows an example

of air flow in a natural draught counterflow wet cooling tower with film fill and trickle or splash fill.

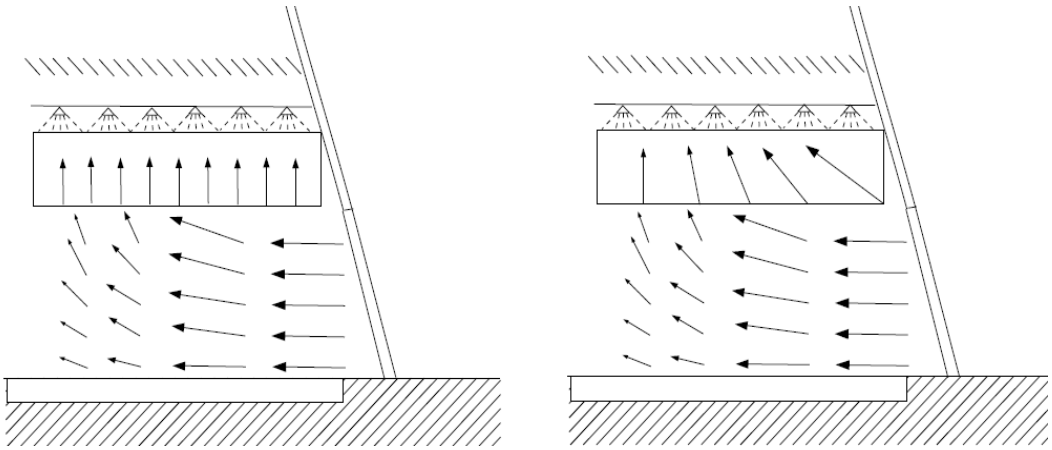

(a) Film fill (b) Splash or trickle fill

Figure 1.7: Velocity vectors of inlet air flow in a circular counterflow wet-cooling tower (Kröger, 2004)

Furthermore, re-circulation can occur near the cooling tower inlet if the fill loss coefficient is low and cross-counterflow effects can often increase under crosswind conditions. Both air re-circulation and cross-winds can considerably reduce the effectiveness of the cooling tower. In most cooling towers the outlet of the fill is level with the top of the cooling tower inlet. Research and experiments have suggested that by hanging the fill into the rain zone, re-circulation and effects of crosswinds can be greatly reduced. Such a setup would only be possible with splash and trickle fills or a combination of those film types and a film fill, see Figure 1.8.

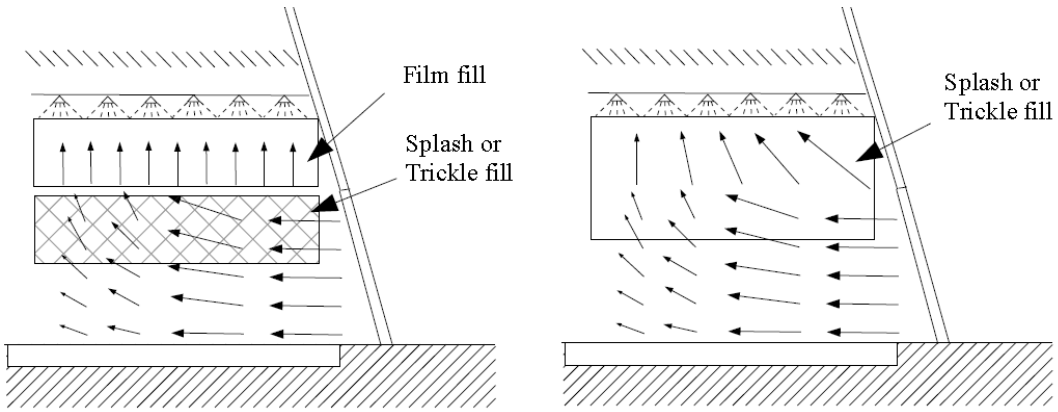

(a) Film and splash or trickle fill (b) Splash or Trickle fill

Figure 1.8 Velocity vectors of inlet air flow in a circular counterflow wet-cooling tower with fill hanging into the rain zone (Kröger, 2004)

1.1.4 Performance prediction and modelling of wet-cooling towers

In counterflow towers, cooling zones are categorized as: spray, fill and rain zones, whereas in crossflow towers there is essentially only a fill zone. In counterflow towers, more than 80% of the cooling can take place in the fill region (Al-Waked, 2006). Merkel (1925) was the first to develop a model to predict the rate of cooling in the fill. To simplify the model, Merkel combined the partial differential equations, describing the rate of change in properties of the water and air, into one simplified equation. The equation is commonly known as the Merkel equation and it describes simultaneous heat and mass transfer from a surface in terms of a coefficient, area and enthalpy driving potential. The Merkel equation is one-dimensional and can be solved with by hand. Zivi and Brand (1956) developed and solved the Merkel model for a crossflow cooling tower. This crossflow model is two-dimensional and is solved numerically using a computer. The more common model used for crossflow towers is an effectiveness-NTU method. Jaber and Webb (1989) adopted the e-NTU method, commonly used for heat exchangers, to be applied to cross- and counterflow wet-cooling towers. The method can be solved one dimensionally for both cross- and counterflow with equal effort. All of these models make simplifying assumptions regarding heat and mass transfer which allows them to be solved more easily. Despite these assumptions they can be used to predict water cooling with sufficient accuracy for most practical cases. In cases where a more accurate prediction of air outlet conditions is needed, such as hybrid towers, these models are not accurate. Poppe and Rögener (1991) developed a model that does not make the same simplifying assumptions as Merkel and can be used for prediction of air outlet conditions. The model consists of four partial differential equations which are functions of each other and solved simultaneously. The differential equations describe water temperature, water flow rate, air enthalpy and humidity. In comparison with the Merkel and e-NTU models, the Poppe model is complicated to solve and understand, and is computationally expensive for both cross- and counterflow conditions.

The Merkel, e-NTU and Poppe model assume that air is either in cross- or counterflow to the water. In film fill these assumptions are generally valid since the air flow is essentially either in cross- or counterflow to the water. In splash or trickle fill the air flow direction can vary across the fill and be in cross-counterflow. When the air is in cross-counterflow conditions none of the models discussed above can take cross-counterflow into account and therefore fail to accurately describe the heat and mass transfer in the fill. With most commercial CFD software such as ANSYS-*Fluent*®, flow in cooling towers can be modelled. By modelling a cooling tower with splash or trickle fill, cross-counterflow conditions and air re-circulation can be identified and quantified. To take these cross-counterflow conditions into account, Reuter (2010) developed a fill performance model from first principles that does not make any simplifying assumptions regarding airflow. By incorporating the Reuter model in a commercial CFD solver, the effects of re-circulation (flow separation) and cross-counterflow conditions in splash or trickle fill can be more accurately predicted.

Furthermore, cooling towers with fill hanging into the rain zone, to reduce cross wind effects, can be simulated.

The model does not make the simplified Merkel assumptions and should therefore give the same result as the Poppe model when air flow is assumed to be in either cross- or counterflow. Reuter implemented the model in ANSYS-*Fluent*® using a user defined function (UDF). The UDF obtains data from ANSYS-*Fluent*® to calculate source terms for the air. The source terms are then used by ANSYS-*Fluent*® to simulate heat and mass transfer in the fill. Governing partial differential equations for water temperature and flow rate are discretized and solved simultaneously within the UDF and stored in user defined memories (UDM).

Reuter presented his derivation for an axisymmetric natural draught wet-cooling tower (NDWCT) with unsaturated air, discretized and solved with a first order upwind differencing scheme. Additionally governing partial differential equations were given for a rectangular cooling tower as well as for supersaturated air. Using the first order scheme, Reuter (2010) concluded that an element size of 0.0125 m to 0.025 m is required to get acceptable grid independence. This cell size is too small to be a practical option for modelling a three-dimensional cooling tower.

The model was verified with a single drop model in unsaturated air and the one-dimensional Merkel method. Even though governing equations were presented for supersaturated air, the model was not verified to any supersaturated cases and the supersaturation equations were not successfully implanted in the UDF. If the model is to be considered for hybrid cooling towers, the supersaturation equations have to be effectively implemented. Furthermore, performance prediction was not compared to the crossflow Merkel method or the cross- and counterflow e-NTU and Poppe methods. To model a cooling tower fill, the transfer characteristics, in the form of the dimensionless Merkel number (Me), for the fill must be predetermined. The Merkel number for a fill is obtained from empirical equations generated from testing the fill material under varying conditions. Merkel numbers for e-NTU and Merkel method are generally at a similar range whereas, Merkel numbers obtained with the Poppe model are 7 to 10% higher (Kloppers, 2003). Thus a Merkel number obtained by the Merkel or e-NTU method cannot be used in the Poppe method to predict cooling without getting a similar difference in cooling range. If the Reuter model is to be used for modelling wet-cooling towers with existing Merkel numbers the model must be compared to the e-NTU, Merkel and Poppe model and differences in performance prediction with the different models analysed.

The above factors can be summarized as:

- The element or cell size required for the Reuter model is too small to be used in a full scale three dimensional model of a wet-cooling tower
- The Reuter model has not been successfully implemented with supersaturated air
- Comparison of performance prediction with the cross- and counterflow Merkel , e-NTU, and Poppe model has not been done.

These factors are important because:

- Three dimensional models are essential for studying cross-wind effects
- Including supersaturated air is essential for modelling hybrid cooling towers
- In order to use existing fill performance data, expected difference in performance prediction between the Reuter, e-NTU, Merkel, Poppe models must be known.

The main objective of this thesis is to include the above stated factors into the Reuter model. The thesis is split into three main chapters, in which the following three topics are covered: derivation of the Reuter model with a comparison to the e-NTU, Merkel and Poppe models; solution method to the Reuter model, where a second order differencing scheme is applied and a comparison to other applied solution methods is given; implementation of the Reuter model in ANSYS-*Fluent*® for a two and three dimensional model with un- and supersaturated air. Main literature sources are the works of Reuter (2010), Kröger (2004) and Kloppers (2003, 2004 and 2005). The same nomenclature is used as by these sources to maintain coherence. Literature review is covered within the introduction section of each chapter for the relevant topics.

1.2 Thesis objectives

The objectives of this thesis are:

- Compare the Reuter model to the existing fill performance models of Merkel, e-NTU and Poppe for both cross- and counterflow. To determine if transfer characteristics (Merkel numbers) obtained using Merkel, e-NTU and Poppe method can be used directly in the Reuter model for performance prediction.
- Verify that the Reuter model gives the same results as when implemented in ANSYS-*Fluent*® as when programmed for fill performance evaluation of test data.
- Verify that the Reuter model results with the same outlet conditions for supersaturated air, when implemented in ANSYS-*Fluent*® as when programmed for fill performance evaluation of test data.

- Suggest improvement to the solution method employed by Reuter (2010) to increase accuracy.
- Model a three-dimensional "block" of fill with ANSYS-*Fluent*®

1.3 Motivation for research

With evidence of global warming getting clearer, demand for carbon emission free power sources is increasing. The technology of these power sources, such as wind and solar, is still limited and expensive compared to conventional energy sources. This often makes conventional sources a more economical choice despite incentives provided by authorities. The conventional energy sources for electricity production most widely used globally are: hydro, coal, gas and nuclear. The coal and gas source along with other fossil fuels used in transportation are considered the main contributes to greenhouse gas emissions in the world. Replacing the conventional energy systems with other alternatives will take a long time and efforts to do so may not happen in time to meet targets of carbon emission reduction. To meet these targets other measures must be taken as well. One of those measures is to try to improve efficiencies of the existing conventional systems economically. By improving efficiency of existing systems the total power output is increased without burning more fuel and without increasing emissions.

One such measure is by improving effectiveness of cooling towers. Cooling towers are used in many steam power plants as well as many industrial processes around the world. The same cooling tower technology is often applied for a variety of applications. By improving the effectiveness of a cooling tower the capacity of its application, such as a steam cycle, can be improved. To find the fields where a cooling tower might be improved requires a detailed study of its operations. By studying air flow in and around cooling towers, effects of flow variation on its operation can be determined and improvements can be proposed. Such solutions lead to a more optimal operation of cooling towers and improved effectiveness.

1.4 Thesis outline

The thesis is split into 5 chapters. The first chapter is an introduction, where a general overview of wet-cooling towers, their basic function, setup and types are discussed. Additionally, different airflow patterns in the fill area of wet-cooling towers are described to emphasize the application of the Reuter model. In the second chapter a derivation of the Reuter model for a rectangular cooling tower for both unsaturated and supersaturated air. Furthermore the e-NTU, Merkel and Poppe models are described and discussed. All four methods are solved and modelled using Scilab and model comparison is given with a sample case used by Kröger (2004) and Kloppers (2003), (example 4.3.1 in Kröger) in cross- and counterflow.

The third chapter presents solution methods to the Reuter model where accuracy of the different solution methods is compared. To give a further comparison, solution methods according to the Merkel and Poppe models are compared to the suggested solution methods of the Reuter model. In chapter four a detailed description on how to implement the Reuter model into ANSYS-*Fluent*® is given and a comparison of the same fill modelled in Scilab and ANSYS-*Fluent*® is presented. The main chapters are followed by thesis conclusions, the 5th chapter, where conclusions of conclusions of each chapter are summarized and discussed.

Three Appendices are given to supplement the thesis. In appendix A, a sample calculation for the Reuter model and the crossflow e-NTU method are given. Appendix B presents experimental data for a trickle fill tested in the cross- and counterflow test facilities at Stellenbosch University is presented. Transfer characteristics (Merkel number) of the fill, obtained by Reuter, e-NTU, Merkel and Poppe models are determined to show difference in Merkel number the different methods. Finally appendix C gives the programming code for the user defined functions of the ANSYS-*Fluent*® model.

2 GOVERNING EQUATION OF HEAT AND MASS TRANSFER IN WET-COOLING TOWER FILLS

2.1 Introduction

Merkel (1925) developed a method to predict fill performance in counterflow wet cooling towers. The method is relatively simple and can be used to cooling tower performance with basic hand calculations. Jaber and Webb (1989) later developed a way to use the effectiveness-NTU approach directly to wet-cooling towers, similar to the e-NTU method normally used for heat exchangers. The e-NTU method has an advantage over the Merkel method, which is it can calculate cooling for cross- or counterflow with equal effort. The Merkel and e-NTU methods make the following simplifying assumptions: change in water flow rate from evaporation is negligible in the energy balance; the air leaving the fill is saturated with water vapour and the Lewis factor is equal to unity. Despite these assumptions the methods allow for an accurate evaluation of water outlet temperature. However, the prediction of air outlet temperature and humidity is inaccurate. For cooling towers with plume abatements like hybrid towers it is essential to determine the conditions of the air leaving the fill correctly. Poppe and Rögener (1991) developed the Poppe method which does not make the same simplifying assumptions as Merkel and can be solved for cross- or counterflow. The Poppe method is not as simple as the e-NTU and Merkel methods and requires solving multiple differential equations. It can be solved one-dimensionally for counterflow but requires a two-dimensional calculation for crossflow.

In cooling towers with anisotropic fill resistance such as trickle and splash fills, the air flow through the fill can, as previously mentioned in chapter 1, be oblique or in cross-counterflow to the water flow, particularly at a cooling tower inlet and when the fill loss coefficient is small (Reuter, 2010 and Kröger, 2004). With CFD models, the oblique flow field in the fill can be modelled. The Merkel, e-NTU and Poppe methods cannot predict cooling tower performance for cross-counterflow. Reuter (2010), however developed a method that can evaluate fill performance of wet-cooling tower in cross-, counter- and cross-counterflow conditions. The method gives the same result as would be obtained in an equivalent CFD model. The method is new and therefore no information exists on transfer characteristics for cooling tower fills determined by the method.

Reuter (2010) derived the governing fundamental partial differential equation to determine the cooling water temperature, water evaporation rate, air temperature and air humidity ratio in a two-dimensional cross-counterflow fill for unsaturated and supersaturated air. The equations are presented in cylindrical co-ordinates for circular sectioned axis-symmetric cooling towers. Governing equations are also given for a rectangular sectioned cooling tower in Cartesian co-ordinates. In this chapter a derivation is given for the Reuter model for a rectangular cooling tower, as well as a description of the e-NTU, Merkel and Poppe methods. A sample case used by Kröger (2004) and Kloppers (2003), in a cross- and counterflow fill

analysis is used as a comparison of performance prediction with the different methods. Experimental data from cross- and counterflow cooling tower test facilities at the University of Stellenbosch is used to illustrate the difference in transfer characteristics for different flow rates and inlet conditions. Description of test facility and full test results are given in Appendix B of this thesis.

2.2 Governing differential equations of heat and mass transfer in a cross-counterflow fill of a rectangular wet-cooling tower for unsaturated air

The following derivations are adopted from Reuter (2010), nomenclature and structure of derivation is kept similar for coherency. Consider the elementary cross-section through a rectangular cooling tower fill with cross-counterflow, in Figure 2.1.

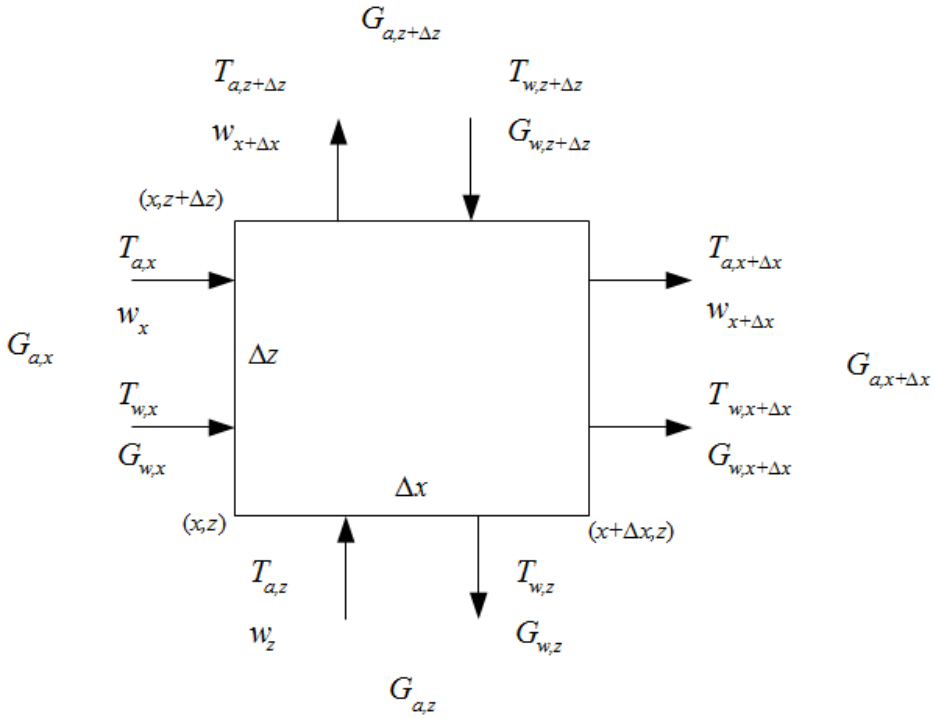

Figure 2.1: Elementary cross-section through a fill region of a rectangular cooling tower (Reuter, 2010)

Dry air mass balance for the above control volume yields,

$$\left(G_{a,x+\Delta x} - G_{a,x}\right)\Delta z + \left(G_{a,z+\Delta z} - G_{a,z}\right)\Delta x = 0 \tag{2.1}$$

Divide Eq. (2.1) by $\Delta x, \Delta z$

$$\frac{\left(G_{a,x+\Delta x}-G_{a,x}\right)}{\Delta x}+\frac{\left(G_{a,z+\Delta z}-G_{a,z}\right)}{\Delta z}=0 \tag{2.2}$$

and let $\Delta x, \Delta z \rightarrow 0$ to obtain,

$$\frac{\partial G_{a,x}}{\partial x}+\frac{\partial G_{a,z}}{\partial z}=0 \tag{2.3}$$

Assume that the horizontal water mass velocity is $G_{w,x}=0$ kg/sm^2 since the water flow in the fill is essentially downwards. Water mass balance for the control volume in Fig 2.1 can therefore be written as

$$\begin{aligned}&\left(G_{w,z+\Delta z}-G_{w,z}\right)\Delta z\\&\quad=\left(G_{a,x+\Delta x}w_{x+\Delta x}-G_{a,x}w_x\right)\Delta x+\left(G_{a,z+\Delta z}w_{z+\Delta z}-G_{a,z}w_z\right)\Delta z\end{aligned} \tag{2.4}$$

Divide Eq. (2.4) by $\Delta x, \Delta z$

$$\begin{aligned}&\frac{\left(G_{w,z+\Delta z}-G_{w,z}\right)}{\Delta z}\\&\quad=\frac{\left(G_{a,x+\Delta x}w_{x+\Delta x}-G_{a,x}w_x\right)}{\Delta z}+\frac{\left(G_{a,z+\Delta z}w_{z+\Delta z}-G_{a,z}w_z\right)}{\Delta x}\end{aligned} \tag{2.5}$$

Let $\Delta x, \Delta z \rightarrow 0$ and substitute Eq. (2.3) to obtain the following differential equation

$$\frac{\partial G_w}{\partial z}=G_{a,x}\frac{\partial w}{\partial x}+G_{a,z}\frac{\partial w}{\partial z} \tag{2.6}$$

From the definition of mass transfer rate by Merkel (1925), the evaporation rate of water in unsaturated air can be expressed as,

$$\frac{\partial G_w}{\partial z}=h_d a_{fi}(w_{sw}-w) \tag{2.7}$$

where h_d is the mass transfer coefficient and a_{fi} is the area density of the fill. By combining Eq. (2.6) and (2.7), the differential equation for humidity ratio of unsaturated air is

$$G_{az}\frac{\partial w}{\partial z}+G_{ax}\frac{\partial w}{\partial x}=h_d a_{fi}(w_{sw}-w) \tag{2.8}$$

Heat and mass transfer at the air/water interface over the control volume can be expressed as

$$c_{pw}\left(T_{w_{z+\Delta z}}G_{w_{z+\Delta z}} - T_{w_z}G_{w_z}\right)\Delta x = \left[ha_{fi}(T_w - T_a) + i_{v(T_w)}h_d a_{fi}(w_{sw} - w)\right]\Delta z\Delta x \tag{2.9}$$

Divide Eq. (2.9) by $\Delta z\Delta x$ and get,

$$\frac{c_{pw}\left(T_{w_{z+\Delta z}}G_{w_{z+\Delta z}} - T_{w_z}G_{w_z}\right)}{\Delta z} = \left[ha_{fi}(T_w - T_a) + i_{v(T_w)}h_d a_{fi}(w_{sw} - w)\right] \tag{2.10}$$

Let $\Delta z, \Delta x \to 0$

$$c_{pw}\frac{\partial(G_w T_w)}{\partial z} = ha_{fi}(T_w - T_a) + i_{v_{(T_w)}}h_d a_{fi}(w_{sw} - w) \tag{2.11}$$

Differentiate equation (2.11) by the chain rule and get

$$c_{pw}\left(G_w\frac{\partial T_w}{\partial z} + T_w\frac{\partial G_w}{\partial z}\right) = ha_{fi}(T_w - T_a) + i_{v_{(T_w)}}h_d a_{fi}(w_{sw} - w) \tag{2.12}$$

Eq. (2.12) can be rewritten for the rate of change in water temperature as,

$$\frac{\partial T_w}{\partial z} = \frac{1}{c_{pw}G_w}\left[ha_{fi}(T_w - T_a) + i_{v(T_w)}h_d a_{fi}(w_{sw} - w) - c_{pw}T_w\frac{\partial G_w}{\partial z}\right] \tag{2.13}$$

Insert Eq. (2.7) into Eq. (2.13)

$$\frac{\partial T_w}{\partial z} = \frac{1}{c_{pw}G_w}\left[ha_{fi}(T_w - T_a) + i_{v(T_w)}h_d a_{fi}(w_{sw} - w) - c_{pw}T_w h_d a_{fi}(w_{sw} - w)\right] \tag{2.14}$$

Use the definition of the Lewis factor to substitute h in Eq. (2.14)

$$Le_f = h/(h_d c_{pma}) \tag{2.15}$$

The definition for enthalpy of water vapour can be expressed as

$$i_{v(T)} = i_{fg(T)} + c_{pw}T \tag{2.16}$$

Substitute Eq. (2.15) and (2.16) into Eq. (2.14) and get

$$\frac{\partial T_w}{\partial z} = \frac{h_d a_{fi}}{c_{pw}G_w}\left[Le_f c_{pma}(T_w - T_a) + (i_{fg(T_w)} + c_{pw}T_w)(w_{sw} - w) - c_{pw}T_w(w_{sw} - w)\right] \tag{2.17}$$

Eq. (2.17) can then be written as

$$\frac{\partial T_w}{\partial z} = \frac{c_{pma}}{c_{pw}} \frac{h_d a_{fi}}{G_w} \left[Le_f (T_w - T_a) + \frac{i_{fg(T_w)}}{c_{pma}} (w_{sw} - w) \right] \tag{2.18}$$

Change in air temperature can be determined from the dry-air enthalpy. The sensible heat and mass transfer of the air over the control volume can be written as

$$\begin{aligned} \left(G_{a,x+\Delta x}\, i_{ma,x+\Delta x} - G_{a,x}\, i_{ma,x}\right) \Delta z + \left(G_{a,z+\Delta z}\, i_{ma,z+\Delta z} - G_{a,z}\, i_{ma,z}\right) \Delta x \\ = \left[h a_{fi} (T_w - T_a) + i_{v(T_w)}\, h_d a_{fi} (w_{sw} - w) \right] \Delta z \Delta x \end{aligned} \tag{2.19}$$

Divide by Eq. (2.19) by $\Delta z \Delta x$ and get

$$\begin{aligned} \frac{\left(G_{a,x+\Delta x}\, i_{ma,x+\Delta x} - G_{a,x}\, i_{ma,x}\right)}{\Delta x} + \frac{\left(G_{a,z+\Delta z}\, i_{ma,z+\Delta z} - G_{a,z}\, i_{ma,z}\right)}{\Delta z} \\ = h a_{fi} (T_w - T_a) + i_{v(T_w)} h_d a_{fi} (w_{sw} - w) \end{aligned} \tag{2.20}$$

Let $\Delta z, \Delta x \to 0$ and substitute Eq. (2.3) and (2.15) to get,

$$G_{ax} \frac{\partial i_{ma}}{\partial x} + G_{az} \frac{\partial i_{ma}}{\partial z} = h_d a_{fi} \left[Le_f c_{pma} (T_w - T_a) + i_{v(T_w)} (w_{sw} - w) \right] \tag{2.21}$$

The governing differential equations for heat and mass transfer in unsaturated air are Eq. (2.7), (2.8), (2.18) and (2.21) where the air temperature can be iteratively determined from the following equation,

$$i_{ma} = c_{pa} T_a + w\, i_{v(T_a)} \tag{2.22}$$

Reuter (2010) took the derivation a step further and substituted Eq. (2.22) into Eq. (2.21) and differentiated with respect to x and z.

$$\frac{\partial i_{ma}}{\partial x} = c_{pa} \frac{\partial T_a}{\partial x} + \frac{\partial w}{\partial x} i_{v(T_a)} + w c_{pv} \frac{\partial T_a}{\partial x} \tag{2.23}$$

$$\frac{\partial i_{ma}}{\partial z} = c_{pa} \frac{\partial T_a}{\partial z} + \frac{\partial w}{\partial z} i_{v(T_a)} + w c_{pv} \frac{\partial T_a}{\partial z} \tag{2.24}$$

Substitute Eq. (2.23) and (2.24) into Eq. (2.21) to get,

$$\begin{aligned} c_{pma} \left(G_{ax} \frac{\partial T_a}{\partial x} + G_{az} \frac{\partial T_a}{\partial z} \right) + i_{v(T_a)} \left(G_{ax} \frac{\partial w}{\partial x} + G_{az} \frac{\partial w}{\partial z} \right) \\ = h_d a_{fi} \left[Le_f c_{pma} (T_w - T_a) + i_{v(T_w)} (w_{sw} - w) \right] \end{aligned} \tag{2.25}$$

The enthalpy of water vapour can either be described with Eq. (2.16) or the following equation,

$$i_{v(T_w)} = i_{fgwo} + c_{pv}T_w \tag{2.26}$$

where i_{fgwo} is the latent heat of vaporization evaluated at 0°C (273 K). Now substitute Eq. (2.8) and (2.26) into Eq. (2.25) to get,

$$\begin{aligned} &c_{pma}\left(G_{ax}\frac{\partial T_a}{\partial x} + G_{az}\frac{\partial T_a}{\partial z}\right) \\ &= h_d a_{fi}\left[\begin{array}{c} Le_f c_{pma}(T_w - T_a) + \\ (i_{fgwo} + c_{pv}T_w)\,(w_{sw} - w) - (i_{fgwo} + c_{pv}T_a)\,(w_{sw} - w) \end{array}\right] \end{aligned} \tag{2.27}$$

where $c_{pma} = c_{pa} + w\,c_{pv}$. Eq. (2.27) can be written in the following form,

$$G_{ax}\frac{\partial T_a}{\partial x} + G_{az}\frac{\partial T_a}{\partial z} = h_d a_{fi}(T_w - T_a)\left[Le_f + \frac{c_{pv}}{c_{pma}}(w_{sw} - w)\right] \tag{2.28}$$

Thus Eq. (2.28), instead of Eq. (2.21), along with Eq. (2.7), (2.8), (2.18) make up the governing partial differential equations for heat and mass transfer in a rectangular cooling tower fill with crossflow, counterflow or cross-counterflow conditions where the air is unsaturated.

2.3 Governing differential equations of heat and mass transfer in a cross-counterflow fill of a rectangular wet-cooling tower for supersaturated air

The air may become saturated before it leaves the fill. When this is the case the governing equations derived in the previous section fail to describe the heat and mass transfer in the fill. If the water temperature is still higher than the air temperature a potential for mass transfer still persists and the air becomes supersaturated (Kröger, 2004). When the air is supersaturated the amount of water per unit of dry air or absolute humidity consists of the water that is saturated in the air stream and the water that has condensed as mist. The humidity can then be written as

$$w = w_{sa} + (w - w_{sa}) \tag{2.29}$$

Consider the control volume presented in Fig. 2.1, by following the same derivation as has been presented for unsaturated air, only by assuming supersaturated air. Dry air mass balance for the control volume gives the same equation as Eq. (2.3). Applying Eq. (2.29) to the water mass balance gives the following equation,

$$\begin{aligned}(G_{w,z+\Delta z} - G_{w,z})\Delta z &= (G_{a,x+\Delta x}w_{x+\Delta x} - G_{a,x}w_x)\Delta x \\ &+ (G_{a,z+\Delta z}w_{z+\Delta z} - G_{a,z}w_z)\Delta z \\ &+ \left[G_{a,x+\Delta x}(w_{x+\Delta x} - w_{sa,x+\Delta x}) - G_{a,x}(w_x - w_{sa,x})\right]\Delta x \\ &+ \left[G_{a,z+\Delta z}(w_{z+\Delta z} - w_{sa,z+\Delta z}) - G_{a,z}(w_z - w_{sa,z})\right]\Delta z\end{aligned} \tag{2.30}$$

Divide Eq. (2.30) by $\Delta z, \Delta x$

$$\begin{aligned}\frac{(G_{w,z+\Delta z} - G_{w,z})}{\Delta z} &= \frac{(G_{a,x+\Delta x}w_{sa,x+\Delta x} - G_{a,x}w_{sa,x})}{\Delta z} \\ &+ \frac{(G_{a,z+\Delta z}w_{sa,z+\Delta z} - G_{a,z}w_{sa,z})}{\Delta x} \\ &+ \frac{\left[G_{a,x+\Delta x}(w_{sa,x+\Delta x} - w_{sa,x+\Delta x}) - G_{a,x}(w_{sa,x} - w_{sa,x})\right]}{\Delta z} \\ &+ \frac{\left[G_{a,z+\Delta z}(w_{z+\Delta z} - w_{sa,z+\Delta z}) - G_{a,z}(w_z - w_{sa,z})\right]}{\Delta x}\end{aligned} \tag{2.31}$$

Let $\Delta z, \Delta x \to 0$ and substitute Eq. (2.31) to obtain the following differential equation

$$\frac{\partial G_w}{\partial z} = G_{a,x}\frac{\partial w_{sa}}{\partial x} + G_{a,z}\frac{\partial w_{sa}}{\partial z} + G_{a,x}\frac{\partial (w - w_{sa})}{\partial x} + G_{a,z}\frac{\partial (w - w_{sa})}{\partial z} \tag{2.32}$$

The first two terms on the right hand side represent the water vapour taken to the air stream and the last two terms represent the mist which condensed from the air.

When the air gets supersaturated with water vapour the evaporation rate will depend on the difference between the saturated humidity at bulk water temperature and the saturation humidity of the air. The governing differential equations for heat and mass transfer in supersaturated air can thus be written as,

$$\frac{\partial G_w}{\partial z} = h_d a_{fi}(w_{sw} - w_{sa}) \tag{2.33}$$

$$\frac{\partial T_w}{\partial z} = \frac{c_{pma}}{c_{pw}}\frac{h_d a_{fi}}{G_w}\left[Le_f(T_w - T_a) + \frac{i_{fg(T_w)}}{c_{pma}}(w_{sw} - w_{sa})\right] \tag{2.34}$$

$$G_{a,z}\frac{\partial w}{\partial z} + G_{a,x}\frac{\partial w}{\partial x} = h_d a_{fi}(w_{sw} - w_{sa}) \tag{2.35}$$

$$\begin{aligned}G_{a,x}\frac{\partial i_{ma,ss}}{\partial x} + G_{a,z}\frac{\partial i_{ma,ss}}{\partial z} \\ = h_d a_{fi}\left[Le_f c_{pma}(T_w - T_a) + i_{v(T_w)}(w_{sw} - w_{sa})\right]\end{aligned} \tag{2.36}$$

The above equation for change in enthalpy can be used as the governing differential equation for air, instead of the governing differential equation for air temperature, by determining the air temperature iteratively from Eq. (2.37).

$$i_{ma,ss} = c_{pa}T_a + w_{sa}\, i_{v(T_a)} + (w - w_{sa})\, c_{pw}\, T_a \tag{2.37}$$

As with the governing equation for unsaturated air, a governing equation for air temperature can be derived by differentiating Eq. (2.37) with regards to x and z,

$$\frac{\partial i_{ma,x}}{\partial x} c_{pa} \frac{\partial T_a}{\partial x} + \frac{\partial w_{sa}}{\partial x} i_{v(T_a)} + (w - w_{sa}) c_{pw} \frac{\partial T_a}{\partial x} \tag{2.38}$$

$$\frac{\partial i_{ma,z}}{\partial z} = c_{pa} \frac{\partial T_a}{\partial z} + \frac{\partial w_{sa}}{\partial z} i_{v(T_a)} + (w - w_{sa}) c_{pw} \frac{\partial T_a}{\partial z} \tag{2.39}$$

Substituting Eq. (2.38), (2.39) into Eq. (2.36) and follow a similar derivation as in the section 2.2, the following differential equation for air temperature can be obtained:

$$\begin{aligned} G_{ax} \frac{\partial T_a}{\partial x} + G_{az} \frac{\partial T_a}{\partial z} = \\ h_d a_{fi} Le_f (T_w - T_a) \frac{c_{pma}}{c_{pma,ss}} \\ + \left[\frac{i_{fg(T_w)} + c_{pw}(T_w - T_a)}{c_{pma,ss}} \right] h_d a_{fi} (w_{sw} - w_{sa}) \\ - \frac{i_{fg(T_a)}}{c_{pma,ss}} \left(G_{ax} \frac{\partial w_{sa}}{\partial x} + G_{az} \frac{\partial w_{sa}}{\partial z} \right) \end{aligned} \tag{2.40}$$

where $c_{pma,ss} = c_{pa} + w_{sa}c_{pv} + (w - w_{sa})c_{pw} = c_{pma,s} + (w - w_{sa})c_{pw}$.

The governing equations for heat and mass transfer when the air is supersaturated are then Eq. (2.34), (2.35), (2.36) and (2.40). See Chapter 3 for detailed descriptions of solving the governing differential equations.

2.4 Transfer characteristics

The Lewis factor, the mass transfer coefficient and the area density of the fill will have to be known or determined to solve the system of governing differential equations. The mass transfer coefficient and area density of the fill in wet-cooling towers are usually described by the Merkel number (Me), whereas the Lewis factor (Le_f) in Eq. (2.15), describes the ratio heat and mass transfer coefficients.

2.4.1 The Lewis factor

Kloppers and Kröger (2005b) described the Lewis factor and analysed its influence on the performance of wet cooling towers. Three different Lewis factor specifications were employed. Lewis factors of 0.5 and 1.3, as Häszler (1999) proposes for upper and lower limits, and the following Lewis factor relation proposed by Bosnjakovic (1965),

$$Le_f = 0.866^{0.667}\left(\frac{w_{sw}+0.622}{w+0.622}-1\right)/\ln\left(\frac{w_{sw}+0.622}{w+0.622}\right) \tag{2.41}$$

Eq. (2.41) is for unsaturated air and for supersaturated it becomes,

$$Le_f = 0.866^{0.667}\left(\frac{w_{sw}+0.622}{w_{sa}+0.622}-1\right)/\ln\left(\frac{w_{sw}+0.622}{w_{sa}+0.622}\right) \tag{2.42}$$

Merkel assumed a Lewis factor of unity (Le_f = 1), which made his derivation simpler. Currently no method has been implemented effectively to measure the Lewis factor and determine it accurately for wet-cooling towers. Hence the Lewis factor is usually assumed to be within the Häszler limits (the Bosnjakovic relation gives a value of approximately 0.92 (Kloppers and Kröger, 2005b)). Kloppers and Kröger pointed out that whatever value is used for the Lewis factor, it is more important to use the same Lewis factor when predicting performance as was used to obtain Merkel number from experimental data.

2.4.2 The Merkel number

The mass transfer coefficient and the area density of the fill are always presented as a term ($h_d a_{fi}$). It is therefore not necessary to calculate them independently. When the system of governing partial differential equations are solved they are expressed in the form of the dimensionless Merkel number,

$$Me = \frac{h_d a_{fi} L_{fi}}{G_w} \quad , \text{ or } \quad Me/L_{fi} = \frac{h_d a_{fi}}{G_w} \quad , \text{ per meter } (\text{m}^{-1}) \tag{2.43}$$

To obtain the Merkel number for a particular fill, tests are made in specialized test facilities with varying air and water flow rates, inlet water temperatures and fill height. For every test, the air temperature, humidity and pressure are measured as well as the water outlet temperature to determine water cooling in the fill. When inlet conditions of the water and air and the outlet water temperatures are known

the Merkel number can be determined iteratively by solving the governing differential equations. Empirical relations can be obtained by fitting a curve through the test results based on the varying parameters with the following equation (Johnson, 1989)

$$Me/L_{fi} = c_1 \, G_{wi}^{c_2} \, G_a^{c_3} \, T_{wi}^{c_4} \tag{2.44}$$

where c_1, c_2, c_3 and c_4 are curve fitting constants. The Merkel number from the empirical formula can be used to predict water outlet temperature in a fill. Reuter (2010) pointed out that there are no test facilities capable of testing cross-counterflow condition and the Merkel number can therefore not be determined from real test data. Instead, Reuter proposed using an interpolation between cross- and counterflow Merkel numbers based on the airflow angle, written as

$$\left(\frac{Me}{L_{fi}}\right) = \left\{\left(\frac{Me}{L_{fi}}\right)_{counter} + \left[\left(\frac{Me}{L_{fi}}\right)_{cross} - \left(\frac{Me}{L_{fi}}\right)_{counter}\right]\left(\frac{90° - \theta}{90°}\right)\right\} \tag{2.45}$$

2.5 Governing differential equations of heat and mass transfer in a cross-, counter-, and cross-counterflow fill based on the Merkel assumptions

Merkel (1925) assumed a Lewis factor equal to unity ($Le_f = 1$) and the evaporative loss to be negligible ($\partial G_w/\partial z = 0$ and $\partial w/\partial z = 0$) in the energy balance. By applying these assumptions only the governing differential equations for the water temperature and air enthalpy remain. In the energy balance of the water and air, the equations for the water temperature simplifies to,

$$\frac{\partial T_w}{\partial z} = \frac{1}{c_{pw} G_w}\left[c_{pma} h_d a_{fi}(T_w - T_a) + i_{v(T_w)} h_d a_{fi}(w_{sw} - w)\right] \tag{2.46}$$

This equation is often written in terms of enthalpies, instead of temperature and humidity. By assuming that the difference in specific heat evaluated at the different temperatures is minimal, the following equations can be obtained,

$$i_{masw} - i_{ma} \approx c_{pma}(T_w - T_a) + i_v(w_{sw} - w) \tag{2.47}$$

By substituting Eq. (2.47) into Eq. (2.46), the governing differential equation for water temperature can be written in terms of enthalpy in the following form,

$$\frac{\partial T_w}{\partial z} = \frac{1}{c_{pw}} \frac{h_d a_{fi}}{G_w}(i_{masw} - i_{ma}) \tag{2.48}$$

Similarly the governing differential equation for enthalpy can be written as,

$$\frac{\partial i_{ma}}{\partial z} = \frac{h_d a_{fi}}{G_{a,z}} (i_{masw} - i_{ma}) \tag{2.49}$$

For crossflow the governing differential equations for enthalpy becomes,

$$\frac{\partial i_{ma}}{\partial x} = \frac{h_d a_{fi}}{G_{a,x}} (i_{masw} - i_{ma}) \tag{2.50}$$

To determine the properties of the air leaving the fill, Merkel (1925) assumed that the air is saturated with water vapour. By applying this last assumption for a counterflow fill, Eq. (2.48) and (2.49) can be combined to form the following,

$$Me = \frac{h_d a_{fi} L_{fi}}{G_w} = \int_{T_{wo}}^{T_{wi}} \frac{c_{pw} dT_w}{i_{masw} - i_{ma}} \tag{2.51}$$

The above equation is the most traditional form of the governing equations for counterflow wet-cooling towers and is commonly referred to as the Merkel equation (Kröger, 2004). The Merkel equation can be solved with any numerical integration method, but is generally solved by the means of the Chebychev method. Zivi and Brand (1956) derived and solved the two governing equations for the Merkel method in crossflow. The governing equations for crossflow have to be solved in a two dimensional domain and usually require an iterative procedure.

One of the advantages of the Reuter model is that it can do cross-, counter- or cross-counterflow by only changing the values $G_{a,x}$ and $G_{a,z}$. It can also be useful to switch between Poppe and Merkel assumptions without altering the governing differential equation substantially. Consider the following form of the governing differential equation for the water temperature,

$$\frac{\partial T_w}{\partial z} = \frac{c_{pma}}{c_{pw}} \frac{h_d a_{fi}}{G_w} \left[Le_f (T_w - T_a) + \frac{i_{fg(T_w)} + \beta_{Me} c_{pw} T_w}{c_{pma}} (w_{sw} - w) \right] \tag{2.52}$$

where $\beta_{Me} = 0$ is for Poppe assumption and $\beta_{Me} = 1$ is for Merkel assumption of the evaporative loss in the energy balance. Using $\beta_{Me} = 1$ and $Le_f = 1$ therefore gives the Merkel assumption, whereas $\beta_{Me} = 0$ and the Bosnjakovic relation for the Lewis factor gives the Poppe assumptions. By solving the governing equations for humidity as well, this form can be implemented in CFD models to give results equivalent of the common Merkel method. A comparison of performance prediction using the Reuter model with Merkel assumption and the full Merkel method is discussed in Section 2.8.

2.6 The effectiveness-NTU method

Jaber and Webb (1989) developed the effectiveness-NTU method to be directly applied to crossflow or counterflow wet-cooling towers. The e-NTU method is very useful for crossflow due to its simplicity compared to other crossflow methods. Kröger (2004) gives a detailed derivation of e-NTU method along with a sample calculation for a counterflow case. The e-NTU method makes the same simplifying assumption as Merkel for evaporation, Lewis factor and air outlet conditions.

The e-NTU method resembles the common e-NTU heat exchanger equation

$$\frac{\partial(i_{masw} - i_{ma})}{i_{masw} - i_{ma}} = h_d \left(\frac{\partial i_{masw}/\partial T_w}{m_w c_{pw}} - \frac{1}{m_a} \right) \partial A \tag{2.53}$$

Two cases can be considered for a wet-cooling tower,

Case 1: $m_a > m_w c_{pw}/(\partial i_{masw}/\partial T_w)$

where $C_{emin} = m_w c_{pw}/(\partial i_{masw}/\partial T_w)$ and $C_{emax} = m_a$

Case 2: $m_a < m_w c_{pw}/(\partial i_{masw}/\partial T_w)$

where $C_{emin} = m_a$ and $C_{emax} = m_w c_{pw}/(\partial i_{masw}/\partial T_w)$

The gradient of the saturated air enthalpy temperature curve is

$$\frac{\partial i_{masw}}{\partial T_w} = \frac{i_{maswi} - i_{maswo}}{T_{wi} - T_{wo}} \tag{2.54}$$

The fluid capacity rate ratio is defined as

$$C = \frac{C_{emin}}{C_{emax}} \tag{2.55}$$

The effectiveness ratio is given by

$$e = \frac{Q}{Q_{max}} = \frac{m_w \, c_{pw} \, (T_{wi} - T_{wo})}{C_{\text{emin}} \, (i_{maswi} - \lambda - i_{mai})} \tag{2.56}$$

where Lambda (λ) is a correction factor proposed by Berman (1961) and is defined by

$$\lambda = (i_{maswo} + i_{maswi} - 2i_{maswm})/4 \tag{2.57}$$

Depending on the flow configuration the effectiveness-NTU formula is given in different forms. For a counterflow the effectiveness formula is given by

$$e = \frac{1 - \exp[-NTU\ (1 - C)]}{1 - C\ \exp[-NTU\ (1 - C)]} \tag{2.58}$$

For crossflow configurations the effectiveness can be defined as

$$e = 1 - \exp\{NTU^{0.22}[\exp(-C\ NTU^{0.78}) - 1]\}/C \tag{2.59}$$

The Merkel number in the effectiveness-NTU method can be determined by

$$Me = \frac{C_{emin}}{m_w} NTU \tag{2.60}$$

If a Merkel number is known for a given fill, the number of transfer units (NTU) can be determined from Eq. (2.60). With the capacity, the effectiveness can be determined and water outlet temperature can be solved from the effectiveness, Eq. (2.56). When a Merkel number is to be determined from measured test data, the effectiveness is first determined from Eq. (2.56). The number of transfer units can then be solved from the effectiveness formulas and the Merkel number determined from Eq. (2.60).

2.7 Cross- and counterflow models with Poppe assumptions

Poppe and Rögener (1991) developed a way to predict the performance of fills without making the simplifying assumptions of Merkel. This approach is normally referred to as the Poppe method. Consider the following governing differential equation for a crossflow Poppe method with unsaturated air,

$$\frac{\partial G_w}{\partial z} = h_d a_{fi}(w_{sw} - w) \tag{2.61}$$

$$G_a \frac{\partial w}{\partial x} = h_d a_{fi}(w_{sw} - w) \tag{2.62}$$

$$\frac{\partial T_w}{\partial z} = \frac{h_d a_{fi}}{c_{pw} G_w} \left[(w_{sw} - w) c_{pw} T_w - B_{us}\right] \tag{2.63}$$

$$G_a \frac{\partial i_{ma}}{\partial x} = h_d a_{fi}(T_w - T_a)\ B_{us} \tag{2.64}$$

where,

$$B_{us} = i_{masw} - i_{ma} + \left(Le_f - 1\right)\left[i_{masw} - i_{ma} - i_v\ (w_{sw} - w)\right] \tag{2.65}$$

For supersaturated air the equations become,

$$\frac{\partial G_w}{\partial z} = h_d a_{fi}(w_{sw} - w_{sa}) \tag{2.66}$$

$$G_a \frac{\partial w}{\partial x} = h_d a_{fi}(w_{sw} - w_{sa}) \tag{2.67}$$

$$\frac{\partial T_w}{\partial z} = \frac{h_d a_{fi}}{c_{pw} G_w} \left[(w_{sw} - w_{sa}) c_{pw} T_w - B_{ss}\right] \tag{2.68}$$

$$G_a \frac{\partial i_{ma}}{\partial x} = h_d a_{fi}(T_w - T_a)\, B_{ss} \tag{2.69}$$

$$B_{ss} = i_{masw} - i_{ma,ss} + \left(Le_f - 1\right)\left[i_{masw} - i_{ma,ss} - i_v\,(w_{sw} - w_{sa})\right] + Le_f c_{pw} T_w (w - w_{sa}) \tag{2.70}$$

The main difference between this form of governing equation and the Reuter model in full crossflow is that it is derived fully in terms of air enthalpy instead of air temperature. A check must be made to determine whether the air is unsaturated or supersaturated, which requires an iterative procedure. The effort of solving these equations is therefore similar to when the governing equations in the Reuter model are solved with the air enthalpy, Eq. (2.21) and Eq. (2.36), and the air temperature iteratively determined. The governing equations for counterflow can be derived from the above crossflow equations by replacing ∂x with ∂z in the equation for enthalpy and humidity, thereby solving the air properties vertically instead of horizontally. The above governing differential equations can be solved with the same solution methods as the Reuter model.

The counterflow Poppe method has been presented in another form where the governing equations are derived in terms of water temperature as opposed to the spatial coordinates. Kloppers and Kröger (2005a) derive this form of the Poppe method, where governing equations for unsaturated air are presented as,

$$\frac{m_w}{m_a} = \frac{m_{wi}}{m_a}\left(1 - \frac{m_a}{m_{wi}}(w_o - w)\right) \tag{2.71}$$

$$\frac{dw}{dT_w} = \frac{c_{pw}\frac{m_w}{m_a}(w_{sw} - w)}{B_{us} - (w_{sw} - w)c_{pw}T_w} \tag{2.72}$$

$$\frac{di_{ma}}{dT_W} = \frac{m_w c_{pw}}{m_a}\left[1 + \frac{(w_{sw} - w)c_{pw}T_w}{B_{us} - (w_{sw} - w)c_{pw}T_w}\right] \tag{2.73}$$

$$\frac{dMe_p}{dT_w} = \frac{c_{pw}}{B_{us} - (w_{sw} - w)c_{pw}T_w} \tag{2.74}$$

where B_{us} is according to Eq. (2.65). For supersaturated air the governing equations are,

$$\frac{m_w}{m_a} = \frac{m_{wi}}{m_a}\left(1 - \frac{m_a}{m_{wi}}(w_o - w_{sa})\right) \tag{2.75}$$

$$\frac{dw}{dT_w} = \frac{c_{pw}\frac{m_w}{m_a}(w_{sw} - w_{sa})}{B_{ss}} \tag{2.76}$$

$$\frac{di_{ma}}{dT_W} = \frac{m_w c_{pw}}{m_a}\left[1 + \frac{(w_{sw} - w_{sa})c_{pw}T_w}{B_{ss}}\right] \tag{2.77}$$

$$\frac{dMe_p}{dT_w} = \frac{c_{pw}}{B_{ss}} \tag{2.78}$$

$$B_{ss} = i_{masw} - i_{ss} + \left(Le_f - 1\right)\left[\begin{matrix} i_{masw} - i_{ss} - (w_{sw} - w_{sa})i_v + \\ (w - w_{sa})c_{pw}T_w \end{matrix}\right] + (w - w_{sw})c_{pw}T_w \tag{2.79}$$

Note that B_{ss} is not the same as before. These governing equations can be solved numerically by dividing the inlet-outlet water temperature difference in to intervals or cells. Kloppers and Kröger (2005a) present a detailed discretization for solving the equations by 4th order Runge-Kutta numerical scheme. Discretization with 4th order Runge-Kutta method is presented and discussed in Chapter 3.

2.8 Model comparison

Kröger (2004) presents two sample calculations for an expanded metal fill (trickle fill) in a wet-cooling tower counterflow test facility where Merkel numbers are determined by the Merkel method and the e-NTU method of analysis. Measured parameters for the test case are given in Table 2.1.

This case has a measured cooling range of $\Delta T_w = 11.90$°C and Merkel numbers per meter fill height of $Me/L_{fi} = 0.365$ m^{-1} using the Merkel equation and $Me/L_{fi} = 0.361$ m^{-1} using the e-NTU method. Kloppers (2003) uses the same case for a sample calculation of the counterflow Poppe method, with a 4th order Runge-Kutta numerical scheme, as well as giving crossflow Merkel numbers and outlet conditions for e-NTU, Merkel and Poppe method. This particular case can therefore be verified and is used to illustrate differences from using the Reuter model with Merkel and Poppe approaches.

Table 2.1: Measured data for an expanded metal fill (Kröger, 2004)

Measured conditions		
Atmospheric pressure (p_a)	101712	N/m^2
Air inlet temperature (T_{ai})	9.70	°C
Air inlet temperature (T_{wb})	8.23	°C
Dry air mass flow rate (m_a)	4.134	kg/s
Water inlet temperature (T_{wi})	39.67	°C
Water outlet temperature (T_{wo})	27.77	°C
Water mass flow rate (m_w)	3.999	kg/s
Static pressure drop across fill	4.5	N/m^2
Fill height (L_{fi})	1.878	m
Fill length and depth	1.5	m

Table 2.2 gives the Merkel numbers per meter fill height for this particular case in cross- and counterflow for the Merkel, e-NTU, Poppe and Reuter model.

Table 2.2: Cross- and counterflow Merkel numbers per meter fill height obtained by the e-NTU, Merkel, Poppe and the Reuter model

Method	e-NTU	Merkel	Poppe	Reuter model	
				with Merkel $\beta_{Me} = 1, Le_f = 1$	with Poppe $\beta_{Me} = 0, Le_f =$ Bosjn.
Counterflow	0.361	0.365	0.392	0.364	0.391
Crossflow	0.394	0.395	0.427	0.394	0.425

To obtain a Merkel number from the Reuter model with Merkel assumptions, the evaporation is neglected ($\beta_{Me} = 1$) in the governing equations for water temperature, Eq. (2.52), and the Lewis factor is equal to unity ($Le_f = 1$). For Poppe assumptions the evaporation is not neglected ($\beta_{Me} = 0$) and the Bosnjakovic relation is used for the Lewis factor. To vary between cross and counterflow the inlet air flow angle is varied from 0° for crossflow and 90° for counterflow. The Merkel numbers obtained correspond well with Merkel numbers determined by the other methods.

The e-NTU and Merkel method determine outlet conditions of the air by assuming the air leaving the fill is saturated. Temperature and humidity are therefore determined by applying this assumption to the enthalpy of the outlet air stream. The Poppe and Reuter model do not make this assumption and solve unsaturated or supersaturated governing equations. Table 2.3 and 2.4 give the difference in air properties across the fill for different methods and approaches with the Merkel numbers obtained in Table 2.2.

Table 2.3: Counterflow results for air properties using the e-NTU, Merkel, Poppe and Reuter models

Method	e-NTU	Merkel	Poppe	Reuter model with Merkel $\beta_{Me} = 1, Le_f = 1$	Reuter model with Poppe $\beta_{Me} = 0, Le_f =$ Bosjn.
Me/L_{fi}, m^{-1}	0.361	0.365	0.392	0.364	0.391
ΔT_a, °C	14.58	14.58	15.00	14.45	14.97
Δw, kg/kg	0.01305	0.01305	0.01535	0.01422	0.01516

Table 2.4: Crossflow results for air properties using the e-NTU, Merkel, Poppe and Reuter models

Method	e-NTU	Merkel	Poppe	Reuter model with Merkel $\beta_{Me} = 1, Le_f = 1$	Reuter model with Poppe $\beta_{Me} = 0, Le_f =$ Bosjn.
Me/L_{fi}, m^{-1}	0.394	0.395	0.427	0.394	0.426
ΔT_a, °C	14.58	14.60	14.85	14.25	14.80
Δw, kg/kg	0.01305	0.01308	0.01521	0.01430	0.01522

It can be seen from Tables 2.3 and 2.4 that the difference between the Poppe method and the Reuter model with Poppe assumptions is insignificant. Whereas the Merkel and e-NTU methods have a significant difference in air temperature and humidity compared with the Reuter model with both the Poppe and Merkel assumptions. The difference is caused by the equation describing rate of change in water temperature being adjusted for Merkel assumptions, but equations for rate of change in water mass flow, air temperature and humidity. The energy balance for the Poppe assumptions is 0.3% whereas, it is -4.7% for the Merkel assumptions. Despite this difference there is a small difference in water cooling. It should be noted that theoretically the Poppe method should give perfect energy balance. The energy balance is not 0% mainly because fluid properties in the models are calculated from empirical equations, and second order terms are neglected.

Accurate predictions of air outlet temperature are usually only important when hybrid systems are considered. The humidity is equally important for hybrid and normal cooling towers to predict total evaporation from the water stream. Predicting the humidity accurately is therefore very important to determine the amount of makeup water needed. The Reuter model with Merkel assumptions predicts humidity closer to the Poppe method than the e-NTU and Merkel method.

From Tables 2.3 and 2.4 it can be seen that differences in Merkel numbers and outlet conditions between the e-NTU and Merkel method and Reuter model with

corresponding assumptions is small. One way of determining the effects of this difference is to use Merkel numbers obtained by the e-NTU, Merkel and Poppe methods directly in the Reuter model to determine outlet conditions. Tables 2.5 and 2.6 give the resulting difference in properties for the case in Table 2.1.

Table 2.5: Counterflow results using the Reuter model with Merkel numbers obtained by the e-NTU, Merkel and Poppe models

Method	with Merkel assumptions		with Poppe assumptions
	(e-NTU)	(Merkel eq.)	(Poppe Method)
Me/L_{fi}, m^{-1}	0.361	0.365	0.392
ΔT_w, °C	11.85	11.92	11.92
ΔT_a, °C	14.40	14.48	14.99
Δw, kg/kg	0.01417	0.01425	0.01518

Table 2.6: Crossflow results using the Reuter model with Merkel numbers obtained by the e-NTU, Merkel and Poppe models

Method	with Merkel assumptions		with Poppe assumptions
	(e-NTU)	(Merkel eq.)	(Poppe Method)
Me/L_{fi}, m^{-1}	0.394	0.395	0.427
ΔT_w, °C	11.91	11.92	11.91
ΔT_a, °C	14.26	14.27	14.84
Δw, kg/kg	0.01431	0.01432	0.01521

Tables 2.5 and 2.6 show that Merkel numbers obtained by a different method can be used directly in Reuter model and predict the same performance. To determine if this applies for different conditions than given in Table 2.1, Merkel numbers are determined with the Merkel, e-NTU, Poppe and Reuter methods for a series of experiments presented in Appendix B. A curve is fitted through the results with Eq. (2.45). Figures 2.2 and 2.3 show Merkel numbers per meter fill using the correlations obtained for the different methods. The curve fit constants, correlation and plot with curve fit and experimental data for all the methods are given in Appendix B.

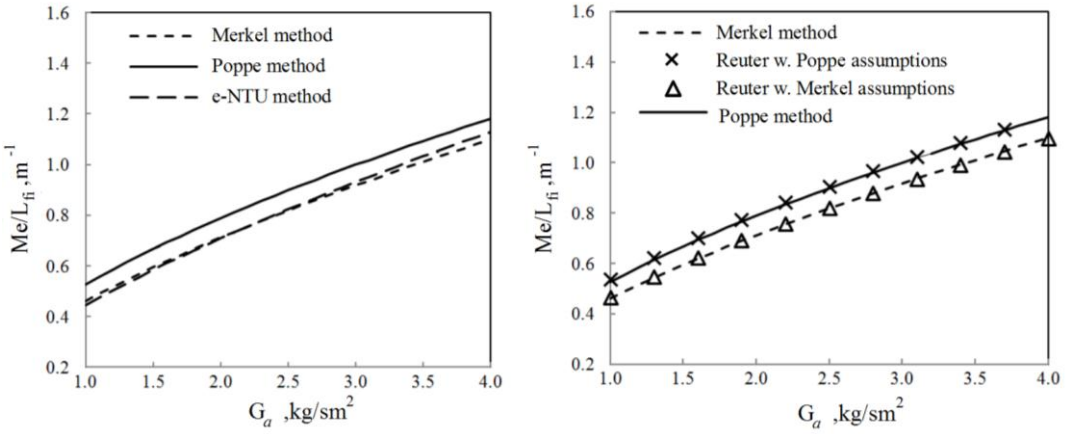

(a) e-NTU, Merkel and Poppe

(b) Merkel, Poppe and Reuter model

Figure 2.2: Performance curves for a trickle fill in counterflow configuration with G_w = 3 kg/m^{2}s and T_{wi} = 40°C

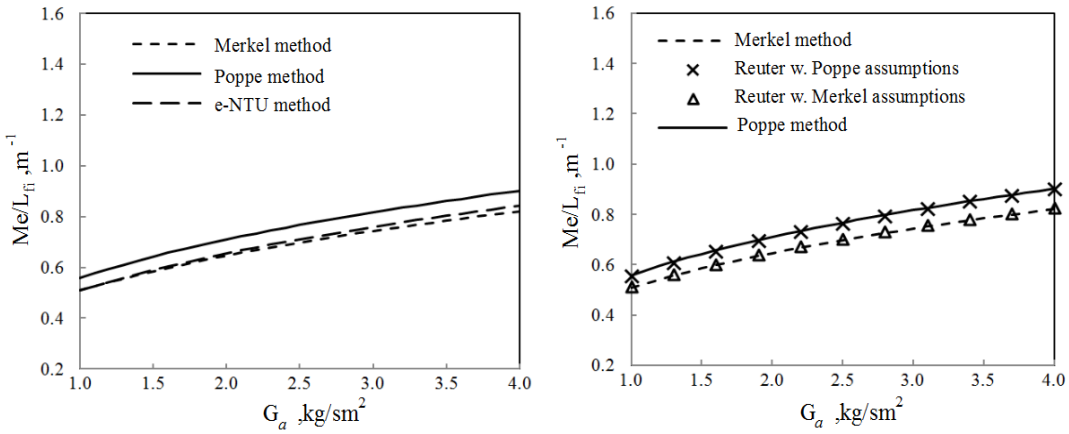

(a) e-NTU, Merkel and Poppe Methods

(b) Merkel, Poppe and Reuter model

Figure 2.3: Performance curves for a trickle fill in crossflow configuration with G_w = 3 kg/s m^2 and T_{wi} = 40°C

The Merkel and Poppe give the same results as the Reuter model with Merkel and Poppe assumptions. The e-NTU method gives a similar result as the Merkel method and Reuter model with Merkel assumptions. The difference between the e-NTU and Merkel increases as the air flow increases. When the airflow becomes two and a half times the water flow the difference between the two starts to increase, see performance graphs in Appendix B. When this is the case, Merkel numbers from the e-NTU method should be used with caution and cannot always be expected to give the same or similar results as the Merkel method or the Reuter model with Merkel assumptions.

2.9 Conclusion and summary

The Reuter model is derived for unsaturated and supersaturated air for a rectangular cooling tower fill. Governing equations for the cross- and counterflow Merkel methods as well as cross-counterflow Merkel method are given. Necessary changes to the derivation by Reuter, to predict performance equivalent to the Merkel method are given. Descriptions of cross and counterflow e-NTU and Poppe methods are presented.

Sample case by Kröger (2004) is presented to illustrate the differences in predicting outlet conditions and performance with these different methods for cross and counterflow. Differences in Merkel numbers are given with varying air flow rate and constant water inlet conditions where the Merkel numbers were determined using curve fit equations obtained from experimental test data presented in Appendix B.

Main results from employing the different methods were the following:

- If the appropriate assumptions are made, the Reuter model results in the same Merkel number and outlet water temperature as the Merkel and e-NTU methods for cross- and counterflow.

- For the same Lewis factor the Reuter model results in the same Merkel number and outlet conditions of water and air as the Poppe method for cross- and counterflow.

- Outlet conditions of air determined by the Reuter model with Merkel approach will not be the same as for the Merkel and e-NTU method.

- The e-NTU method gives the same result as the Reuter model with Merkel assumptions for most cases. In some cases the e-NTU method can differ significantly, particularly when the airflow rate is two to three times the water flow rate. This is not the case for the Merkel method, as it gives consistently the same result as the Reuter model with Merkel assumptions

The Merkel method has been around for a long time and is relatively simple for a counterflow case. Therefore, extensive information exists for performance prediction for different fill materials. The same applies for the e-NTU method except it is equally simple for cross- and counterflow. Therefore, information on performance prediction exists for both counter- and crossflow. The traditional Poppe methods are more complex, similar to the Reuter method and less information exists on performance prediction with the Poppe method. The Reuter model is new and no information is available where the Reuter model is applied directly. New experiment for various different cooling tower fill materials would be time consuming and expensive. As has been shown with a comparison, the cross-counterflow model can use transfer characteristics obtained with Merkel or Poppe method if the right assumption and modification are made.

3 SOLVING THE GOVERNING DIFFERENTIAL EQUATION OF HEAT AND MASS TRANSFER IN WET-COOLING TOWER FILLS

3.1 Introduction

The governing partial differential equations describing the heat and mass transfer in wet cooling towers can be solved with finite differences. The methods of Merkel, Poppe and Reuter have all been presented with specific solution methods. The Merkel equation is in the form of an integral and is commonly solved with Chebychev numerical integration (Merkel, 1925 and Kröger, 2004). The crossflow Merkel method is in the form of two differential equations and has been solved with a first order backward differencing scheme (Zivi and Brand, 1956 and Kloppers, 2003). The same applies for the crossflow Poppe method except here four equations are solved (Kloppers, 2003). The counterflow Poppe method was presented by Kröger and Kloppers (2005a) with a 4^{th} order Runge-Kutta method differencing scheme. The Runge-Kutta method is of 4^{th} order and gives considerably better accuracy in terms of grid dependence compared to the a first order method. First order differencing methods are often chosen for multi-dimensional problems because they are relatively easy to implement. Reuter (2010) presents the cross-counterflow model with a first order upwind differencing scheme where the properties in each control volume or cell are determined in the cell centre. This approach can be used with meshes created and used by CFD software packages such as ANSYS-*Fluent*®.

Reuter (2010) gives a discretized form of the governing differential equation for unsaturated air. In this section the governing differential equations are given with first and second order upwind differences for unsaturated and supersaturated air. Procedures to solve the system of discretized governing equations are given, as well as methods to avoid numerical instabilities. Grid independence and convergence is analysed for different cases and guidelines are given for solving the Reuter method. Solution of other traditional fill performance methods are discussed where numerical accuracy is compared to the first and second order upwind differencing scheme.

3.2 Discretization of the governing partial differential equations

To solve the governing partial differential equations of heat and mass transfer in a cross-counterflow wet cooling tower fill, the equations are discretized and gradient in the cell are described with source terms (Versteeg, 2007). Consider the governing differential equations or gradients for unsaturated air as source terms in the following form,

$$S_{Gw} = \frac{\partial G_w}{\partial z} = G_w \left(\frac{Me}{L_{fi}}\right) (w_{sw} - w) \tag{3.1}$$

$$S_{Tw} = \frac{\partial T_w}{\partial z} = \left(\frac{Me}{L_{fi}}\right)\frac{c_{pma}}{c_{pw}}\left[Le_f(T_w - T_a) + \frac{i_{fg(T_w)} + \beta_{Me}c_{pw}T_w}{c_{pma}}(w_{sw} - w)\right] \tag{3.2}$$

$$S_w = G_{a,z}\frac{\partial w}{\partial z} + G_{a,x}\frac{\partial w}{\partial x} = G_w\left(\frac{Me}{L_{fi}}\right)(w_{sw} - w) \tag{3.3}$$

$$S_{Ta} = G_{a,x}\frac{\partial T_a}{\partial x} + G_{a,z}\frac{\partial T_a}{\partial z} = G_w\left(\frac{Me}{L_{fi}}\right)(T_w - T_a)\left[Le_f + \frac{c_{pv}}{c_{pma}}(w_{sw} - w)\right] \tag{3.4}$$

$$S_{ima} = G_{a,x}\frac{\partial i_{ma}}{\partial x} + G_{a,z}\frac{\partial i_{ma}}{\partial z} = G_w\left(\frac{Me}{L_{fi}}\right)\left[Le_f c_{pma}(T_w - T_a) + i_{v(T_w)}(w_{sw} - w)\right] \tag{3.5}$$

When the air in the fill becomes supersaturated the source terms become,

$$S_{Gw,ss} = \frac{\partial G_w}{\partial z} = G_w\left(\frac{Me}{L_{fi}}\right)(w_{sw} - w_{sa}) \tag{3.6}$$

$$S_{Tw,ss} = \frac{\partial T_w}{\partial z} = \left(\frac{Me}{L_{fi}}\right)\frac{c_{pma}}{c_{pw}}\left[Le_f(T_w - T_a) + \frac{i_{fg(T_w)} + \beta_{Me}c_{pw}T_w}{c_{pma}}(w_{sw} - w_{sa})\right] \tag{3.7}$$

$$S_{w,ss} = G_{a,z}\frac{\partial w}{\partial z} + G_{a,x}\frac{\partial w}{\partial x} = G_w\left(\frac{Me}{L_{fi}}\right)(w_{sw} - w_{sa}) \tag{3.8}$$

$$S_{ima,ss} = G_{a,x}\frac{\partial i_{ma}}{\partial x} + G_{a,z}\frac{\partial i_{ma}}{\partial z} = G_w\left(\frac{Me}{L_{fi}}\right)\left[Le_f c_{pma}(T_w - T_a) + i_{v(T_w)}(w_{sw} - w_{sa})\right] \tag{3.9}$$

$$S_{Ta,ss} = G_{a,x}\frac{\partial T_a}{\partial x} + G_{a,z}\frac{\partial T_a}{\partial z} = (S_1 + S_2 - S_3) \tag{3.10}$$

where S_1, S_2 and S_3 are,

$$S_1 = G_w \left(\frac{Me}{L_{fi}}\right)\left[Le_f\ (T_w - T_a)\frac{c_{pma}}{c_{pma,ss}}\right] \tag{3.11}$$

$$S_2 = G_w \left(\frac{Me}{L_{fi}}\right)\left[\frac{i_{fg(T_w)} + c_{pw}(T_w - T_a)}{c_{pma,ss}}\right] \tag{3.12}$$

$$S_3 = \frac{i_{fg(T_a)}}{c_{pma,ss}}\left[G_{a,x}\frac{\partial w_{sa}}{\partial x} + G_{a,z}\frac{\partial w_{sa}}{\partial z}\right] \tag{3.13}$$

To solve the discrete form of the governing differential equations the cooling tower fill area is discretized into control volumes or cells for a computational domain, see Figure 3.1.

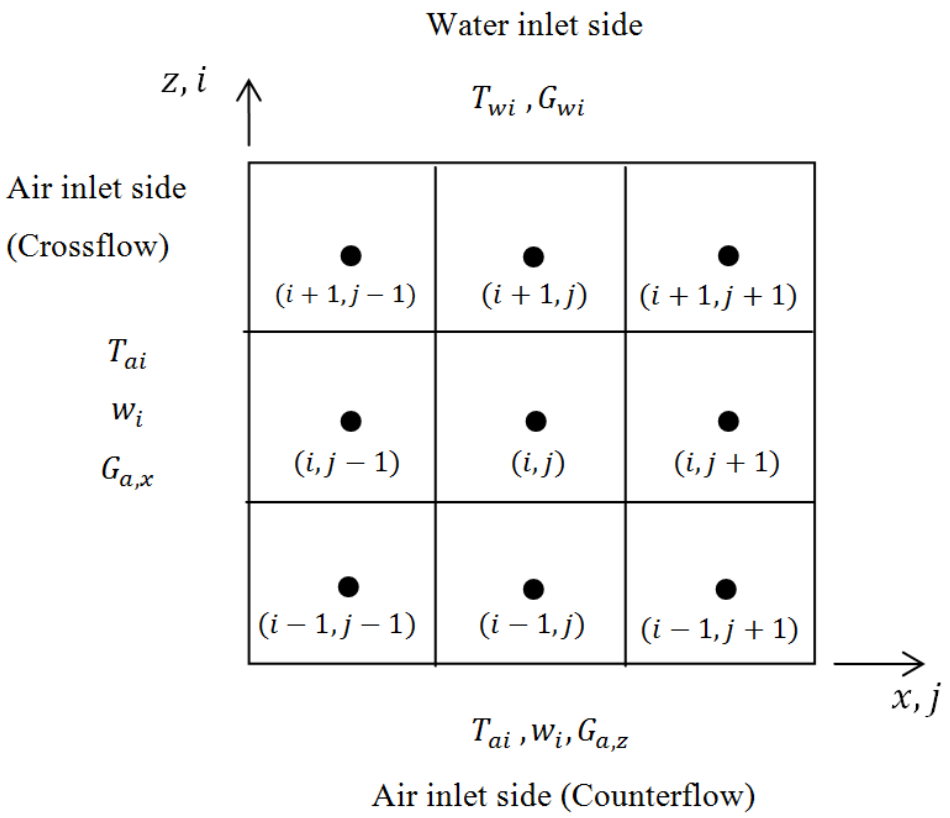

Figure 3.1: Computational domain for a cross-counterflow fill.

When a computational domain has been defined, the change in water and air properties can be approximated by employing finite differences. Where the gradient of a property φ over cell (i, j) can be approximated accordingly,

$$\frac{\partial \varphi_{(i,j)}}{\partial x} \approx \frac{\varphi_{e(i,j)} - \varphi_{w(i,j)}}{\Delta x} \tag{3.14}$$

$$\frac{\partial \varphi_{(i,j)}}{\partial z} \approx \frac{\varphi_{n(i,j)} - \varphi_{s(i,j)}}{\Delta z} \tag{3.15}$$

where $\varphi_{e(i,j)}$, $\varphi_{w(i,j)}$, $\varphi_{n(i,j)}$ and $\varphi_{s(i,j)}$ are the values of φ at the east, west, north and south faces of cell (i,j).

3.2.1 First order upwind differencing scheme

With first order differences the value of φ at the cell faces can be approximated from the central or nodal values of φ in cell (i,j) and its neighbouring cells. With the first order upwind a property at the downstream cell face with the value in the cell and the upstream face with the value in the upstream cell can be approximated accordingly (Versteeg, 2007),

$$\varphi_{e(i,j)} \approx \varphi_{n(i,j)} \approx \varphi_{(i,j)} \tag{3.16}$$

$$\varphi_{w(i,j)} \approx \varphi_{(i,j-1)} \tag{3.17}$$

$$\varphi_{s(i,j)} \approx \varphi_{(i-1,j)} \tag{3.18}$$

Substituting Eq. (3.16), (3.17) and (3.18) into Eq. (3.14) and (3.15) gives,

$$\frac{\partial \varphi_{(i,j)}}{\partial x} \approx \frac{\varphi_{(i,j)} - \varphi_{(i,j-1)}}{\Delta x} \tag{3.19}$$

$$\frac{\partial \varphi_{(i,j)}}{\partial z} \approx \frac{\varphi_{(i,j)} - \varphi_{(i,j-1)}}{\Delta z} \tag{3.20}$$

Reuter (2010) derives and uses the same method for the first order upwind differencing scheme to solve the governing differential equations.

The system of equations can be solved by replacing the properties with φ. The water properties only change vertically in z direction and can be discretized by means of equation (3.20) only,

$$\frac{\partial G_w}{\partial z} \approx \frac{G_{w(i,j)} - G_{w(i-1,j)}}{\Delta z} = S_{Gw(i,j)} \tag{3.21}$$

From the above equation a discrete form of the governing differential equations for water flow rate can be written as,

$$G_{w(i,j)} = G_{w(i-1,j)} + S_{Gw(i,j)}\,\Delta z \tag{3.22}$$

The governing equation for the water temperature can be discretized similarly to obtain

$$T_{w(i,j)} = T_{w(i-1,j)} + S_{Tw(i,j)}\,\Delta z \tag{3.23}$$

The air properties are subjected to change both horizontally and vertically, they therefore have to be discretized with Eq. (3.19) and (3.20). The governing differential equations for the air side properties can be written in the following discretized form,

$$T_{a(i,j)} = \frac{G_{a,x}T_{a(i,j-1)}\,\dfrac{\Delta z}{\Delta x} + G_{a,z}T_{a(i-1,j)} + S_{Ta(i,j)}\Delta z}{G_{a,x}\dfrac{\Delta z}{\Delta x} + G_{a,z}} \tag{3.24}$$

$$w_{(i,j)} = \frac{G_{a,x}w_{(i,j-1)}\,\dfrac{\Delta z}{\Delta x} + G_{a,z}w_{(i-1,j)} + S_{w(i,j)}\Delta z}{G_{a,x}\dfrac{\Delta z}{\Delta x} + G_{a,z}} \tag{3.25}$$

$$i_{ma(i,j)} = \frac{G_{a,x}\,i_{ma(i,j-1)}\,\dfrac{\Delta z}{\Delta x} + G_{a,z}\,i_{ma(i-1,j)} + S_{ima(1,1)}\,\Delta z}{G_{a,x}\dfrac{\Delta z}{\Delta x} + G_{a,z}} \tag{3.26}$$

When the system of equations is solved a check must be made to determine whether the air in cell (i,j) is unsaturated or supersaturated to choose the relevant source term. In the source term equation for temperature of supersaturated air ($S_{Ta,ss}$) the part of the equation defined as S_3 contains gradient terms for saturated humidity of air ($\partial w_{sa}/\partial x$ and $\partial w_{sa}/\partial z$). The saturated humidity of the air is only a function of air temperature and pressure and is determined from empirical equations for thermophysical properties. The gradient can be calculated by the difference in saturated humidity as a function of the difference in the air temperature and pressure between cell (i,j) and its neighbouring cell,

$$S_{3(i,j)} = \frac{i_{fg(T_a)}}{c_{pma,ss}}\left[G_{a,x}\frac{\Delta z}{\Delta x}\left(w_{sa(i,j)} - w_{sa(i,j-1)}\right) + G_{a,z}\left(w_{sa(i,j)} - w_{sa(i-1,j)}\right)\right] \tag{3.27}$$

Properties are calculated for the cell centre and boundaries are discretized separately. At the boundary of the computational domain the property at the face is $\varphi_{f(i,j)} = \varphi_{BC}$ and the gradient is over half the cell. Eq. (3.19) and (3.20) can now be written as,

$$\frac{\partial \varphi}{\partial x} \approx \frac{(\varphi_{(i,j)} - \varphi_{BC})}{\Delta x/2} \tag{3.28}$$

$$\frac{\partial \varphi}{\partial z} \approx \frac{(\varphi_{(i,j)} - \varphi_{BC})}{\Delta z/2} \tag{3.29}$$

On the water side boundary, separate discretization is only needed for cells $(1, j)$,

$$G_{w(1,j)} = G_{wo} + \frac{S_{Gw(1,j)}}{2}\Delta z \tag{3.30}$$

$$T_{w(1,j)} = T_{wo} + \frac{S_{Tw(1,j)}}{2}\Delta z \tag{3.31}$$

On the air side, separate boundary discretization is needed for cells (1,1), $(1, j)$ and $(i, 1)$. For the humidity the discretized equations become,

$$w_{(1,1)} = w_i + \frac{S_{w(1,1)}\,\Delta z}{2\,G_{a,x}\frac{\Delta z}{\Delta x} + 2\,G_{a,z}} \tag{3.32}$$

$$w_{(1,j)} = \frac{G_{a,x}w_{(i,j-1)}\frac{\Delta z}{\Delta x} + 2\,G_{a,z}w_i + S_{w(1,j)}\,\Delta z}{G_{a,x}\frac{\Delta z}{\Delta x} + 2\,G_{a,z}} \tag{3.33}$$

$$w_{(i,1)} = \frac{2\,G_{a,x}w_i\frac{\Delta z}{\Delta x} + G_{a,z}w_{(i-1,j)} + S_{w(i,1)}\Delta z}{2\,G_{a,x}\frac{\Delta z}{\Delta x} + G_{a,z}} \tag{3.34}$$

For the air temperature they become,

$$T_{a(1,1)} = T_{ai} + \frac{S_{Ta(1,1)}\Delta z}{2\,G_{a,x}\frac{\Delta z}{\Delta x} + 2\,G_{a,z}} \tag{3.35}$$

$$T_{a(1,j)} = \frac{G_{a,x}T_{a(i,j-1)}\frac{\Delta z}{\Delta x} + 2\,G_{a,z}T_{ai} + S_{Ta(1,1)}\Delta z}{G_{a,x}\frac{\Delta z}{\Delta x} + 2\,G_{a,z}} \tag{3.36}$$

$$T_{a(i,1)} = \frac{2\,G_{a,x}T_{ai}\frac{\Delta z}{\Delta x} + G_{a,z}T_{a(i-1,j)} + S_{Ta(1,1)}\Delta z}{G_{a,x}\frac{\Delta z}{\Delta x} + 2\,G_{a,z}} \tag{3.37}$$

where the S_3 term in the air temperature source term at the boundaries is,

$$S_{3(1,1)} = \frac{i_{fg(T_a)}}{c_{pma,ss}}\left[2\,G_{a,x}\frac{\Delta z}{\Delta x}\left(w_{sa(i,j)} - w_{sai}\right) + 2\,G_{a,z}\left(w_{sa(i,j)} - w_{sai}\right)\right] \tag{3.38}$$

$$S_{3(1,j)} = \frac{i_{fg(T_a)}}{c_{pma,ss}}\left[G_{a,x}\frac{\Delta z}{\Delta x}\left(w_{sa(i,j)} - w_{sa(i,j-1)}\right) + 2\,G_{a,z}\left(w_{sa(i,j)} - w_{sai}\right)\right] \tag{3.39}$$

$$S_{3(i,1)} = \frac{i_{fg(T_a)}}{c_{pma,ss}}\left[2\,G_{a,x}\frac{\Delta z}{\Delta x}\left(w_{sa(i,j)} - w_{sai}\right) + G_{a,z}\left(w_{sa(i,j)} - w_{sa(i-1,j)}\right)\right] \tag{3.40}$$

The discretized equations for air enthalpy at the boundaries become,

$$i_{ma(1,1)} = i_{mai} + \frac{S_{ima(1,1)}}{2\,G_{a,x}\frac{\Delta z}{\Delta x} + 2\,G_{a,z}}\Delta z \tag{3.41}$$

$$i_{ma(1,j)} = \frac{G_{a,x}\,i_{ma(i,j-1)}\frac{\Delta z}{\Delta x} + 2\,G_{a,z}\,i_{mai} + S_{ima(1,j)}\Delta z}{G_{a,x}\frac{\Delta z}{\Delta x} + 2\,G_{a,z}} \tag{3.42}$$

$$i_{ma(i,1)} = \frac{2\,G_{a,x}\,i_{mai}\frac{\Delta z}{\Delta x} + G_{a,z}\,i_{ma(i-1,j)} + S_{ima(i,1)}\Delta z}{2\,G_{a,x}\frac{\Delta z}{\Delta x} + G_{a,z}} \tag{3.43}$$

3.2.2 Second order linear upwind differencing scheme

The first order differencing scheme is relatively easy to implement and understand. Accuracy is often limited for first order method, because it needs relatively small cell sizes to obtain acceptable grid independence. For improved numerical accuracy better grid independence, higher order differencing schemes can be considered. To obtain a second order differencing scheme, properties at the faces of the cell are approximated by both the property in the cell and its gradient (ANSYS-*Fluent*® v13.0 - *Theory Guide*, 2011),

$$\varphi_f = \varphi + \Delta\varphi = \varphi_{(i)} + \frac{\varphi_{(i)} - \varphi_{(i-1)}}{2} \tag{3.44}$$

With second order upwind the property at the downstream face (φ_e and φ_s) is approximated from the property and gradient in cell (i,j), and the property at the upstream face (φ_w and φ_n) with the properties and gradients in cells $(i-1,j)$ and $(i,j-1)$. By substituting Eq. (3.44) into Eq. (3.14) and (3.15) the following discrete equations can be obtained,

$$\frac{\partial \varphi}{\partial x} \approx \frac{3\,\varphi_{(i,j)} - 4\,\varphi_{(i,j-1)} + \varphi_{(i,j-2)}}{2\Delta x} \tag{3.45}$$

$$\frac{\partial \varphi}{\partial z} \approx \frac{3\,\varphi_{(i,j)} - 4\,\varphi_{(i-1,j)} + \varphi_{(i-2,j)}}{2\Delta z} \tag{3.46}$$

Water side equations only change vertically in z direction and can be written as follows,

$$S_\varphi = \frac{\partial \varphi}{\partial z} \approx \frac{3\,\varphi_{(i,j)} - 4\,\varphi_{(i-1,j)} + \varphi_{(i-2,j)}}{2\Delta z} \tag{3.47}$$

From the above equations the properties of water in cell (i,j) can be written as,

$$\varphi_{(i,j)} = \frac{4\varphi_{(i-1,j)} - \varphi_{(i-2,j)} + 2\,S_{\varphi(i,j)}\Delta z}{3} \tag{3.48}$$

where φ represent either the water temperature (T_w) or flow rate (G_w). On the air side the equations for humidity, temperature and enthalpy can be written as,

$$\varphi_{(i,j)} = \frac{G_{a,x}\frac{\Delta z}{\Delta x}\left(4\,\varphi_{(i,j-1)} - \varphi_{(i,j-2)}\right) + G_{a,z}\left(4\,\varphi_{(i-1,j)} - \varphi_{(i-2,j)}\right) + S_{\varphi(i,j)}\Delta z}{3\,\left(G_{a,x}\frac{\Delta z}{\Delta x} + G_{a,z}\right)} \tag{3.49}$$

where φ can represent either the humidity (w), air temperature (T_a) or enthalpy (i_{ma}).

Three points are used for approximation in the second order method and therefore, boundary discretization is required for cells at the boundary and their neighbouring cells. For the cells next to the boundary the gradient approximation is the same as for the first order method, using Eq. (3.28) and (3.29). For the cells neighbouring the cell at the boundary, the point outside the domain can be approximated accordingly,

$$\varphi_0 = 2\,\varphi_{BC} - \varphi_{(i,j)} \tag{3.50}$$

Insert Eq. (3.50) into Eq. (3.45) and (3.46) and get,

$$\frac{\partial \varphi_{(i,j)}}{\partial x} \approx \frac{3\,\varphi_{(i,j)} - 5\,\varphi_{(i,j-1)} + 2\,\varphi_{BC}}{2\Delta x} \tag{3.51}$$

$$\frac{\partial \varphi_{(i,j)}}{\partial z} \approx \frac{3\,\varphi_{(i,j)} - 5\,\varphi_{(i-1,j)} + 2\,\varphi_{BC}}{2\Delta z} \tag{3.52}$$

On the water side, cells $(1,j)$ employ the same boundary discretization as the first order method, and cells $(2,j)$ are discretized as,

$$\varphi_{(2,j)} = \frac{5\,\varphi_{(1,j)} - 2\,\varphi_{BC} + S_{\varphi(2,j)}\Delta z}{3} \tag{3.53}$$

On the air side, separate boundary discretization is needed for cells $(1,1),(1,2),(2,1),(2,2),(i,1),(1,j),(i,2)$ and $(j,2)$ where $i > 2$ and $j > 2$. Cell $(1,1)$ is the same as for the first order method. Using Eq. (3.28), (3.29), (3.51) and (3.52), cells $(1,2)$ and $(2,1)$ can be discretized in the following form,

$$\varphi_{(2,1)} = \frac{(5/2)G_{a,z}\,\varphi_{(1,1)} + \left(2\,G_{a,x}\frac{\Delta z}{\Delta x} - G_{a,z}\right)\varphi_{BC} + S_{\varphi(2,1)}\Delta z}{2\,G_{a,x} + (3/2)\,G_{a,z}} \tag{3.54}$$

$$\varphi_{(1,2)} = \frac{(5/2)G_{a,x}\frac{\Delta z}{\Delta x}\varphi_{(1,1)} - \left(G_{a,x}\frac{\Delta z}{\Delta x} - 2\,G_{a,z}\right)\varphi_{BC} + S_{\varphi(2,1)}\Delta z}{(3/2)\,G_{a,x}\frac{\Delta z}{\Delta x} + 2\,G_{a,z}} \tag{3.55}$$

and for cell $(2,2)$ the discrete equations can be written as,

$$\varphi_{(2,2)} = \frac{5G_{a,x}\frac{\Delta z}{\Delta x}\varphi_{(2,1)} + 5G_{a,z}\,\varphi_{(1,2)} - 2\left(G_{a,x}\frac{\Delta z}{\Delta x} + G_{a,z}\right)\varphi_{BC} + 2\,S_{\varphi(2,1)}\Delta z}{3\left(G_{a,x}\frac{\Delta z}{\Delta x} + G_{a,z}\right)} \tag{3.56}$$

For cells $(i,1)$ and $(1,j)$ the equations become,

$$\varphi_{(i,1)} = \frac{2G_{a,z}\,\varphi_{(i-1,1)} - (1/2)G_{a,z}\,\varphi_{(i-2,1)} + 2\,G_{a,x}\frac{\Delta z}{\Delta x}\,\varphi_{BC} + 2\,S_{\varphi(i,1)}\Delta z}{2\,G_{a,x} + (3/2)\,G_{a,z}} \tag{3.57}$$

$$\varphi_{(1,j)} = \frac{2G_{a,x}\frac{\Delta z}{\Delta x}\varphi_{(1,j-1)} - (1/2)\,G_{a,x}\frac{\Delta z}{\Delta x}\,\varphi_{(1,j-2)} + 2\,G_{a,z}\,\varphi_{BC} + 2\,S_{\varphi(1,j)}\Delta z}{(3/2)\,G_{a,x}\frac{\Delta z}{\Delta x} + 2\,G_{a,z}} \tag{3.58}$$

and for cells $(i,2)$ and $(2,j)$ they become,

$$\varphi_{(i,2)} = \frac{5\,G_{a,x}\frac{\Delta z}{\Delta x}\varphi_{(i-1,1)} - 2\,G_{a,x}\frac{\Delta z}{\Delta x}\varphi_{BC}}{3\left(G_{ax}\frac{\Delta z}{\Delta x} + G_{az}\right)} + \frac{4G_{az}\,\varphi_{(i-1,2)} - G_{az}\varphi_{(j-1,2)}}{3\left(G_{ax}\frac{\Delta z}{\Delta x} + G_{az}\right)} + \frac{2\,S_{\varphi(i,2)}\Delta z}{3\left(G_{ax}\frac{\Delta z}{\Delta x} + G_{az}\right)} \tag{3.59}$$

$$\varphi_{(2,j)} = \frac{4\,G_{a,x}\frac{\Delta z}{\Delta x}\varphi_{(2,j-1)} - G_{a,x}\frac{\Delta z}{\Delta x}\varphi_{(2,j-2)}}{3\left(G_{ax}\frac{\Delta z}{\Delta x} + G_{az}\right)} + \frac{5\,G_{az}\,\varphi_{(2,j-1)} - 2\,G_{az}\varphi_{BC}}{3\left(G_{ax}\frac{\Delta z}{\Delta x} + G_{az}\right)} + \frac{2S_{\varphi(2,j)}\Delta z}{3\left(G_{ax}\frac{\Delta z}{\Delta x} + G_{az}\right)} \tag{3.60}$$

3.2.3 Solving the system of discretized governing equations

The gradient or source in the system of equations is a function of the properties in the cells and will therefore have to be solved iteratively. To solve the system of equations and determine the source terms simultaneously point-iterative methods such as the Gauss-Siedel method can be employed. Consider the discrete form of the governing equation for the property φ,

$$\varphi_{(i,j)}^{(1)} = \varphi_{(i-1,j)}^{(1)} + S_{\varphi(i,j)}^{(0)}\Delta z \tag{3.61}$$

where the source term is calculated by a guessed or previously calculated value for φ. The residual of the equation is the difference between the right and left hand side of the equations or the difference between the old and the new value.

$$\varphi_{(i,j)}^{(1)} - \varphi_{(i,j)}^{(0)} = r_{i,j} \tag{3.62}$$

The equation is considered solved or converged when the residuals reach zero ($r_{i,j}\rightarrow 0$). In a computational domain of size (n,m) the absolute average of the total residuals $\bar{r}$ is used as an indicator of convergence.

$$\bar{r} = \frac{1}{n\,m}\sum_{j=1}^{n}\sum_{i=1}^{m} r_{i,j} \tag{3.63}$$

When using a method such as the upwind method, where upstream values are used for approximation, each cell can be converged before the next cell is calculated. For cell (1,1) that means its neighbouring upstream cell are only the boundaries. Therefore cell (1,1) can be iterated to convergence without solving the entire domain. When cell (1,1) is converged, cell (1,2) or cell (2,1) can be iterated to convergence without calculating any other cells. Continuing in a similar way through the domain, means that convergence of the entire solution is not reached until all cells have been converged individually. This often results in a more stable solution and shorter converging time. In an unstructured grid or complex geometries this procedure may not be possible and the average residual is used instead. When the Reuter model is implemented in a CFD solver such as ANSYS-*Fluent*® the program does not allow for this approach and the average residual (Eq. 3.63) is used.

To make the solution more stable a relaxation factor can be introduced,

$$\varphi_{(i,j)}^{(1)} = (1-\alpha)\,\varphi_{(i,j)}^{(0)} + \alpha\left(\varphi_{(i-1,j)}^{(1)} + S_{\varphi(i,j)}^{(0)}\Delta z\right) \tag{3.64}$$

The relaxation factor does not only give more stable solutions, it can improve the convergence rate as well (Versteeg 2007). When solving the different cross- and counterflow test cases in Appendix B it was found that a relaxation factor of $\alpha = 0.8$ gave the best result. This may vary slightly between individual cases.

When the discretized governing equations for supersaturation are solved with the air temperature equations, Eq. (3.24) and Eq. (3.10) for the source term, convergence can be difficult to obtain. This is mainly caused by the gradient term for saturated air humidity in Eq. (3.13). When the air becomes supersaturated, water liquid condenses from the air stream. The energy released from the condensation transfers to the air, resulting in an increase in air temperature gradient and saturated humidity gradient. The sudden increase in air temperature gradient often causes the solution to become unstable and diverge. A further analysis of the transition between un- and supersaturated air and methods of solving this problem is given in Chapter 4. One way of avoiding this problem is to use the discrete form of the enthalpy equations, Eq. (3.26), instead of the air temperature equations. When the enthalpy equations are used the air temperature has to be determined iteratively for each cell. This results in more computation for every time the domain is solved. On the other hand the solution becomes more stable and converges quicker, often resulting in less computing time than if the air temperature equation is used in full.

For a cross-counterflow fill in a wet-cooling tower the properties known are the inlet conditions of the water and air, as well performance characteristics of the fill. The inlet conditions of the water and air are usually not at the same side of the domain and the outlet conditions of both are therefore unknown. To obtain correct solutions, either one will have to be determined iteratively. In this research the outlet water temperature is determined iteratively. If the outlet air properties are used, both the outlet air temperature and humidity will have to be guessed and iteratively determined. The upwind method solves the system of equations in the direction of airflow and the outlet water temperature is iterated until the resulting inlet water temperature ($T_{wi,new}$) is the same as actual inlet water temperature (T_{wi}). When the Merkel number is to be determined, it is iterated until the outlet temperatures of the water is the same as measured.

3.3 Convergence and grid independence of the numerical solution

To determine the accuracy of a solution, Roache (1997) gave the following equation for estimating discretization error of a numerical solution,

$$E_i = \frac{U_{i+1} - U_i}{1 - k^p} \tag{3.65}$$

where U is an outcome parameter, k the refinement ratio ($k = h_i/h_{i+1}$), h the cell size and p the order of the numerical scheme. To determine the accuracy of a numerical solution with the presented differencing schemes, consider the case presented by Kröger (2004) (see Table 2.1) used in the previous chapter to illustrated differences in fill performance models. Tables 3.1 and 3.2 show the error in water cooling over the fill ($\Delta T_w = T_{wi} - T_{wo}$) using the initial cell size of 0.1 m and grid refinement ratio of $h = 0.5$. Solutions are obtained by solving the system of discretized equations using the Poppe assumptions with $Me/L_{fi} = 0.391$ for counterflow and $Me/L_{fi} = 0.424$ for crossflow. The error is normalized by using the temperature difference ($\Delta T_w = 11.90$°C) from the test case.

Table 3.1: Counterflow Reuter model first order upwind discretization error (E_i) and energy balance with grid refinement ratio of 0.5

Domain	Cell Size	Error		Energy
(n, m)	$\Delta z, \Delta x$ (m)	E_i (°C)	$E_i/\Delta T_w$	balance
(19,1)	0.100			0.33%
(38,1)	0.050	-0.0500	-0.42 %	0.30%
(75,1)	0.025	-0.026	-0.22 %	0.28%
(150,1)	0.013	-0.014	-0.11 %	0.27%
(300,1)	0.006	-0.007	-0.06 %	0.26%

Table 3.2: Crossflow Reuter model first order upwind discretization error (E_i) and energy balance with grid refinement ratio of 0.5

Domain	Cell Size	Error		Energy
(n, m)	$\Delta z, \Delta x$ (m)	E_i (°C)	$E_i/\Delta T_w$	balance
(19,15)	0.100			-3.04%
(38,30)	0.050	-0.1859	-1.56 %	-1.43%
(75,60)	0.025	-0.0949	-0.80 %	-0.60%
(150,120)	0.013	-0.0474	-0.40 %	-0.17%
(300,240)	0.006	-0.0237	-0.20 %	0.25%

Table 3.3: Counterflow Reuter model second order upwind method Discretization error (E_i) and energy balance with grid refinement ratio of 0.5

Domain	Cell Size	Error		Energy
(n,m)	$\Delta z, \Delta x$ (m)	E_i (°C)	$E_i/\Delta T_w$	balance
(19,1)	0.100			0.26%
(38,1)	0.050	-0.0002	0.00%	0.26%
(75,1)	0.025	-0.0001	0.00%	0.26%

Table 3.4: Crossflow Reuter model second order upwind discretization error (E_i) and energy balance with grid refinement ratio of 0.5

Domain	Cell Size	Error		Energy
(n,m)	$\Delta z, \Delta x$ (m)	E_i (°C)	$E_i/\Delta T_w$ (%)	Balance
(19,15)	0.100			0.26%
(38,30)	0.050	-0.0088	-0.07%	0.26%
(75,60)	0.025	-0.0023	-0.02%	0.26%

It can be seen from the Tables 3.1 and 3.2 that there is considerable difference between the errors in counter- and crossflow. To obtain a crossflow solution with equivalent grid independence to a counterflow solution, the crossflow cells must be quarter of the size. It is clear that by applying the first order method for a crossflow case requires a relatively fine grid. The grid independence of the second order method presented in Tables 3.3 and 3.4 is very good in comparison to the first order method. The initial cell size of 0.1 m can be expected to give grid independence solutions in counterflow. This can be said for the crossflow case as well, although the grid dependence in crossflow is considerable more than in counterflow. The numerical error of the second order solution is so small that it indicates that the cell size may be larger and still maintain good grid independence. Table 3.5 gives the resulting ΔT_w when the cell sizes are increased by decreasing the number of intervals in the domain to a minimum of 3 intervals. The Merkel number used for cross- and counterflow is determined using cell size of 0.025 m and gives exactly 11.90 °C. How far ΔT_w is from 11.90 °C for the relevant cell size indicates the grid dependence.

In the counterflow case it is clear that as few as three intervals are needed to get a solution with grid independence. In crossflow, cell sizes larger than 0.1 m can result in a considerable loss of grid independence.

Table 3.5: Cross- and counterflow Reuter model second order upwind cooling (ΔT_w) and energy balance with cells larger than 0.1 m

Domain	Counterflow		Energy Balance	Crossflow		Energy Balance
(n,m)	Δz (m)	ΔT_w (°C)		Δx (m)	ΔT_w (°C)	
(3,3)	0.626	11.899	0.28%	0.500	12.033	0.30%
(5,5)	0.376	11.901	0.27%	0.300	11.957	0.28%
(10,10)	0.188	11.900	0.26%	0.150	11.916	0.26%
(15,15)	0.125	11.900	0.26%	0.100	11.906	0.26%

The numerical error can differ with varying flow rates. To demonstrate this difference, error in Merkel numbers for three counter- and three crossflow cases from the experimental data in Appendix B (counterflow cases nr. 9, 11, 13 and crossflow cases nr. 5, 6, and 8) are determined. The cases have a similar water flow rate and inlet temperature. The air flow is varied, giving an air to water flow ratio (G_a/G_w) ranging from 0.5 to 1.25. The water outlet temperature is measured for each case, typically giving a low Merkel number for low ratio and high for higher ratio. The cases are refined with the same refinement as in Tables 3.1 and 3.2. Figure 3.2 shows the differences in error from the determined Merkel number with different flow ratios. The error is normalized by a Merkel number obtained using cell size of 0.0125 m and the first order method.

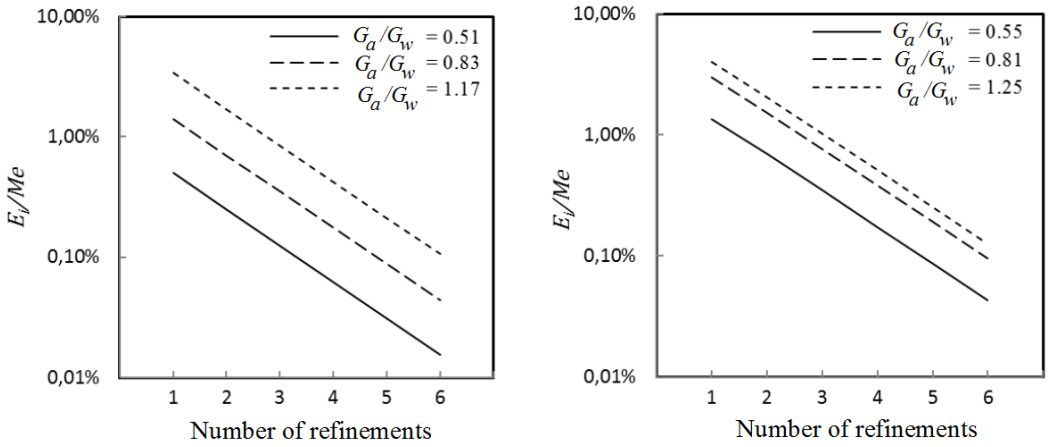

(a) Counterflow (b) Crossflow

Figure 3.2: First order upwind discretization error (E_i/Me) for increasing air to water flow ratio

It can be seen from the Figure 3.2 that an additional refinement is needed between air to water mass flow ratio 0.51 and 0.83, and two refinements between 0.51 and 1.17 in the counterflow cases. The crossflow cases give a similar trend for the

difference from air to water mass flow ratio of 0.51 to 0.81 whereas the difference between 0.81 and 1.25 is smaller. If the curve fit comparison given in Figure 2.3 is reviewed it can be seen that the increase in crossflow Merkel numbers with increased airflow is significantly lower than in counterflow. A low Merkel number indicates less heat and mass transfer. This means that it is the rate of heat and mass transfer that affects the total error and not just the air to water ratio. The Merkel number describes the rate of heat and mass transfer in the fill, indicating that the high Merkel numbers give a higher error and more grid dependence. Care must therefore be taken when selecting cell or grid size to obtain a solution. If the Merkel number is relatively high, indicating high heat and mass transfer, cells must be smaller to give numerical accuracy equivalent to a case with relatively low Merkel number. To determine the necessary grid refinement for a particular case, Roache (1997) rearranged Eq. (3.65) to give the following error estimation formula,

$$E_{i+1} = r^p \left(\frac{U_{i+1} - U_i}{1 - r^p} \right) \tag{3.66}$$

Roache pointed out that even though a numerical scheme is of a certain order, p will not necessarily be of the exact same order. To determine more accurately the error and refinement the following equation is applied,

$$\tilde{p} = ln\left(\frac{U_{i+2} - U_{i+1}}{U_{i+1} - U_i} \right) / \ln(k) \tag{3.67}$$

where k is a constant refinement ratio and $\tilde{p}$ is used in Eq. (3.66) instead of p. Using the first three values in Table 3.2 and Table 3.4,a $\tilde{p} = 0.95$ for the first order method and $\tilde{p} = 1.95$ for the second order method are obtained.

The convergence rate of point iterative methods such as the Gauss-Seidel can be higher for coarse grids and less for finer grids (Versteeg, 2007). To analyse this effect, the average residual ($\bar{r}$) for the water temperature (T_w) is plotted against number of iterations in Figure 3.3.

Figure 3.3 shows that the difference in convergence rate for the crossflow solution is significant whereas this effect seems minimal for the counterflow solution. In a case of cross- or cross-counterflow where air and water side change in two or three dimensions, larger cell sizes are therefore not just beneficial in term cells to calculate but convergence rate as well.

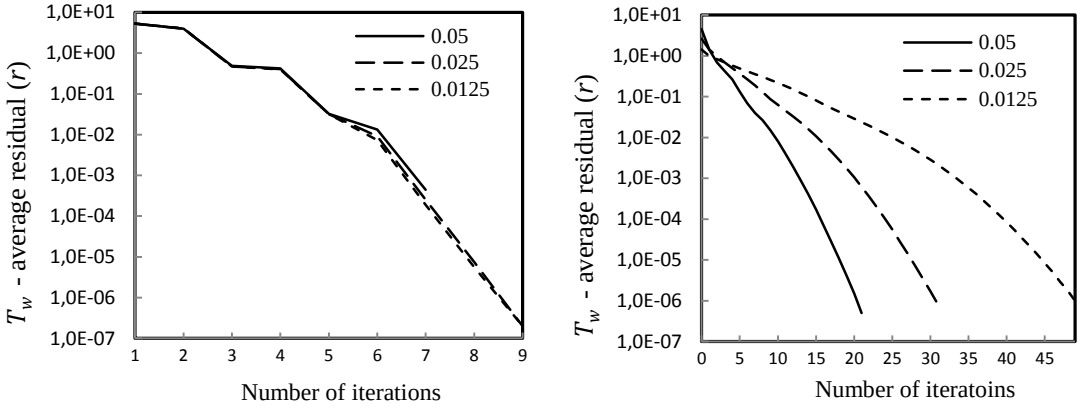

(a) Counterflow (b) Crossflow

Figure 3.3: Cross- and counterflow convergence rate for a decreasing cells size

3.4 Discretizing and solving governing differential equations based on Merkel assumptions

The crossflow Merkel method presented by Zivi and Brand (1991) can be solved using the same differencing scheme as has been presented for the cross-counterflow model in the previous section. Only two differential equations need to be solved. Source terms for air enthalpy and water temperature can be written as,

$$S_{Tw} = \frac{\partial T_w}{\partial z} = \frac{1}{c_{pw}} \left(\frac{Me}{L_{fi}} \right) (i_{masw} - i_{ma}) \tag{3.68}$$

$$S_{ima} = G_a \frac{\partial i_{ma}}{\partial x} = \left(\frac{Me}{L_{fi}} \right) G_w (i_{masw} - i_{ma}) \tag{3.69}$$

where $G_a = G_{a,x}$ and G_w is constant. To solve the crossflow Merkel model it is more convenient to solve for the water temperature from inlet to outlet. For this purpose a backward differencing scheme can be used. Discrete form of the governing differential equations can be written as,

$$T_{w(i,j)} = T_{w(i-1,j)} - S_{Tw(i,j)} \, \Delta z \tag{3.70}$$

$$i_{ma(i,j)} = i_{ma(i,j-1)} + S_{ima(i,j)} \, \Delta z \tag{3.71}$$

where $i = 1$ at the water inlet side and $j = 1$ at the air inlet side. By employing this form, iterating the water temperature can be avoided and considerably reducing computing time. This form is only beneficial in a fully crossflow case. In a counter- or cross-counterflow case the air outlet conditions at the top of the fill need to be determined iteratively in the same way as with the upward scheme,

resulting in similar computational expense. Table 3.6 gives the discretization error in the same way as was presented for the first order upwind method for the same case and normalized with $\Delta T_w = 11.90$ °C.

Table 3.6: Crossflow Merkel model first order backwind discretization error (E_i) and energy balance with grid refinement ratio of 0.5

Domain	Cell Size	Error	
(n,m)	$\Delta z, \Delta x$ (m)	E_i (°C)	$E_i/\Delta T_w$ (%)
(19,15)	0.100		
(38,30)	0.050	0.0584	0.49%
(75,60)	0.025	0.0292	0.25%
(150,120)	0.013	0.0146	0.12%
(300,240)	0.006	0.0073	0.06%

The initial error is about third of the initial error of the upwind method in Table 3.2 and the error decreases at a similar rate with refinement. The error is all positive as opposed to negative for the upwind method, indicating that a grid independent solution is approached from a different direction.

The cross-counterflow Merkel method presented in the previous chapter can be discretized in the same way as the Reuter model. Source terms for a cross-counterflow Merkel method can be written as,

$$\frac{S_{Tw}}{\Delta z} = \frac{\partial T_w}{\partial z} = \frac{1}{c_{pw}} \left(\frac{Me}{L_{fi}} \right) (i_{masw} - i_{ma}) \tag{3.72}$$

$$\frac{S_{ima}}{\Delta z} = G_{a,x} \frac{\partial i_{ma}}{\partial x} + G_{a,z} \frac{\partial i_{ma}}{\partial z} = \left(\frac{Me}{L_{fi}} \right) G_w (i_{masw} - i_{ma}) \tag{3.73}$$

The cross-counterflow Merkel method can be used to calculate performance based on the Merkel assumption for cross-, counter or cross-counterflow fill. Outlet conditions of the air for both the cross-, and cross-counterflow Merkel methods are determined by assuming that air leaving the fill is saturated with water vapour.

Merkel (1925) combined the two differential equations to the following Merkel equation,

$$Me = \frac{h_d a_{fi} L_{fi}}{G_w} = \int_{T_{wo}}^{T_{wi}} \frac{c_{pw} dT_w}{i_{masw} - i_{ma}} \tag{3.74}$$

By assuming energy balance, Merkel was able to determine the dry air enthalpy of the outlet air from the water temperature.

$$i_{mao} = m_w c_{pwm}(T_{wi} - T_{wo})/m_a + i_{mai} \tag{3.75}$$

The Merkel equation can be solved with numerical integration. Merkel proposed using the Chebychev integration method. The method is a four point method that uses 0.1, 0.4, 0.6 and 0.9 as calculation intervals. With these intervals the integral can then be approximated accordingly,

$$\int_{T_{wo}}^{T_{wi}} \frac{c_{pw} dT_w}{i_{masw} - i_{ma}} \approx \frac{c_{pwm}(T_{wi} - T_{wo})}{4}\left(\frac{1}{\Delta i_{(0.1)}} + \frac{1}{\Delta i_{(0.4)}} + \frac{1}{\Delta i_{(0.6)}} + \frac{1}{\Delta i_{(0.9)}}\right) \tag{3.76}$$

where

$$T_{w(0.1)} = T_{wo} + 0.1\,(T_{wi} - T_{wo}) \tag{3.77}$$

$$\Delta i_{(0.1)} = i_{masw(0.1)} - m_w c_{pwm}\left(T_{w(0.1)} - T_{wo}\right)/m_a + i_{mai} \tag{3.78}$$

$$i_{masw(0.1)} = c_{pa}\, T_{w(0.1)} + w_{sw}(i_{fgwo} + c_{pv}\, T_{w(0.1)}) \tag{3.79}$$

Points 0.4, 0.6 and 0.9 can be calculated in the same way. Other forms of numerical integration can be applied to the integral in a similar way. The most common are the rectangular-, trapezoidal- and Simpson rule which can be written for the Merkel equation in the following way,

$$Me_{rect} \approx \frac{c_{pwm}(T_{wi} - T_{wo})}{4}\left(\frac{1}{i_{maswm} - i_{mam}}\right) \tag{3.80}$$

$$Me_{trapz} \approx \frac{c_{pwm}(T_{wi} - T_{wo})}{4}\left(\frac{1}{i_{maswo} - i_{mao}} + \frac{1}{i_{maswi} - i_{mai}}\right) \tag{3.81}$$

$$Me_{simps} \approx \frac{c_{pwm}(T_{wi} - T_{wo})}{4}\left(\frac{1}{i_{maswo} - i_{mao}} + \frac{2}{i_{maswm} - i_{mam}} + \frac{1}{i_{maswi} - i_{mai}}\right) \tag{3.82}$$

All these methods are relatively simple to calculate and can be solved with hand calculations. Their accuracy on the other hand is limited in this form. To get a more accurate result a composite form is applied. In a composite numerical integration the interval between T_{wi} and T_{wo} is split into n number of intervals and the numerical integration in the above equations is applied to each interval. In

Table 3.7 Merkel numbers are presented for the varying flow ratio rate test cases used in Figure 3.2, with 1, 10 and 100 intervals.

Table 3.7: Counterflow Merkel equations Merkel numbers obtained with rectangle, trapezoidal, Simpson and Chebychev numerical integration methods

G_a/G_w =	0.51	0.83	1.17
n		Me/L_{fi}	
1	0.712	0.993	1.197
10	0.675	0.949	1.195
100	0.674	0.948	1.195

(a) Rectangle

G_a/G_w =	0.51	0.83	1.17
n		Me/L_{fi}	
1	0.605	0.863	1.175
10	0.673	0.947	1.195
100	0.674	0.948	1.195

(b) Trapezoidal

G_a/G_w =	0.51	0.83	1.17
n		Me/L_{fi}	
1	0.658	0.928	1.186
10	0.674	0.948	1.195
100	0.674	0.948	1.195

(c) Simpson

G_a/G_w =	0.51	0.83	1.17
n		Me/L_{fi}	
1	0.673	0.947	1.194
10	0.674	0.948	1.195
100	0.674	0.948	1.195

(d) Chebychev

Table 3.7 shows that integration methods all give the same Merkel number in a composite form with 100 intervals. 10 intervals give the same or similar result as the 100 interval solution. In the single interval form the Chebychev method gives Merkel numbers closest to the 10 and 100 intervals. The Chebychev method can therefore be expected to give results with insignificant numerical error with a single interval. The Simpsons rule gives good result for single interval but should be used with more than one interval to give results equivalent to Chebychev. Rectangle and Trapezoidal should use at least 10 intervals to get accuracy equivalent to the Chebychev method.

Merkel numbers for the same test cases determined using the Reuter model in counterflow ($G_{ax} = 0$) with a Merkel assumptions ($Le_f = 1$ and $\beta_{Me} = 1$) are given in Table 3.8. Merkel numbers are also given for the counterflow Merkel method by solving the two governing differential equations of the Merkel method instead of the integral in the Merkel equation. Both methods are discretized with the second order linear upwind method as has been presented in this chapter, using 30 intervals ($\Delta z = 0.05$).

Table 3.8: Counterflow Reuter model Merkel numbers and energy balance with Merkel assumptions

G_a/G_w =	0.51	0.83	1.17
Me/L_{fi}	0.670	0.942	1.185
EB =	-4.58%	-4.00%	-3.62%

(a) Reuter model w. Merkel assumptions ($Le_f = 1$ and $\beta_{Me} = 1$)

G_a/G_w =	0.51	0.83	1.17
Me/L_{fi}	0.673	0.947	1.194
EB =	0.01%	0.11%	0.17%

(b) cross-counter Merkel method

The Merkel numbers in part (b) of Table 3.8, determined by the counterflow Merkel method are within 0.05% from the Merkel equation in Table 3.7. The Merkel numbers in part (a) in Table 3.8 are about -0.5% to -0.8% lower than the Merkel numbers determined by the composite numerical integrations in Table 3.7 and part b. It can be seen in the previous section that the numerical error cannot account for this difference. The reason for the difference can be seen in the energy balance. The energy balance for the Reuter model with Merkel assumptions in Table 3.8 is all negative, whereas it is close to zero for the Merkel method. This indicates that the energy from the water is not all transferred to the air. The reason for this imbalance is that the governing differential equations on the air side are not modified to account for the neglected evaporation term in the water temperature equation. The Merkel number for the Merkel approach will therefore give a lower air outlet temperature even though the water outlet temperature is the same. Sample calculation for the Merkel methods are given in Appendix A.

3.5 Discretizing the governing equations of the Poppe method

Kloppers and Kröger (2004) give a discretized form of governing equations for the counterflow Poppe method using a 4th order Runge-Kutta method. For a crossflow Poppe method Kloppers and Kröger (2005a) give a discretized form of governing differential equations using a first order backwind method solved on a staggered grid. In this thesis the crossflow Poppe method is solved using cell central nodes the same way as the Reuter model. The governing differential equations of the crossflow Poppe method are given in Chapter 2. The differential equations can be discretized in the same way as for the Reuter model in this chapter with $G_{a,z}$= 0. Instead the equations are solved with first order backward differences as purely crossflow for the same reason as for the crossflow Merkel method. Discretization error using from applying the crossflow Poppe method to the case in Table 2.1, is given in Table 3.9.

Table 3.9: Crossflow Poppe model first order backwind discretization error (E_i) and energy balance with grid refinement ratio of 0.5

Domain	Cell size	Error	
(n, m)	$\Delta z, \Delta x$ (m)	E_i (°C)	$E_i/\Delta T_w$
(19,15)	0.100		
(38,30)	0.050	-0.1184	1.00%
(75,60)	0.025	-0.0612	0.51%
(150,120)	0.013	-0.0324	0.25%
(300,240)	0.006	-0.0153	0.13%

Table 3.9 shows that the initial error is about two thirds of the error from the Reuter model with first order upwind and it decreases at a similar rate. As with the crossflow Merkel method, the difference from using the upwind and the backwind method is that the error is positive versus negative. Care must be taken when a Merkel number, that has been obtained using a backwind method, is used to determine outlet water temperature with an upwind method because the numerical error can accumulate.

For the counterflow Poppe method the governing equations are derived in terms of change in water temperature (∂T_w) as oppose too spatially (∂z and ∂x). To solve the counterflow Poppe differential equations, given in section 2.9, with a 4th order Runge-Kutta method consider the equations in the following form,

$$\frac{\partial \varphi}{\partial T_w} = f(w, i_{ma}, T_w) \tag{3.83}$$

where φ can represents Me, i_{ma} or w and f represents the right hand side of the governing equations. The temperature difference $(T_{wi} - T_{wo})$ is split into n intervals and the property φ discretised accordingly,

$$\varphi_{(i+1)} \approx \varphi_{(i)} + (\phi_{(i,1)} + 2\,\phi_{(i,2)} + 2\,\phi_{(i,3)} + \phi_{(i,4)})/6 \tag{3.84}$$

where ϕ is,

$$\phi_{(i,1)} = \Delta T_w\, f(w_{(i)}, i_{ma(i)}, T_{w(i)}) \tag{3.85}$$

$$\phi_{(i,2)} = \Delta T_w\, f\left(w_{(i)} + \frac{w_{(i,1)}}{2}, i_{ma(i)} + \frac{i_{ma(i,1)}}{2}, T_{w(i)} + \frac{\Delta T_w}{2}\right) \tag{3.86}$$

$$\phi_{(i,3)} = \Delta T_w\, f\left(w_{(i)} + \frac{w_{(i,2)}}{2}, i_{ma(i)} + \frac{i_{ma(i,2)}}{2}, T_{w(i)} + \frac{\Delta T_w}{2}\right) \tag{3.87}$$

$$\phi_{(i,4)} = \Delta T_w \, f\left(w_{(i)} + w_{(i,3)}, i_{ma(i)} + i_{ma(i,3)}, T_{w(i)} + \Delta T_w\right) \tag{3.88}$$

and ΔT_w is the temperature change over each interval (i). At the air inlet boundary $(i = 1)$ the humidity and enthalpy are determined from inlet conditions $(w_{(1)} = w_i,\ i_{ma(1)} = i_{mai})$ and the Merkel number is equal to zero $(Me_{(1)} = 0)$. At the boundary $i = n$ the system of equations will result the outlet conditions of the air and the Merkel number for the fill. To get a solution the mass balance equation (Eq. 2.60) is solved by guessing the outlet humidity (w_o). The solution is considered converged when resulting outlet humidity $(w_{(n)})$ is the same as the guessed outlet humidity.

The method is of 4th order and its accuracy relatively good. Only a few intervals are needed to get good prediction of the Merkel number. Table 3.10 gives Merkel numbers for the three counterflow test cases, used in the previous section, with different number of intervals. For comparison Merkel numbers determined using the Reuter model with Poppe assumptions and solved with the second order linear upwind are given in the parenthesis.

Table 3.10: Counterflow Poppe model 4th order Runge-Kutta Merkel numbers and Reuter model second order upwind Merkel numbers

Intervals		Me/L_{fi}		
n	Δz (m)	G_a/G_w = 0.51	G_a/G_w = 0.83	G_a/G_w = 1.17
(3)	0.50	0.750 (0.756)	1.029 (1.035)	1.285 (1.270)
(5)	0.30	0.753 (0.755)	1.030 (1.034)	1.286 (1.280)
(10)	0.15	0.753 (0.754)	1.032 (1.035)	1.287 (1.287)
(15)	0.10	0.753 (0.754)	1.033 (1.035)	1.288 (1.288)
(25)	0.06	0.753 (0.754)	1.033 (1.035)	1.288 (1.289)

Table 3.10 shows that with only 10 intervals the Runge-Kutta solution outcome does not change significantly from the more refined grids. Large cells can therefore be used to obtain a grid independent prediction of a Merkel number and outlet conditions. In comparison the Merkel numbers determined by the Reuter model with second order upwind show similar grid independence. Higher Merkel numbers seem to have more effect on grid dependence for the second order method than the R-K method. Sample calculation for the counterflow Poppe method solved with the fourth order Runge-Kutta method is given in Appendix B.

3.6 Discussion of results and conclusion

The Reuter model is discretized with the first order upwind differencing scheme, as presented by Reuter (2010), as well as with a second order linear upwind scheme proposed in this thesis. A description of how to solve the system of equations is given with suggestions related to the relaxation factor and calculation procedure. Discretization error and convergence rate for cross- and counterflow conditions are presented for the first and second order upwind discretization.

The Method of solving the Merkel method is discussed for cross-, counterflow and cross-counterflow. For solving the Merkel equations the Rectangle, Trapezoidal, Simpson and Chebychev integration methods are applied in a single interval and composite form. Comparison is given for the composite and single interval form as well as to the cross-counterflow Merkel method and Reuter model with Merkel assumptions.

The crossflow Poppe method is discussed and its numerical accuracy compared to the Reuter model with Poppe assumptions. A description of the 4th order Runge-Kutta method is given for the counterflow Poppe method and accuracy compared to the second order linear upwind scheme.

The following was concluded based on results obtained by the different methods:

- There is a significant difference in numerical accuracy for the same cell size between cross- and counterflow. Cells in a computational domain of a crossflow fill have to be at least quarter of the size of cells in a counterflow fill to obtain a similar numerical accuracy.
- There is a significant difference in numerical accuracy between the second order linear upwind method and the first order method. The second order method only needed 0.1 m cell size to obtain a grid independent solution for the sample case in both cross- and counterflow and first order method needed 0.006 m.
- Convergence rate of crossflow solutions decreases with grid refinement, but does not for counterflow solutions.
- Merkel numbers obtained from the Merkel equation using different numerical integration methods can differ considerably. Comparison between one interval integration and multi-interval (composite) shows Merkel numbers do not change significantly for 10 intervals and more. The single interval method of Chebychev will give a Merkel number within 0.1% of the 10 interval composite form. The Simpson rule needs two intervals to get results equivalent of single interval Chebychev and the Rectangle and Trapezoidal need 10 intervals.
- A counterflow Merkel number obtained using the Reuter model in counterflow condition ($G_{a,x} = 0$) and with Merkel approach ($Le_f = 1$ and $\beta_{Me} = 1$) can be 0.5% to 0.8% lower than Merkel numbers obtained by the Chebychev numerically integrated Merkel equations.

- Numerical error in the crossflow Poppe method solved with a first order backwind differencing scheme is about two thirds of the error in the first order upwind method. The error decreases at the same rate with grid refinement.
- Merkel numbers obtained using the counterflow Poppe method with 4th order Runge-Kutta differencing scheme only need a few intervals (3 to 10) to get a relatively accurate prediction. Comparison to the second order upwind method shows that the two discretization schemes give similar numerical accuracy. Except when the Merkel number are relatively high ($Me/L_{fi} > 1.0$) the accuracy of the second order method is poorer with fewer than 10 intervals

Reuter (2010) concluded that his sample case with a cell size of 0.0125 m gave a grid independence using the first order upwind method. For the sample case in this chapter a cell size of 0.0125 m had a discretization error of 0.1% for counterflow and 0.4% for crossflow. The error was higher for the test cases that had higher Merkel numbers, going up to 1.0% in crossflow. The reason for this difference is that Reuter used a relatively low Merkel number obtained from a single drop model in the grid independence study. In this chapter it has been shown that higher Merkel numbers result in higher numerical error using this scheme. The second order upwind method gives accuracy which is almost equivalent to the 4^{th} order Runge-Kutta method and it can be applied to cross-, counter- and cross-counterflow, whereas the Runge-Kutta method as presented by Kröger and Kloppers (2005a) is only for counterflow. Using the second order scheme a cell size of 0.1 m will be sufficient for most cases in cross- and counterflow. If the Merkel numbers used is relatively high, a cell size 0.05 m will give a grid independent solution with the second order method.

4 CFD MODELING OF HEAT AND MASS TRANSFER IN A CROSS-COUNTERFLOW WET-COOLING TOWER FILL

4.1 Introduction

With computing power becoming more affordable and capabilities of commercial CFD software increasing every year, full scale CFD models of cooling towers are becoming a practical option. With a CFD model of a cooling tower, flow can be modelled in all areas of the tower simultaneously. Al-Waked (2006) modelled a full scale three-dimensional natural draught wet-cooling tower (NDWCT) with CFD, where all heat and mass transfer was modelled with a discrete phase model (DPM). Fill volume was simulated by manipulating droplet velocity to get correct fill characteristics. Influence of cross wind was analysed and found to have both positive and negative effects on cooling tower performance. Williamson (2008) modelled a two-dimensional axis-symmetric NDWCT, where a DPM was used for the rain and spray zone. A Poppe model was used for the fill area by assuming counterflow. Klimanek (2009, 2010) created a three-dimensional model of a NDWCT. A DPM was used for the rain zone and a one dimensional Poppe style counterflow model for the fill area. From these studies it was pointed out that re-circulation can occur near the cooling tower inlet and influences of cross winds can be considerable. Experiments have suggested that by hanging a splash or trickle fill into the rain zone of natural or mechanical DWCT these effects can be reduced. Modelling of such a setup is not valid if the air is assumed to be only in counterflow.

Reuter (2010) modelled a two-dimensional axisymmetric NDWCT where the model studied in this thesis was used for the fill area and a DPM for the rain zone. Reuter studied many aspects of a NDWCT, including the rain zone, fill, spray zone, losses and more. The fill model was implemented in ANSYS-*Fluent*® using a User Defined Function (UDF) to simulate heat and mass transfer in the fill area. The water side, i.e. the cooling and evaporative loss in the water stream, was solved within the UDF. The model uses source terms to exchange energy and vapour to the ANSYS-*Fluent*® solver and the water properties for the fill are stored in user defined memory (UDM). The model was represented using a first order discretization for the water side and second order for the air side. To verify the model, Reuter used a single drop model. From the single drop model, a numerical solution which can be obtained for transfer characteristics as well as cooling of a single droplet under any airflow direction. The transfer characteristics in the form of a Merkel number was then used in the ANSYS-*Fluent*® model to compare energy and mass transfer. The model was implemented in ANSYS-*Fluent*® only for unsaturated air. The fill model was verified by comparing it to the DPM with the same transfer characteristics.

The main objective of this chapter is to fulfil the last four objectives of this thesis,

- Verify that the Reuter model results in the same cooling as when implemented in ANSYS-*Fluent*® and when programmed for fill performance evaluation.

- Verify that the Reuter model results in the same outlet conditions for supersaturated air, when implemented in ANSYS-*Fluent*® and when programmed for fill performance evaluation.

- Suggest improvement to the solution method employed by Reuter (2010) to increase accuracy.

- Model a three-dimensional block of fill with ANSYS-*Fluent*®

To fulfill these objectives, a description on how to model heat and mass transfer in the fill area using ANSYS-*Fluent*® is given. Description of how the UDF operates and its structure are explained and discussed. Instructions on how to implement the second order upwind method, presented in Chapter 3, in the UDF to match the second order discretization of ANSYS-*Fluent*® is given. To verify the model, heat and mass transfer is simulated in a block of fill with fixed flow and compared with a Scilab model used in to solve the system of equations in the previous chapters. The last objective is fulfilled by modelling a three-dimensional block of fill with cross-counterflow conditions and a wedge or sector applicable to a circular cooling tower.

4.2 Implementing the Reuter model in ANSYS-*Fluent*®

The main purpose of using ANSYS-*Fluent*® or any other commercial CFD software to model wet-cooling towers is to utilize the solvers ability to solve conservation equations for mass, momentum, energy and species mixing. Most commercial CFD packages can employ a variety of turbulence models to allow for a more accurate modelling of global flow fields. Furthermore, CFD packages such as ANSYS-*Fluent*® come with a design modeller for geometry creation, mesh generators and comprehensive post processors.

Heat and mass transfer from the water to the air is modelled with energy and mass source terms. Source terms for energy and mass with unsaturated can be written as,

$$S_q = \left\{ \left(\frac{Me}{L_{fi}} \right) G_w (T_w - T_a) \left[Le_f c_{pma} + c_{pv} \left(w_{sw} - w \right) \right] \right\}_{(i,j)} \tag{4.1}$$

$$S_m = \left[\left(\frac{Me}{L_{fi}} \right) G_w \left(w_{sw} - w \right) \right]_{(i,j)} \tag{4.2}$$

When the air becomes saturated with water vapour, mass transfer continues as long as the water is warmer than the air and the air gets supersaturated. Source terms for supersaturated air can be written as,

$$S_q = \left\{\left(\frac{Me}{L_{fi}}\right) G_w \left[Le_f c_{pma}(T_w - T_a)c_{pma} + (w_{sw} - w_{sa})\left[i_{fg(T_w)} + c_{pw}(T_w - T_a)\right]\right] - S_{wsa}\, i_{fg(T_a)}\right\}_{(i,j)} \tag{4.3}$$

$$S_m = \left[\left(\frac{Me}{L_{fi}}\right)\frac{G_w}{\Delta z}\,(w_{sw} - w_{sa})\right]_{(i,j)} \tag{4.4}$$

where,

$$S_{wsa} = \left[\frac{G_{a,x}}{\Delta x}\left(w_{sa(i,j)} - w_{sa(i,j-1)}\right) + \frac{G_{a,z}}{\Delta z}\left(w_{sa(i,j)} - w_{sa(i-1,j)}\right)\right] \tag{4.5}$$

The source terms are functions of properties of the water and air, which are not constant throughout the fill. To obtain correct source term, the water and air properties have to be determined. Governing differential equations for air are discretized and solved within the ANSYS-*Fluent*® solver and governing differential equations for the water are discretized and solved separately within a UDF. Properties for the water are stored in user defined memories (UDM). Figure 4.1 shows a schematic diagram for the process of solving heat and mass transfer equations for water an air.

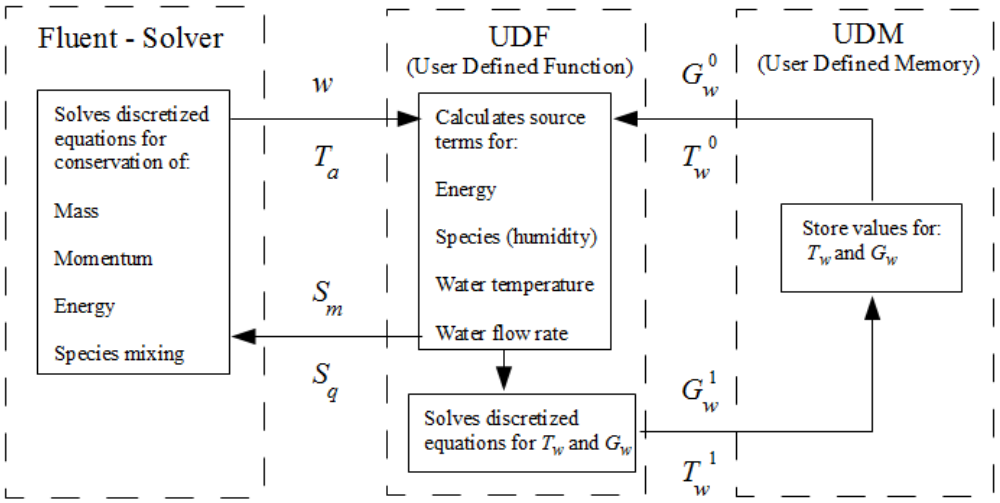

Figure 4.1: Process diagram for solving heat and mass transfer with ANSYS-*Fluent*® and a user defined function

To solve the system of equations, values for all properties are initialized and source terms calculated from the initial values. The UDF carries out its calculation procedure after every iteration of the solver. It extracts current values from the solver and UDM; calculates source terms; sends heat and mass sources back to the solver; discretizes and solved and water properties. When the difference between the values used to calculate the source terms and the resulting values becomes smaller than a specified convergence the solver is stopped.

The Merkel number in the source term equations is determined from the empirical relation (curve fits), characterizing the fill to be modelled. The curve fits are given with Eq. (2.44) from chapter 2,

$$Me/L_{fi} = c_1 \, G_{wi}^{c_2} \, G_a^{c_3} \, T_{wi}^{c_4} \tag{2.44}$$

where c_1, c_2, c_3 and c_4 are curve fitting constants. The Merkel numbers is a function of the water inlet temperature, water mass velocity, air mass velocity and fill depth. The fill depth does have an effect on the Merkel number per meter fill, i.e. it will be higher in shallower fills and decreases when the fill height increases. When a fill is performance tested, the same or similar fill height should be used as is intend to be used in the cooling tower application. When the momentum equations are solved, the air flow may vary considerably in magnitude and direction between cells. The Merkel number is therefore calculated individually within every cell and will vary according to airflow. To calculate the Merkel number in every cell the velocity components are extracted from the solver in the same way as with humidity and air temperature. Additionally when a cooling tower fill is modelled the velocity components are used to calculate loss coefficient from empirical equations. The loss coefficient is used to determine momentum- and pressure loss. This thesis mainly focuses on the heat and mass transfer and momentum loss is not specifically analysed.

4.2.1 Discretizing and solving water properties within the UDF

The source terms for water temperature and flow rate can be written in the same way as displayed in chapter 3, by Eq. (3.1) and (3.2),

$$S_{Gw} = G_w \left(\frac{Me}{L_{fi}}\right) (w_{sw} - w) \tag{3.1}$$

$$S_{Tw} = \left(\frac{Me}{L_{fi}}\right) \frac{c_{pma}}{c_{pw}} \left[Le_f (T_w - T_a) + \frac{i_{fg(T_w)} + \beta_{Me} c_{pw} T_w}{c_{pma}} (w_{sw} - w) \right] \tag{3.2}$$

For supersaturated air the source terms are describe by Eq. (3.6) and (3.7).

$$S_{Gw,ss} = G_w \left(\frac{Me}{L_{fi}}\right) (w_{sw} - w_{sa}) \tag{3.6}$$

$$S_{Tw,ss} = \\ = \left(\frac{Me}{L_{fi}}\right)\frac{c_{pma}}{c_{pw}}\left[Le_f(T_w - T_a) + \frac{i_{fg(T_w)} + \beta_{Me}c_{pw}T_w}{c_{pma}}(w_{sw} - w_{sa})\right] \quad (3.7)$$

The UDF is an "execute at end" function and the solver controls the order in which the cells are calculated. To know where the solver is located in the computational domain, the UDF initially allocates a reference numbers to every cell. The reference number is then used to find the corresponding properties in the UDM.

The water properties, T_w and G_w, can be discretized with the first order upwind method as presented in Chapter 3. To solve the discretized equations, properties in the upstream cell must be found. The UDF searches the neighbouring cells with a "face loop" function and by comparing their vertical position, the upstream cell can be identified with its cell reference number. The cell reference number is then used to find the corresponding value for T_w and G_w in the UDM. With the upstream cell properties known, a new value for cell (i, j) can be calculated according to the first order upwind method given in Eq. (3.21) and (3.22).

$$G_{w(i,j)} = G_{w(i-1,j)} + S_{Gw(i,j)}\,\Delta z \quad (3.21)$$

$$T_{w(i,j)} = T_{w(i-1,j)} + S_{Tw(i,j)}\,\Delta z \quad (3.22)$$

ANSYS-*Fluent*® has several different discretization methods built into its solver, giving its user a range of options from a drop down menu. Both the first and second order upwind methods are part of the selection. To implement a second order method in the same way as it was presented in chapter 3, requires an additional "face loop" around the upstream cell $(i-1, j)$ to find its upstream cell, that is cell $(i-2, j)$. An additional face loop makes the UDF more complicated in terms of programming and increases implication of the computational procedure. Instead, the gradient of each cell is stored in a UDM as well as the property. When the gradient and property of the upstream cell $(i-1, j)$ are known, a second order discretization can be applied in the following form,

$$\varphi_{(i,j)} = \varphi_{(i-1,j)} + \frac{1}{3}\Delta\varphi_{(i-1,j)} + \frac{2}{3}S_{\varphi(i,j)} \quad (4.6)$$

where φ can represent either T_w or G_w. The gradient in the upstream cell, cell $(i-1, j)$, can be written as

$$\Delta\varphi_{(i-1,j)} = \varphi_{(i-1,j)} - \varphi_{(i-2,j)} \quad (4.7)$$

For the current cell, cell (i, j), the gradient becomes

$$\Delta\varphi_{(i,j)} = \varphi_{(i,j)} - \varphi_{(i-1,j)} \quad (4.8)$$

The gradient in the current cell is calculated and stored in a UDM to be extracted and used for the downstream cell. Inserting Eq. (4.7) for the gradients into equations Eq. (4.6) will result in Eq. (3.44) and Eq. (3.45) for the second order upwind method presented in Chapter 3.

4.2.2 Modelling supersaturated air

If the source term equations of the un- and supersaturated air are compared it can be seen that the supersaturated equations are more complicated. When the air becomes supersaturated, water vapour condenses. The energy released from the condensation process is transferred to the air stream, resulting in an increase in air temperature gradient. See Figure 4.2 for air temperature and gradient for the sample case from Kröger (2004) given in Table 2.1.

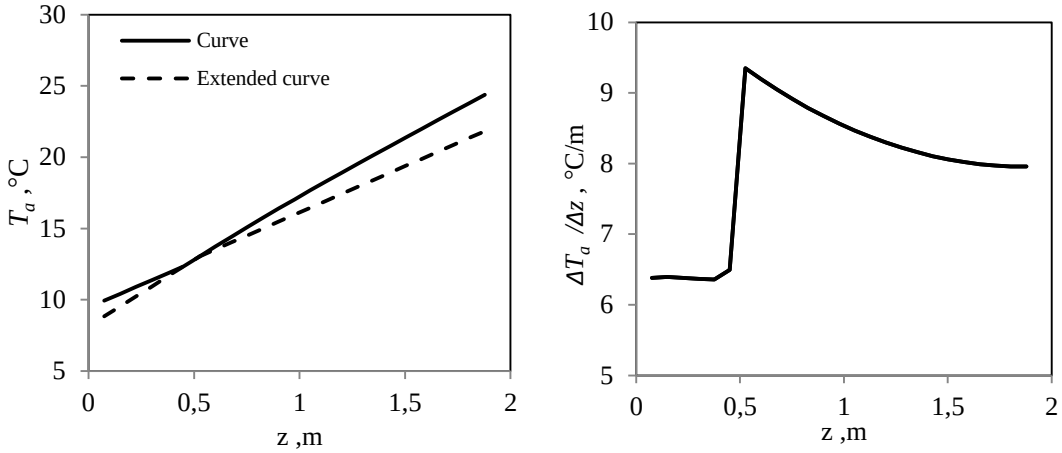

(a) Air temperature

(b) Air temperature gradient

Figure 4.2: Air temperature and gradient over fill height with supersaturated air

It can be seen from Figure 4.2 that the air temperature gradient increases by 45% when the air becomes supersaturated. In Eq. (4.3) for the energy source term, one of the terms is the gradient, or source, of humidity of saturated air (S_{wsa}). This term is calculated by the difference in empirically determined saturated humidity using the air temperature, Eq. (4.5). Therefore, an increase in air temperature gradient results in an increase in saturated humidity gradient. At the point of transitions between unsaturated and supersaturated air, only the gradient of unsaturated air is known. Using the gradient for the unsaturated air causes an over prediction in energy source. When this over prediction occurs, the CFD solution becomes unstable and divergences. This problem can be avoided by introducing a transition factor (α_{ss}). The transition factor can be used to adjust the saturated humidity gradient at transition. Energy source term with the transition factor can be written,

$$S_q = \left\{\left(\frac{Me}{L_{fi}}\right) G_w \left[Le_f c_{pma}(T_w - T_a)c_{pma} + (w_{sw} - w_{sa})\left[i_{fg(T_w)} + c_{pw}(T_w - T_a)\right]\right] - \alpha_{ss} S_{wsa} i_{fg(T_a)}\right\}_{(i,j)} \quad (4.9)$$

In Figure 4.3 the energy source (S_q) is given with and without the transitions factor, for the same case as in Figure 4.2.

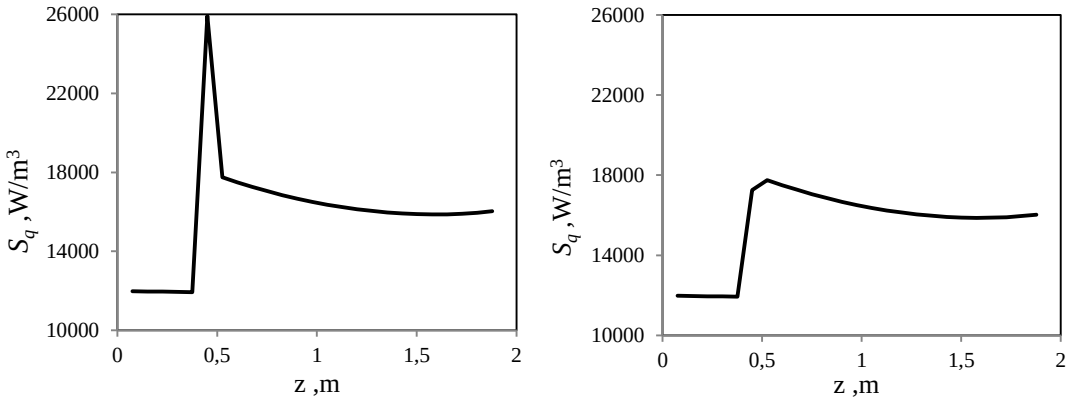

(a) Energy source (S_q), W/m^3, without transition factor ($\alpha_{ss} = 1.0$)

(b) Energy source (S_q), W/m^3, with transition factor ($\alpha_{ss} = 1.4$)

Figure 4.3: Energy source with (b) and without (a) transition coefficient for supersaturated air

It is clear from the Figure 4.3 that the transition factor makes a large difference to the solution. This results in a more stable transition, allowing the solutions to converge.

4.2.3 Three-dimensional model

The Reuter model can be applied to a three dimensional fill space without making any significant changes. Horizontal water flow is assumed to be none ($G_{w,x} = 0$ kg/sm^2 and $G_{w,y} = 0$ kg/sm^2), thus an extra dimension does not affect the discretization in the UDF. ANSYS-*Fluent*® is programmed to solve two and three dimensional flows and with source terms given volumetrically, the air flow can be modelled without any major additions.

For unsaturated air, the only addition is that the UDF loops around six faces of a three dimensional cell to find the upstream cell. For supersaturated air the gradient or source of saturated air humidity will have to be determined with the extra dimension as well. The saturated humidity source for supersaturated air in three dimensions can be determined from the following,

$$S_{wsa} = \left[\frac{G_{a,x}}{\Delta x}\left(w_{sa(i,j,k)} - w_{sa(i,j-1,k)}\right) + \frac{G_{a,z}}{\Delta z}\left(w_{sa(i,j,k)} - w_{sa(i-1,j,k)}\right) + \frac{G_{a,y}}{\Delta y}\left(w_{sa(i,j,k)} - w_{sa(i,j,k-1)}\right)\right] \tag{4.10}$$

4.3 CFD model of a wet-cooling tower fill

Two-dimensional computational flow simulations of the CFD model are meshed with a structured grid (quadrilateral) with 0.05m x 0.05m cells. Computational domains for the cross- and counterflow cases are presented in Figure 4.4.

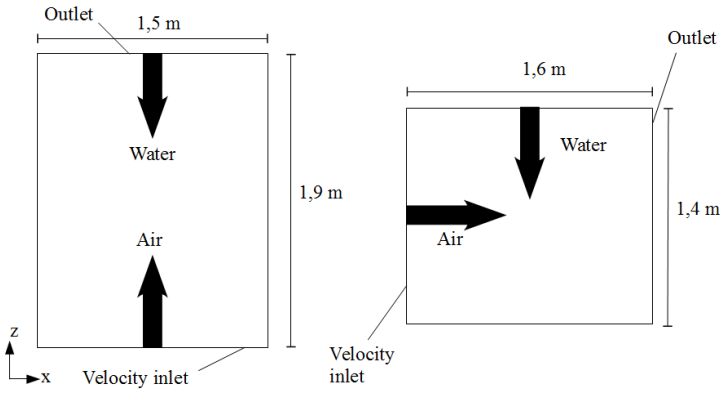

(a) Counterflow (b) Crossflow

Figure 4.4: Computational domains for wet-cooling tower fills

The counterflow domain resembles the case given by Kröger (2004). The crossflow domain is not based on any specific case and is only used for demonstration in this thesis. Horizontal length is made longer than the vertical length to increase the difference between the air inlet and outlet.

To get cross-counterflow conditions, velocity component for air are fixed in every cell. By fixing the velocity in every cell, momentum and continuity equations of the ANSYS-*Fluent*® solver are disabled. The cross-counterflow case is modelled with the same domain as the crossflow case, for convenience in solution setup, with air flowing at 45° through the fill. The cross-counterflow computational domain is presented in Figure 4.5.

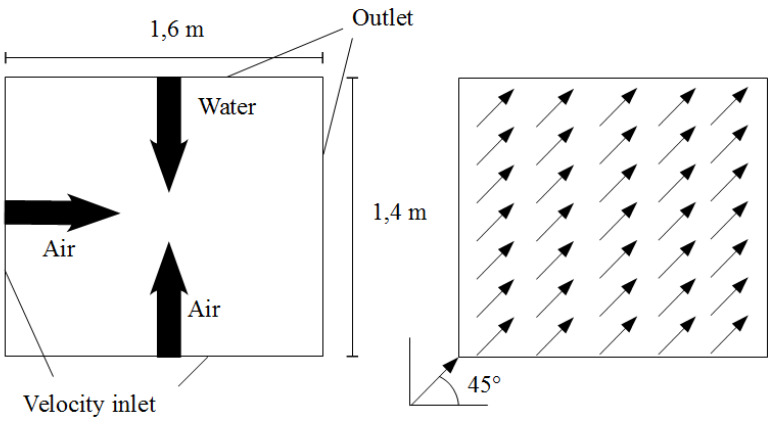

(a) Cross-counterflow (b) Fixed velocity (45°)

Figure 4.5: Computational domain for a cross-counterflow fill

Three-dimensional fill cases are presented with a rectangular cooling tower fill and sector from a circular cooling tower. The rectangular block is meshed with structured hexahedral cells (0.1 m x 0.1m x 0.1m) and the sector with a cut cell mesh of the same size. Computational domains for the three-dimensional cases are presented in Figure 4.6 and 4.7. The rectangular block is modelled with constant airflow angle of 45° in all directions.

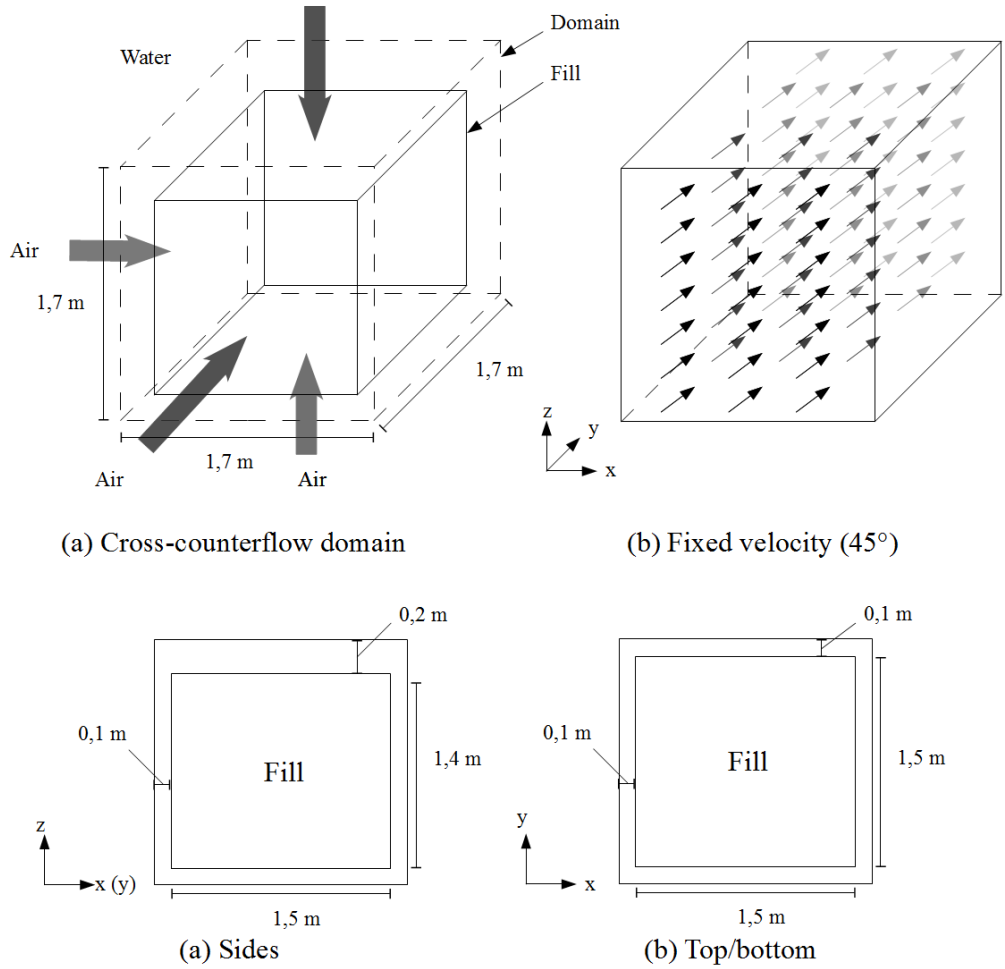

Figure 4.6: Computational domain for a three-dimensional rectangular cross-counterflow fill

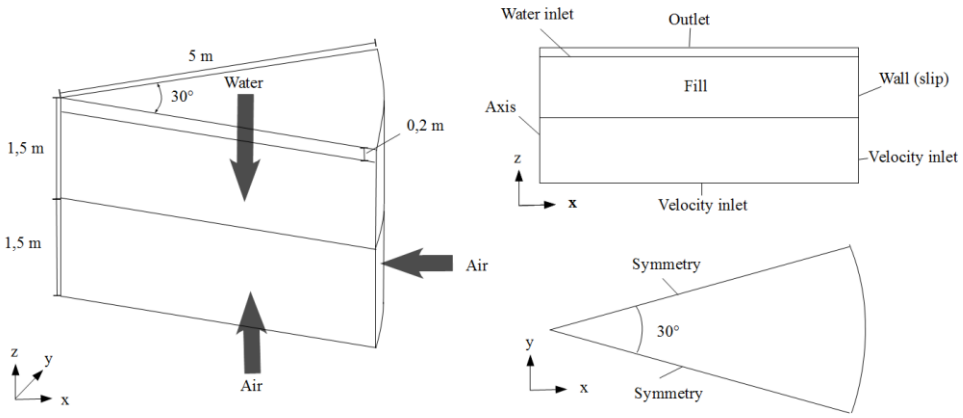

Figure 4.7: Computational domain for a sector of a circular cooling tower

The three dimensional rectangular block in Figure 4.6 does not have all sides of the same length to better distinct between the top and the sides of the domain. The aim the wedge model is only to demonstrate that the Reuter model can be used for circular cooling tower. To reduce modelling time, dimensions are made smaller than in a typical NDWCT. In a circular cooling tower rain zone is usually several times higher than the fill height to get sufficient mass flow rate of air in the fill. To accommodate for the small size of the current domain, and the fact that heat and mass transfer in the rain zone is not modelled, air is allowed to flow in at the bottom and side to get differential equations valid in zones where air is not saturated.

ANSYS-*Fluent*® is used to solve equations for conservation of momentum, mass, energy and species mixing by applying the two- and three dimensional double precision steady state solver. In cases where velocity is not fixed (counterflow and 3D wedge) the *k-ε* realizable turbulence model is applied and SIMPLE algorithm used for pressure-velocity coupling. Second order upwind discretization is applied to all governing equations, including water temperature and flow rate within the UDF.

4.4 CFD results

4.4.1 Counterflow fill

Data presented for the counterflow case is based on conditions from Table 2.1 (example 4.3.1 in Kröger, 2004) with fill height of 1.9 m instead of 1.878 m. ANSYS-*Fluent*® results for the counterflow fill are presented for an inlet air velocity of v_{av} = 1.487 m/s (G_a= 1.843 kg/sm^2). The airflow is essentially vertical and properties of water and air do not vary horizontally. Results can therefore be presented as one dimensional. Table 4.1 gives comparison of main properties from ANSYS-*Fluent*® and Scilab with Poppe ($\beta_{Me} = 0$ and Le_f according to Eq. (2.41)) and Merkel assumptions ($\beta_{Me} = 1$ and Le_f = 1).

The results in Table 4.1 compare well. With Poppe assumptions the difference between ANSYS-*Fluent*® and Scilab is less than 0.1 % in cooling range, 0.2% for water flow rate, 0.5 % in air temperature and 1.0 % in humidity. With Merkel assumptions the difference is the same or less as for the Poppe assumptions.

Table 4.1: Counterflow results from ANSYS-*Fluent*® and Scilab with Poppe and Merkel assumptions

Model	Assumptions	Me/L_{fi} (m^{-1})	ΔT_w (°C)	ΔG_w (kg/sm^2)	ΔT_a (°C)	Δw [kg/kg]
Fluent	Poppe	0.391	11.96	0.02804	15.04	0.01540
Scilab	Poppe	0.391	11.97	0.02801	14.97	0.01525
Fluent	Merkel	0.365	11.99	0.02637	14.56	0.01448
Scilab	Merkel	0.365	12.00	0.02638	14.52	0.01436

The importance of applying the differential equations valid in the saturated zone is best analysed by comparison to a solution where differential equations valid in the unsaturated zone are applied in all zones. In Table 4.2 results for the same case are presented. The case is modelled with unsaturated governing equations throughout the domain, despite the air becoming supersaturated.

Table 4.2: Counterflow results using only unsaturated equations

Model	Assumptions	Me/L_{fi} (m^{-1})	ΔT_w (°C)	ΔG_w (kg/sm^2)	ΔT_a (°C)	Δw (kg/kg)
Scilab	Poppe	0.391	11.96	0.02730	12.09	0.01486
Scilab	Merkel	0.365	12.00	0.02586	12.16	0.01408

Results show that difference in applying the unsaturated equations only, or applying the equations for supersaturated air when it occurs, only have a significant influence on the air temperature. The influence on the cooling range prediction is less than 0.1%. Difference in air temperature prediction is about 20% between the supersaturated and unsaturated solutions.

Solving the differential equations valid in the saturated zone requires considerably more effort than solving the equations for the unsaturated zones. Solving the equations for saturated zones makes the solution more unstable, due to the rapid increase in energy source at the point of saturation (see Figure 4.3). To obtain a convergence, a supersaturated solution requires relaxation factors lower than for unsaturated solution, causing slower rate of convergence. The differential equations for saturated zones should therefore not be used unless an accurate prediction of the outlet air temperature is required, such as in a hybrid cooling tower.

4.4.2 Two dimensional crossflow and cross-counterflow fill

Data presented for the two dimensional crossflow and cross-counterflow cases is based on atmospheric pressure of 101325 Pa; an ambient air temperature of 288.15 K (15°C); absolute humidity of $w_i = 0.006423$ kg/kg (60% relative humidity and T_{wb} = 284.01 K); water inlet temperature of T_{wi} = 313.15 K (40°C); water inlet flow rate of G_{wi} = 3.0 kg/sm^2 and inlet air velocity magnitude of 2.0 m/s. Reuter (2010) used the same conditions for model verification, except for the water mass and air flow. The crossflow and cross-counterflow solutions are compared to the Scilab model used to evaluate performance in the previous chapters. The Merkel number is obtained using Eq. (2.44) with crossflow and counterflow curve fit constants (c_1, c_2, c_3 and c_4). In the cross-counterflow case the vertical and horizontal air velocity components are calculated from velocity magnitude and inlet airflow angle,

$$v_{a,x} = v_{av} \sin\theta, \tag{4.14}$$

$$v_{a,z} = v_{av} \cos\theta \tag{4.15}$$

The cross-counterflow airflow angle is assumed to be 45°, which results in vertical and horizontal velocity components ($v_{a,x}$ and $v_{a,z}$) of 1.414 m/s The dry-air mass velocity can then be calculated from the following,

$$G_a = \frac{\rho_a \sqrt{v_{a,x}^2 + v_{a,z}^2}}{(1+w)} \tag{4.16}$$

Using the curve fits constants given in Appendix B, a Merkel number of Me/L_{fi} = 0.76 for crossflow and Me/L_{fi} = 0.78 for cross-counterflow are obtained. Vertical and horizontal velocity components are fixed in the ANSYS-*Fluent*® solver to get an accurate comparison of ANSYS-*Fluent*® and Scilab in cross-counterflow. When the energy of the air increases, the temperature increases and density decreases. Mass flow rate of air is defined as $m_a = \rho v A$ and decreasing density result in increased air velocity. With the velocity fixed and the density decreasing the mass flow rate decreases across the computational domain, resulting in an under prediction of water cooling. To get an accurate comparison between ANSYS-*Fluent*® and Scilab, the density is calculated locally in every cell in the Scilab model and the density used to get a mass velocity with fixed velocity components. The result is the same loss of mass flow rate in the Scilab model as in the ANSYS-*Fluent*®. This approach contradicts conservation of mass and is only used to get a comparison of heat and mass transfer between the models. It should not be used in any practical purpose and was not used to generate any of the previously presented data in this thesis.

Comparison between the Scilab and ANSYS-*Fluent*® models for crossflow and cross-counterflow is given graphically for the difference in water and air properties across the fill in Figures 4.8 to 4.12.

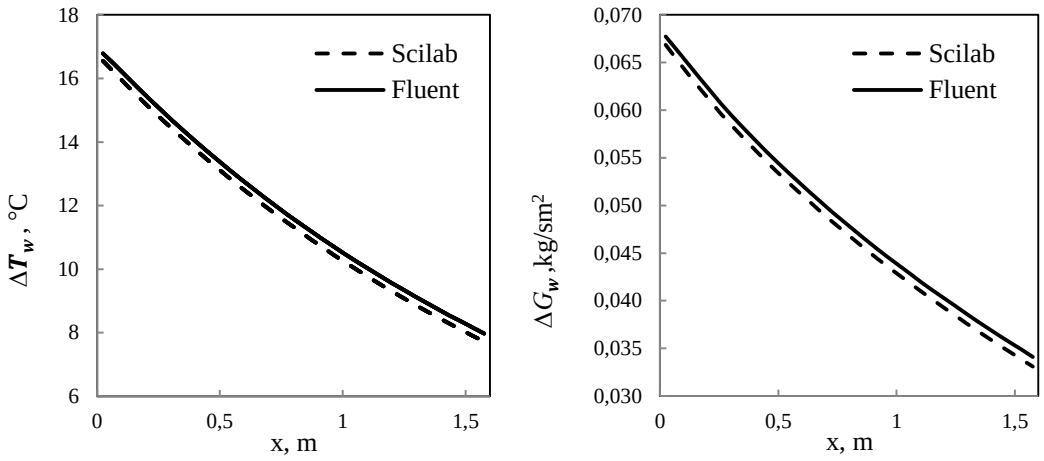

(a) Water temperature (b) Water mass velocity

Figure 4.8: Water temperature and mass velocity across the crossflow fill

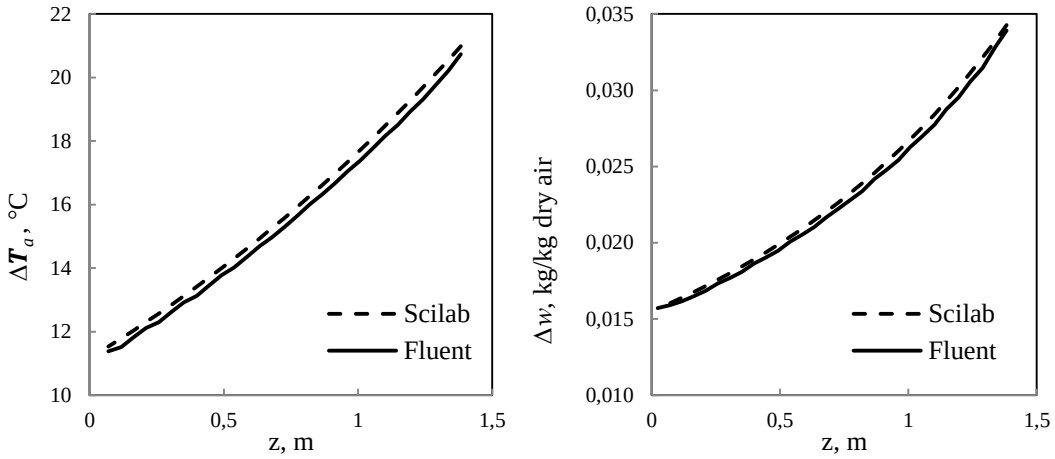

(a) Air temperature (b) Humidity

Figure 4.9: Air temperature and humidity over the crossflow fill

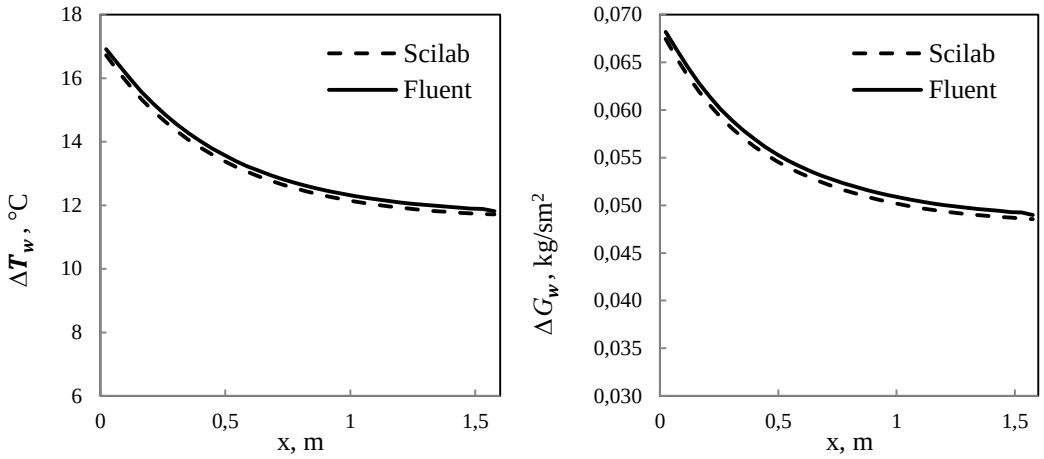

(a) Air temperature (b) Humidity

Figure 4.10: Water temperature and mass velocity across the cross-counterflow fill

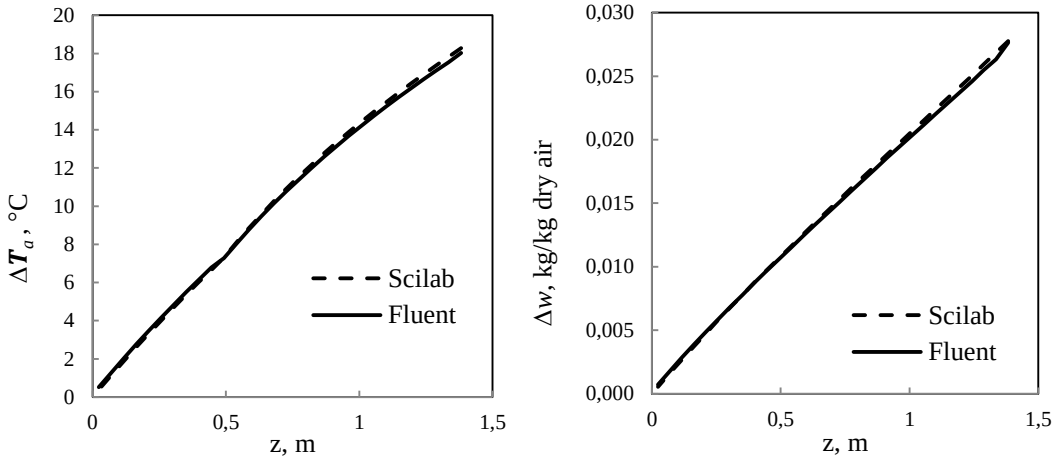

(a) Air temperature (b) Humidity

Figure 4.11: Air temperature and humidity over (horizontally) the cross-counterflow fill

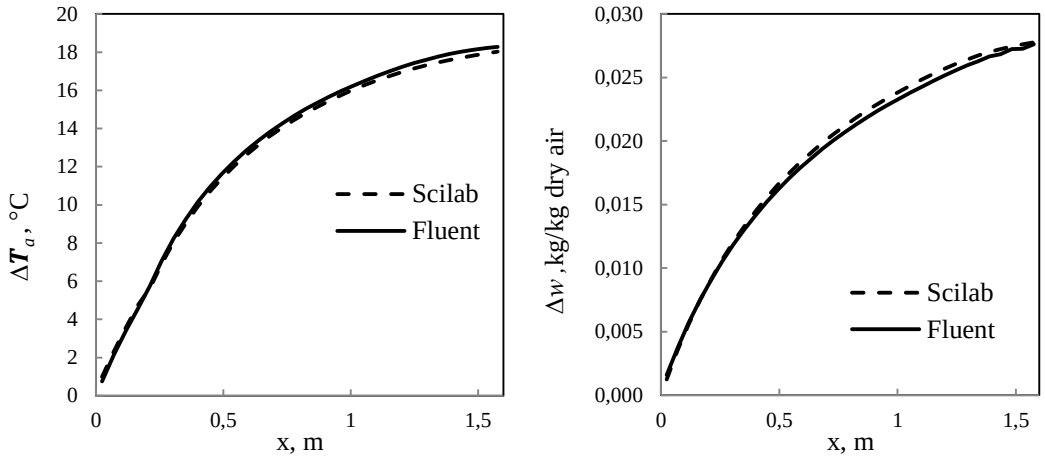

(a) Air temperature (b) Humidity

Figure 4.12: Air temperature and humidity across (vertically) the cross-counterflow fill

The Figures show that there is a small difference between the ANSYS-*Fluent*® and Scilab model in crossflow and cross-counterflow. The difference is approximately 2.0% for all the properties in the crossflow fill. For the cross-counterflow fill the difference between the air properties is 1.0% for the air temperature, 1.4% for humidity and 1.3% for the water temperature and mass velocity. The Reasons for this difference are partly numerical error, although an increase refinement of both models only yielded a marginal decrease in the error. Grid independent solutions for the cross-counterflow model gave a difference of 1.0% in cooling.

4.4.3 Three dimensional cross-counterflow fill

Data presented for the three dimensional cross-counterflow cases is based on the same conditions as the two dimensional cross-counterflow cases, with the exception that inlet air velocity magnitude is 2.6 m/s. The cross-counterflow airflow angle is assumed to be 45° in all direction, which results in all velocity components ($v_{a,x}$, $v_{a,y}$ and $v_{a,z}$) of 1.5 m/s. The Merkel number is assumed to be Me/L_{fi} = 0.96 m^{-1} and momentum losses are assumed to be none. The reason for the momentum loss not being accounted for is that, these cases only serve as demonstrations of modelling heat and mass transfer in three-dimensions and flow is not specifically analysed.

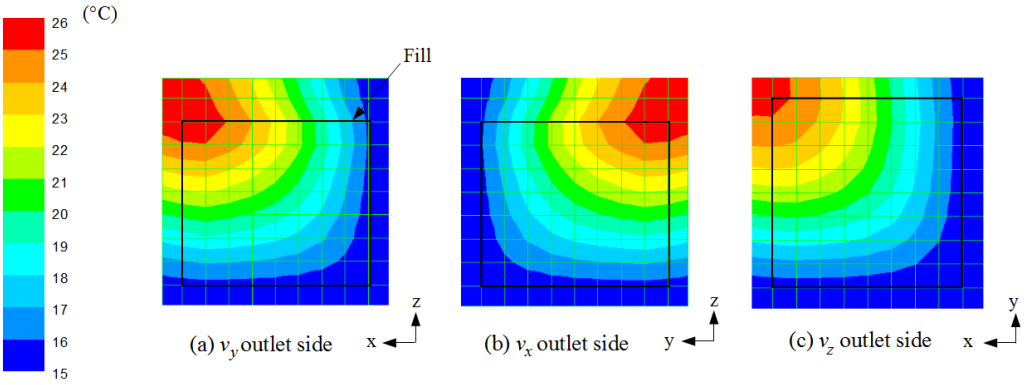

Figure 4.13: Air temperature profiles at outlets of the three-dimensional cross-counterflow fill

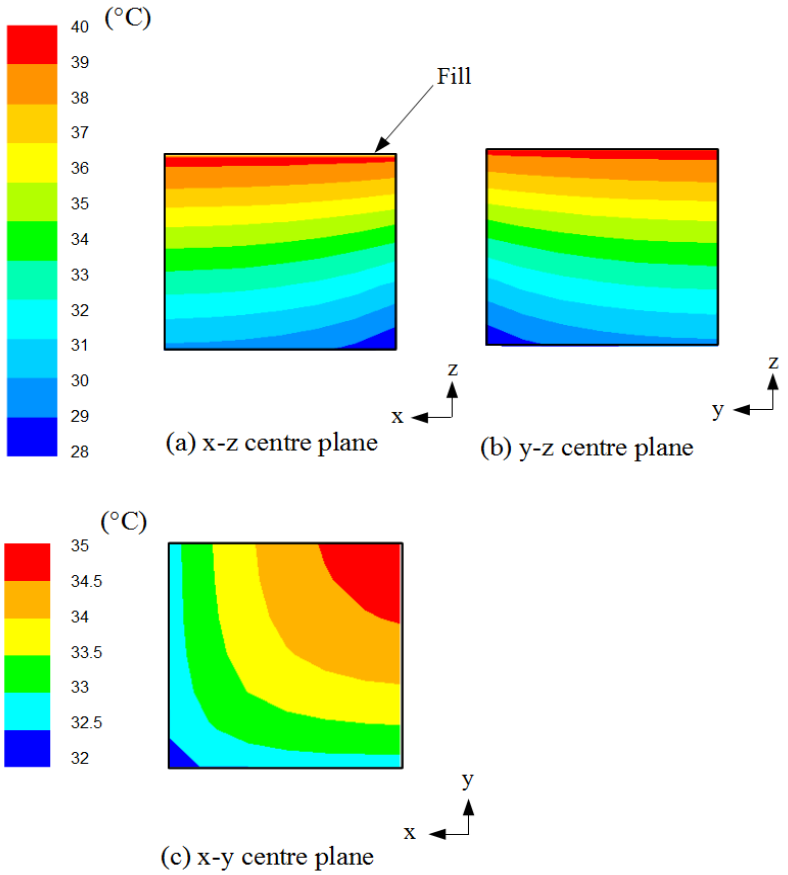

Figure 4.14: Water temperature profiles in three-dimensional cross-counterflow fill

Air temperature profiles are presented graphically at the air outlets (two sides and top) in Figure 4.13. The water temperature profiles are presented graphically at

three observation planes, two vertical centre planes and one horizontal centre plane. Water temperature profiles are presented in Figure 4.14.

From Figures 4.13 and 4.14 it can be seen that the heat and mass transfer is taking place in three dimensions.

4.4.4 Three-dimensional sector model of circular cooling tower

Data presented for the wedge is based on the same conditions as the rectangular block, except for air velocity. Air entering at the bottom of the domain (counterflow) has initial velocity of 2.0 m/s and air entering the side (crossflow) has initial velocity of 1.5 m/s. Properties are presented for the two symmetry sides of the wedge and a plane parallel to the z-axis at 4 m from the origin of the domain. Observatory planes are presented in Figure 4.15.

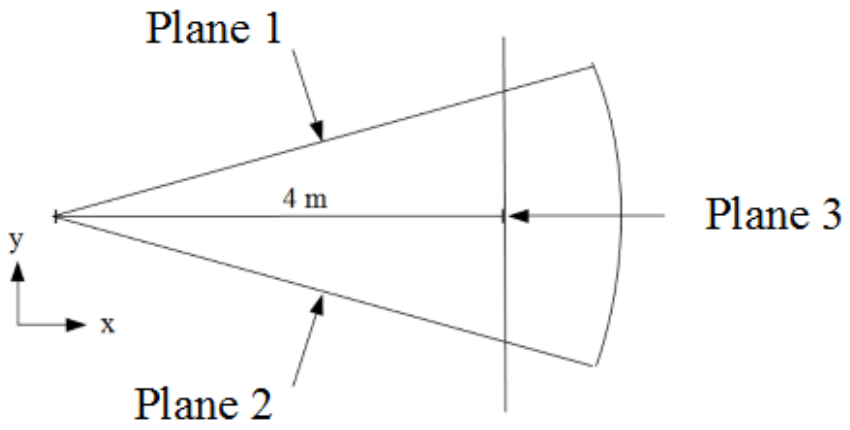

Figure 4.15: Observation planes in the sector model of a circular cooling tower

Velocity magnitude is presented for the three observation planes and with an isometric vector plot. Velocity profiles are given in Figure 4.16 and 4.17. The air and water temperature profiles are presented for the three planes in Figures 4.18 – 4.19.

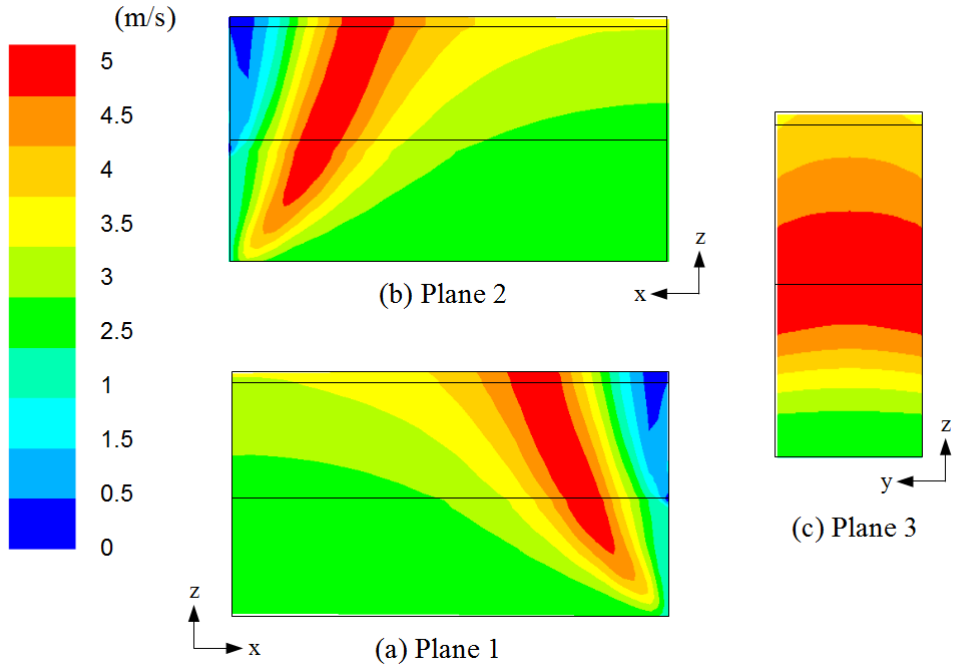

Figure 4.16: Velocity magnitude profiles in the sector model of a circular cooling tower

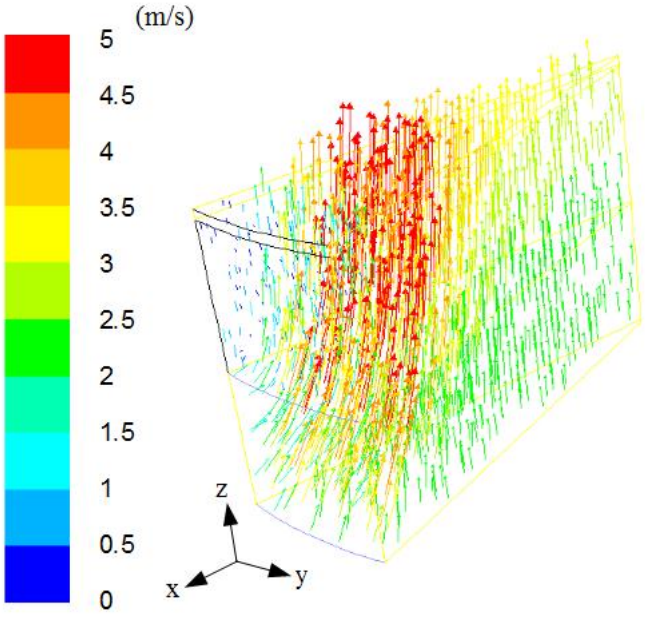

Figure 4.17: Velocity magnitude vectors in the sector model of a circular cooling tower

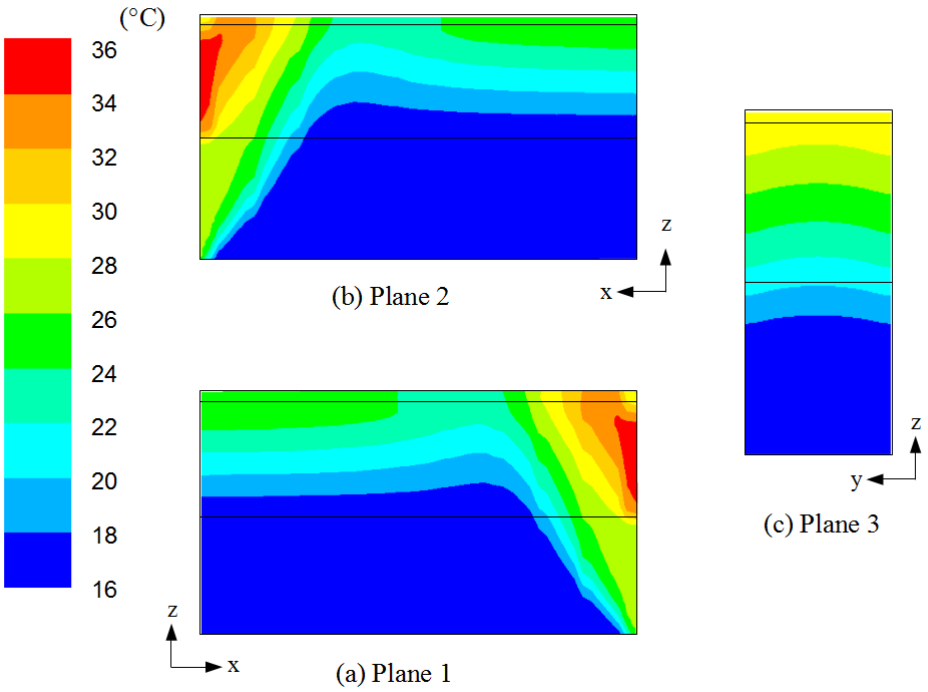

Figure 4.18: Air temperature profiles in the sector model of a circular cooling tower

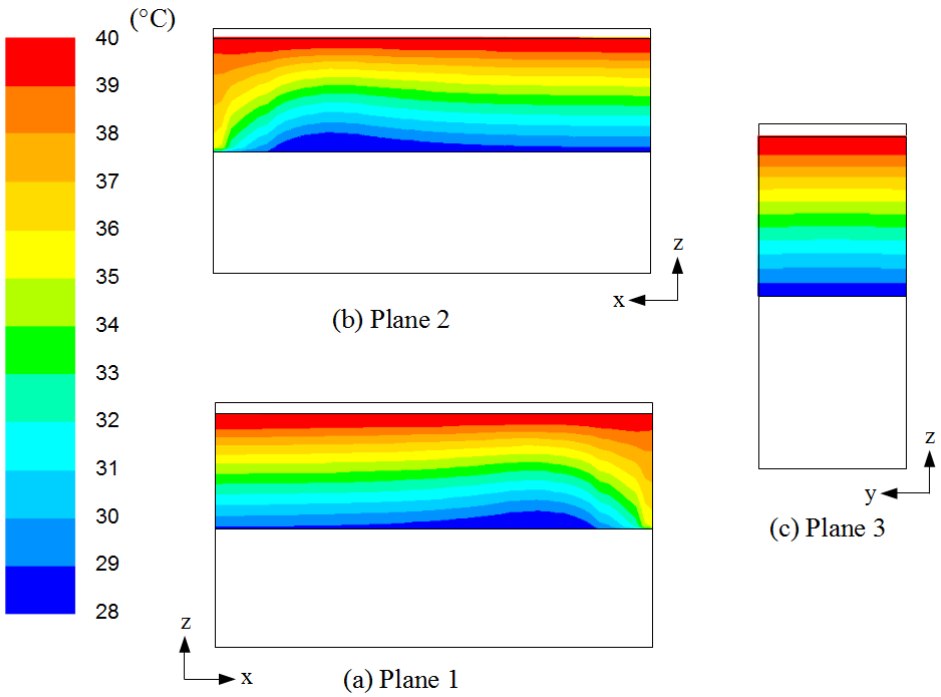

Figure 4.19: Water temperature profiles in the sector model of a circular cooling tower

The temperature and velocity profiles on the sides show little or no variation between the two, despite the three dimensional airflow. If the plane going through the domain is examined it can be seen that there is a minor variation in cooling across the fill from left to right. This matches the minor difference in velocity magnitude in the same plane in Figure 4.19. This indicates that the heat transfer is taking place in all three dimensions.

4.5 Discussion of results and conclusions

A description on how to implement the Reuter model with the second order upwind method in ANSYS-*Fluent*® is presented. Modelling supersaturated air is discussed and solutions to overcome divergence problems when the point of transitions between un- and supersaturated state occurs are presented.

Two-dimensional counterflow, crossflow and cross-counterflow rectangular fills are modelled in ANSYS-*Fluent*®. The ANSYS-*Fluent*® results are compared to the Reuter model solved with Scilab. The cases are modelled for un- and supersaturated air. A detailed comparison in a tabular form is given for the counterflow case and comparison of crossflow and cross-counterflow cases is presented graphically.

A three dimensional rectangular block of fill is modelled as well as a sector from a circular cooing tower. Air temperature profiles are given for the two outlet sides and top. Water temperature profiles are given for the fill at two planes vertically and one horizontally through the fill centre.

Main results from the fill modelling were as follows:

- By storing gradient for water temperature and mass velocity in UDM a second order discretization, equivalent of the second order method presented in chapter 3 can be applied in the UDF.
- Sudden increase in energy source at the point of transition between unsaturated and supersaturated air causes the numerical solutions to become unstable and diverge. To solve the problem a transition coefficient is introduced. The transitions coefficient is only applied to the first cell that become supersaturated and allows for a smoother transition.
- A detailed comparison between ANSYS-*Fluent*®/UDF and Scilab for a counterflow fill gave a difference of less than 0.1 % for cooling with both Merkel and Poppe assumptions. Difference in humidity and air temperature was between 0.5% and 1.0%. Difference in crossflow and cross-counterflow fill ranged between 1.0% and 2.0%.
- Difference in modelling fill with unsaturated equations despite the air becoming supersaturated, was less than 0.1% for water cooling, water flow rate and humidity. The difference in air temperature was more than 20%.
- Modelling of a three-dimensional block shows that both air and water were affected by change in three-dimensions and behaviour of water and

air temperature profile in two-dimensional plane views, gave good resemblance to the two dimensional graphs of the cross-counterflow case.

- The three-dimensional circular cooling tower sector model showed that in the presented form, the Reuter model can effectively be used for three dimensional CFD models of circular cooling towers with air flowing in cross-counterflow to the water.

With the second order method implemented in the UDF, the grid size can be reduced. With an element size of 0.1 m, a fill in circular cooling tower with 1.5 m fill height and 50 m in diameter, such as is common in natural draft wet-cooling towers, can be modelled with approximately 3 million cells. Obtaining a solution through an iterative procedure for a solutions domain of 3 million cells can be done within acceptable time limits. To put these numbers into perspective, the same solutions domain, with a cell size of 0.025m would require about 190 million cells, i.e. approximately 63 time more cells.

5 CONCLUSION AND RECOMMENDATION

5.1 Conclusions

In order to use the performance prediction model presented by Reuter (2010) to better study wet-cooling towers and widening the model's range of application, the following objectives were given in Chapter 1:

- Compare the Reuter model to the existing fill performance models of Merkel, e-NTU and Poppe for both cross- and counterflow to determine if transfer characteristics (Merkel numbers) obtained using Merkel, e-NTU and Poppe methods can be used directly in the Reuter model for performance prediction.
- Verify that the Reuter model gives the same results as when implemented in ANSYS-*Fluent*® as when programmed for fill performance evaluation of test data.
- Verify that the Reuter model results in the same outlet conditions for supersaturated air, when implemented in ANSYS-*Fluent*® as when programmed for fill performance evaluation of test data.
- Suggest improvement to the solution method employed by Reuter (2010) to increase accuracy.
- Model a three-dimensional block of fill with ANSYS-*Fluent*®

Work done to achieve these goals is summarized and discussed below:

First objective: Chapter 2 discusses and compares the cross- and counterflow Merkel, e-NTU and Poppe methods to the Reuter model. The Reuter model is found to result in the same performance prediction as the Poppe model if the same Lewis factor (Le_f) is used and the air is assumed to be in either cross- or counterflow. By setting the presented constant, β_{Me} and Lewis factor to 1 the Reuter model also results in the same Merkel number as the Merkel and e-NTU method. The models are verified with a sample case used by Kloppers (2003, 2005a and 2005b) and Kröger (2004, example. 4.3.1). Further verification is given by using performance curves of a trickle fill in cross- and counterflow. The performance curves are obtained from a range of tests conducted in the cross- and counterflow test facility at Stellenbosch University. Performance characteristics, data and descriptions of the test facility are given in Appendix B.

Second objective: Chapter 3 discusses and compares solution methods presented for the Merkel, Poppe and Reuter models. A second order upwind method, equivalent of the second order upwind method used by ANSYS-*Fluent*® is presented. It is demonstrated with examples that by applying the second order method, element size can be increased by a factor of 4 to 10, to give equivalent results to the first order method. By applying the second order upwind method a cell (element) size of 0.1 m can be expected to give grid independent solutions in both cross- and counterflow for most practical cases.

Third and fourth objectives: In Chapter 4, a two-dimensional counterflow case is modelled in ANSYS-*Fluent*® where the air becomes supersaturated. The case is modelled with both the Merkel ($\beta_{Me} = 1$ and $Le_f = 1$) and the Poppe ($\beta_{Me} = 0$ and Le_f according to Eq. (2.41)) assumptions. A transitional coefficient α_{ss} is introduced to the governing equations to enable a smooth transition between unsaturated and supersaturated source term equations. The result is compared to the same case with the Reuter model in programmed in Scilab. The difference in cooling range (ΔT_w) and evaporation (ΔG_w) is found to be less than 0.2%, whereas the difference in air temperature change (ΔT_a) is 0.5% and humidity ratio change (Δw) is 1.0%. Additionally, a two-dimensional simulation is given for cross- and cross-counterflow with a graphical comparison. The supersaturation equations can make the solution become unstable in cross- and cross-counterflow and should only be used if accurate predictions of air outlet conditions are necessary.

Fifth objective: In Chapter 4, it is demonstrated that the Reuter model can be used to model a rectangular fill and a sector from a circular cooling tower in three-dimensions with the unsaturated air. This can be done without making any significant modification to the model, because the water property equations are essentially one-dimensional. The source terms for energy and humidity are given per unit volume so the same values can be used for both two- and three-dimensions simulations. With supersaturated air the equations for energy source terms are functions of the air flow and the same value cannot be used for two- and three-dimensional simulations. To simulate a cooling tower with supersaturated air in three-dimensions all three velocity components are used in the user defined functions to calculate the source terms.

This thesis provides information for other researchers to use and apply the Reuter model. From the experience gained in this research, modelling of fill with supersaturated air is the most complicated aspect of simulating wet-cooling towers with CFD. With the solution provided in this thesis, those implication can be overcome, providing opportunities for further research on modelling of hybrid cooling towers with CFD.

5.2 Further work and recommendations

With the additions to the Reuter model given in this thesis, the model can use existing fill performance data (generally from the Merkel or e-NTU method) and design specifications to analyse performance of cooling towers.

With an improved solution method, the model can now be used in a three-dimensional model of a wet-cooling tower simulate cross-wind effects. Furthermore, the Reuter model is the only model that can effectively model a cooling tower with a splash or a trickle fill hanging into the rain zone.

With supersaturation implemented, the model can now also be used to model hybrid cooling tower, with induced, forced and fan assisted natural draught.

APPENDIX A – Sample calculations for evaluation of fill performance

A.1 Introduction

Sample calculations are given for the Reuter method of analysis for cross-counterflow fill as well as a case 2 crossflow e-NTU method. Refer to Kröger (2004) for an e-NTU case 1 counterflow and Merkel equation sample calculation, (ex. 4.3.1 and 4.3.2). Refer to Kloppers (2003) for a detailed derivation and a sample calculation using the Poppe method with 4th order Runge-Kutta discretization for the same counterflow case (the expanded metal fill). All thermal properties are calculated according to Appendix A in Kröger (2004).

A.2 Reuter method of analysis

A sample calculation for the Reuter method is presented. Two cells are calculated for demonstration, an unsaturated boundary cell and a supersaturated internal cell. The expanded metal fill sample case presented in Table A.1 (ex. 4.3.1 in Kröger, 2004) is solved with the second order upwind method, assuming constant air flow angle of 45°.

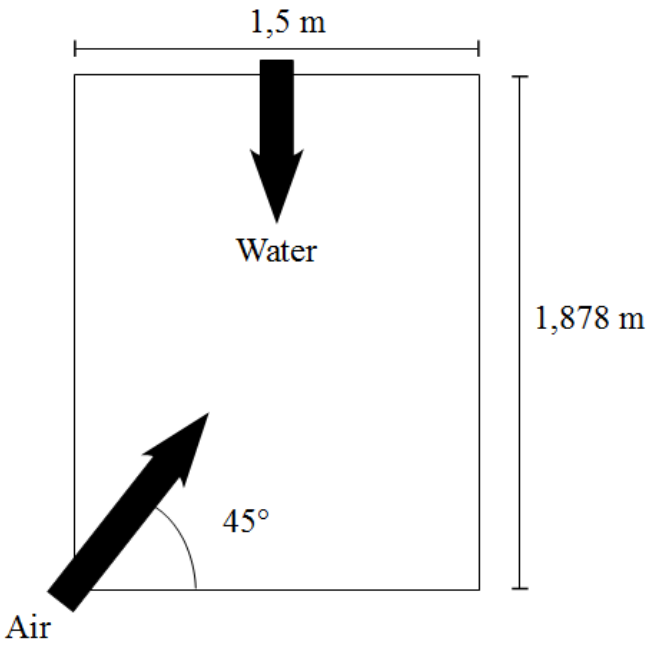

Figure A.1: Computational domain of a cross-counterflow fill with a 45° air flow angle

Table A.1: Measured conditions from an expanded metal fill performance test

Measured conditions		
Atmospheric pressure (p_a)	101712	N/m^2
Air inlet temperature (T_{ai})	9.70	°C
Air inlet temperature (T_{wb})	8.23	°C
Dry air mass velocity (G_a)	1.837	kg/sm^2
Water inlet temperature (T_{wi})	39.67	°C
Water outlet temperature (T_{wo})	27.77	°C
Water mass flow rate (m_w)	3.999	kg/s
Static pressure drop across fill	4.5	N/m^2
Fill height (L_{fi})	1.878	m
Fill length and depth	1.5	m

The inlet air has a humidity of $w_i = 0.006163$ kg/kg dry air (relative humidity of 82.4%) and dry air enthalpy of $i_{ma} = 25292.94$ J/kg.

All thermal properties are calculated according to the equations in Appendix A in Kröger (2004). The computational domain is split into 6x5 intervals ($\Delta z = 0.313$ and $\Delta x = 0.300$ m). A Merkel number of 0.373 per meter fill is obtained by solving the Reuter model with Poppe assumptions.

Mass velocities are calculated accordingly,

$$G_{wi} = \frac{m_w}{A_{bt}} = \frac{3.999}{2.25} = 1.777 \text{ kg/sm}^2$$

$$G_{az} = G_a \sin\left(\frac{\theta}{180}\pi\right) = 1.837 \sin\left(\frac{45}{180}\pi\right) = 1.299 \text{ kg/sm}^2$$

$$G_{ax} = G_a \sin\left(\frac{\theta}{180}\pi\right) = 1.837 \cos\left(\frac{45}{180}\pi\right) = 1.299 \text{ kg/sm}^2$$

Unsaturated boundary - Cell (1,1)

Upstream cells of cell (1,1) are only the boundaries, $T_{wo(1)}, G_{wo(1)}, T_{ai}, w_i$. The converged solution results in the following properties of water and air,

$T_{w(1,1)}$ = 300.5 K $T_{a(1,1)}$ =283.5 K $w_{(1,1)}$ =0.00679 kg/kg $G_{w(1,1)}$ = 1.752 kg/sm^2

Table A.2: Thermal properties of unsaturated air determined from empirical relations

Thermal Property	Function of	Value	Unit
Specific heat of dry air (c_{pa})	T_a	1006	J/kg K
Specific heat of vapour (c_{pv})	T_a	1871	J/kg K
Specific heat of air-vapour mixture(c_{pma})	T_a,w	1019	J/kg K
Specific heat of water (c_{pw})	T_w	4180	J/kg K
Partial pressure of water vapor (p_{vsw})	T_w	3614	N/m^2
Partial pressure of dry air (p_{vsa})	T_a	1254	N/m^2
humidity of air saturated with water vapor (w_{sa})	p_{vsw},T_a,	0,00780	kg/kg
humidity of saturated air (w_{sw})	p_{vsa},T_w	0,02313	kg/kg
Latent heat of vaporization (i_{fg})	T_w	2437052	J/kg

The saturation humidity (w_{sa}) is lower than the absolute humidity $w_{(1,1)}$ making the air unsaturated. The Lewis factor for unsaturated air can be calculated according to Eq. (2.41)

$$Le_f = 0.865^{\frac{2}{3}} \frac{\left(\frac{w_{sw} + 0.622}{w_{(i,j)} + 0.622} - 1\right)}{ln\left(\frac{w_{sw} + 0.622}{w_{(i,j)} + 0.622}\right)} = 0.920$$

Source terms for unsaturated air can be calculated with Eq. (3.1), (3.2) (3.3) and (3.4) as presented in chapter 3.

$$S_{Gw} = G_w \left(\frac{Me}{L_{fi}}\right) (w_{sw} - w) = 0.0060981$$

$$S_{Tw} = \left(\frac{Me}{L_{fi}}\right) \frac{c_{pma}}{c_{pw}} \left[Le_f (T_w - T_a) + \frac{i_{fg(T_w)}}{c_{pma}} (w_{sw} - w)\right] = 4.976928$$

$$S_w = G_w \left(\frac{Me}{L_{fi}}\right) (w_{sw} - w) = 0.0033447$$

$$S_{Ta} = G_w \left(\frac{Me}{L_{fi}}\right) (T_w - T_a) \left[Le_f + \frac{c_{pv}}{c_{pma}} (w_{sw} - w)\right] = 10.548709$$

The above source term can now be used to solve discretized form of the governing equations, Eq. (3.22), (3.23) (3.24) and (3.25),

$$G_{w(1,j)} = G_{wo} + \frac{S_{Gw(1,j)}}{2}\Delta z = 1.752$$

$$T_{w(1,j)} = T_{wo} + \frac{S_{Tw(1,j)}}{2}\Delta z = 300.5$$

$$w_{(1,1)} = w_i + \frac{S_{w(1,1)}\,\Delta z}{2\,G_{a,x}\frac{\Delta z}{\Delta x} + 2\,G_{a,z}} = 0.00679$$

$$T_{a(1,j)} = T_{ai} + \frac{S_{Ta(1,1)}\,\Delta z}{2\,G_{a,x}\frac{\Delta z}{\Delta x} + 2\,G_{a,z}} = 283.5$$

Supersaturated internal cell - Cell (4,4)

The converged solution results in the following properties of water and air for cell (4,4),

$T_{w(4,4)}$ =307.6 K $T_{a(4,4)}$ =292.7 K $w_{(4,4)}$=0.01518 kg/kg $G_{w(4,4)}$ = 1.765 kg/m^{2}s

Table A.3: Thermal properties of supersaturated air determined from empirical relations

Thermal Property	Function of	Value	Unit
Specific heat of dry air (c_{pa})	T_a	1007	J/kg K
Specific heat of vapour (c_{pv})	T_a	1879	J/kg K
Specific heat of air-vapour mixture(c_{pma})	T_a,w	1035	J/kg K
Specific heat of water (c_{pw})	T_w	1037	J/kg K
Partial pressure of water vapor (p_{vsw})	T_w	4177	N/m^2
Partial pressure of dry air (p_{vsa})	T_a	5458	N/m^2
humidity of air saturated with water vapor (w_{sa})	p_{vsw},T_a,	2266	kg/kg
humidity of saturated air (w_{sw})	p_{vsa},T_w	0.01424	kg/kg
Latent heat of vaporization (i_{fg})	T_w	0.03546	J/kg

The saturation humidity (w_{sa}) is higher than the absolute humidity ($w_{(4,4)}$) making the air supersaturated. The Lewis factor for supersaturated air can be calculated according to Eq. (2.42),

$$Le_f = 0.865^{\frac{2}{3}} \frac{\left(\frac{w_{sw} + 0.622}{w_{sa} + 0.622} - 1\right)}{ln\left(\frac{w_{sw} + 0.622}{w_{sa} + 0.622}\right)} = 0.923$$

Source terms for supersaturated air can then be calculated with Eq. (3.6), (3.7) (3.8) and (3.9) as presented in chapter 3.

$$S_{Gw,ss} = G_w \left(\frac{Me}{L_{fi}}\right) (w_{sw} - w_{sa}) = 0.00792$$

$$S_{Tw,ss} = \left(\frac{Me}{L_{fi}}\right) \frac{c_{pma}}{c_{pw}} \left[Le_f (T_w - T_a) + \frac{i_{fg(T_w)} + \beta_{Me} c_{pw} T_w}{c_{pma}} (w_{sw} - w_{sa})\right] = 5.86$$

$$S_{w,ss} = G_w \left(\frac{Me}{L_{fi}}\right) (w_{sw} - w_{sa}) = 0.01397$$

$$S_{Ta,ss} = (S_1 + S_2 - S_3) = 8.45$$

where S_1, S_2 and S_3 are according to Eq. (3.11), (3.12) and (3.13),

$$S_1 = G_w \left(\frac{Me}{L_{fi}}\right) \left[Le_f (T_w - T_a) \frac{c_{pma}}{c_{pma,ss}}\right] = 9.07$$

$$S_2 = G_w \left(\frac{Me}{L_{fi}}\right) \left[\frac{i_{fg(T_w)} + c_{pw}(T_w - T_a)}{c_{pma,ss}}\right] (w_{sw} - w_{sa}) = 33.45$$

$$S_3 = \frac{i_{fg(T_a)}}{c_{pma,ss}} \left[G_{a,x} \frac{\partial w_{sa}}{\partial x} + G_{a,z} \frac{\partial w_{sa}}{\partial z}\right] = 34.08$$

The above source term can now be used to solve discrete form of the governing equations. To solve the discrete equations, the values for neighbouring cells are needed,

$T_{w(3,4)}$ =305.8 K $T_{a(3,4)}$ =290.4 K $w_{(3,4)}$= 0.01301 kg/kg $G_{w(3,4)}$ = 1.760 kg/sm^2

$T_{w(2,4)}$ =304.1 K $T_{a(2,4)}$ =287.6 K $w_{(2,4)}$= 0.01045 kg/kg $G_{w(2,4)}$ = 1.756 kg/sm^2

$T_{a(4,3)}$ =290.9 K $T_{a(4,2)}$ =288.1 K $w_{(4,3)}$= 0.01347 kg/kg $w_{(4,2)}$ = 0.01102 kg/kg

With the above properties the discretized form of the governing equations can be solved in the form of Eq. (3.48) and (3.49)

$$T_{w(i,j)} = \frac{4\, T_{w(i-1,j)} - T_{w(i-2,j)} + 2\, S_{Tw(i,j)} \Delta z}{3} = 307.6 \text{ K}$$

$$G_{w(i,j)} = \frac{4\,G_{w(i-1,j)} - G_{w(i-2,j)} + 2\,S_{Gw(i,j)}\Delta z}{3} = 1.765\ \text{kg/sm}^2$$

$$T_{a(i,j)} = \frac{G_{a,x}\frac{\Delta z}{\Delta x}\left(4\,T_{a(i,j-1)} - T_{a(i,j-2)}\right) + G_{a,z}\left(4\,T_{a(i-1,j)} - T_{a(i-2,j)}\right) + S_{Ta(i,j)}\Delta z}{3\left(G_{a,x}\frac{\Delta z}{\Delta x} + G_{a,z}\right)}$$

$$= 292.7\ \text{K}$$

$$w_{(i,j)} = \frac{G_{a,x}\frac{\Delta z}{\Delta x}\left(4\,w_{(i,j-1)} - w_{(i,j-2)}\right) + G_{a,z}\left(4\,w_{(i-1,j)} - w_{(i-2,j)}\right) + S_{w(i,j)}\Delta z}{3\left(G_{a,x}\frac{\Delta z}{\Delta x} + G_{a,z}\right)}$$

$$= 0.01518\ \text{kg/kg}$$

Outlet conditions and Energy Balance

Outlet conditions are calculated in the following way,

$$T_{wi} = \frac{T_{w(6,1)} - T_{w(5,1)}}{2} + T_{w(6,1)} = \frac{311.37 - 308.49}{2} + 311.38 = 312.82\ K$$
$$= 39.67°C$$

Outlet conditions for the whole domain are given in Table A.4 to A.6.

Table A.4: Water outlet conditions at bottom of the cross-counterflow fill

Cell nr. (j)	1	2	3	4	5
G_{wo}	1.751	1.752	1.752	1.752	1.753
T_{wo}	299.7	300.5	301.1	301.5	301.8

Table A.5: Air outlet conditions at top of the cross-counterflow fill

Cell nr. (j)	1	2	3	4	5
$T_{ao,z}$	285.1	290.5	294.1	296.7	298.5
$w_{o,z}$	0.0089	0.0134	0.0170	0.0200	0.0222
$i_{mao,z}$	34173	49016	60961	70520	77927

Table A.6: Air Outlet conditions at side of the cross-counterflow fill

Cell nr. (i)	1	2	3	4	5	6
$T_{ao,z}$	284.2	287.7	291.2	294.1	296.5	298.5
$w_{o,z}$	0.00765	0.01068	0.01375	0.01672	0.01969	0.02207
$i_{mao,z}$	30459	40852	51175	60897	69631	77631

Energy of the air can be calculated by,

$$Q_a = mean\left(\frac{G_{a,z}}{A_{top}}\left(i_{mao,z} - i_{mai}\right)\right) + mean\left(\frac{G_{a,x}}{A_{side}}\left(i_{mao,x} - i_{mai}\right)\right)$$

$= 206250$ W

where the area of the top and bottom are, A_{top}= 2.25 m^2 and A_{side}= 2.817 m. Energy of the water can be calculated from,

$$Q_w = mean\left(\frac{G_{wi}}{A_{top}} c_{pw(T_{wi})}(T_{wi} - 273.15) + \frac{G_{wo}}{A_{bottom}} c_{pw(T_{wo})}(T_{wo} - 273.15)\right)$$

$= 205417$ W

Area at the bottom of the fill is the same as on top. The energy balance can now be calculated from,

$$EB = \frac{Q_a - Q_w}{Q_w} = \frac{206250 - 205417}{205417} = 0.004 = 0.4\ \%$$

A.3 e-NTU method of analysis

Kröger (2004) presents a sample calculation for the e-NTU method with the same test data as presented in Table A.1 The example given by Kröger is a counterflow case 1. In this sample calculation a crossflow case 2 is analysed. The calculation procedure follows the sample calculation by Kröger to maintain coherency.

Inlet and outlet conditions area measured for fill in crossflow test facility. The measured data is given in Table A.7

Table A.7: Measured conditions from a crossflow trickle fill performance test

Measured conditions		
Atmospheric pressure (p_a)	100380	N/m^2
Air inlet temperature (T_{ai})	14.50	°C
Air inlet temperature (T_{wb})	12.35	°C
Dry air mass flow rate (m_a)	8.860	kg/s
Water inlet temperature (T_{wi})	32.77	°C
Water outlet temperature (T_{wo})	24.92	°C
Water mass flow rate (m_w)	13.241	kg/s
Static pressure drop across fill	75	N/m^2
Fill height (L_{fi})	2.0	m
Fill length and depth	1.55	m

The dry air enthalpy of the inlet air can be calculated from Eq. (2.22),

$i_{mai} = 35271.6\,\text{J/kg}$

where $w_i = 0.008319\,\text{kg/kg}$

To obtain a Merkel number the effectiveness is determined from Eq. (2.56),

$$e = \frac{Q}{Q_{max}} = \frac{m_w\, c_{pw}\, (T_{wi} - T_{wo})}{C_{\text{emin}}\, (i_{maswi} - \lambda - i_{mai})}$$

To determine the heat transfer rate Q a specific heat is determined at the average of T_{wi} and T_{wo}

$$\frac{T_{wi} + T_{wo}}{2} = \frac{305.92 + 298.07}{2} = 302.995\ \text{K}$$

$c_{pwm} = 4179.094\ \text{J/kg K}$

The heat transfer rate is determined by,

$Q = m_w\, c_{pwm}\, (T_{wi} - T_{wo}) = 13.241\ 4179.094\ (305.92 - 298.07) = 434382.7\ \text{J/kg}$

To find Q_{max}, enthalpies of saturated air at the water inlet and outlet temperature are determined. To evaluated the enthalpies at the outlet, the specific heat of dry air at (273.15 + T_{wo}/2) = (273.15 + 24.92/2) = 285.61 K is determined,

$c_{pao} = 1006.54\ \text{J/kg K}$, $c_{pvo} = 1873.18\ \text{J/kg K}$

Pressure of water vapour at T_{wo} = 298.07 K can be determined

$p_{vo} = 3151.7\ \text{Pa}$

Using the pressure of water vapour the humidity of saturated air at 298.07 K can be determined,

$w_{swo} = 0.0202655\ \text{kg/kg}$

The enthalpy of saturated air evaluated at the local bulk water temperature 298.07 K can now be determined

$$i_{maswo} = c_{pao}\,(T_{wo} - 273.15) + w_{swo}\,(i_{fgwo} + c_{pvo}(T_{wo} - 273.15) =$$

$$= 76725.1\,\mathrm{J/kg}$$

Following the same calculation steps the enthalpy at water inlet T_{wi} = 305.92 K can be determined,

$$i_{maswi} = c_{pai}\,(T_{wi} - 273.15) + w_{swi}\,(i_{fgwo} + c_{pvi}(T_{wi} - 273.15) =$$
$$= 116390.0\ \mathrm{J/kg}$$

The enthalpy at T_{wm} = (305.92+298.07) / 2 = 302.995 K is,

$$i_{maswm} = c_{pam}\,(T_{wm} - 273.15) + w_{swm}\,(i_{fgwo} + c_{pvm}\,(T_{wm} - 273.15)$$
$$= 94819.8\ \mathrm{J/kg}$$

With these values the approximate gradient of the saturated air enthalpy i_{masw} – water temperature T_w curve can be determined from Eq. (2.54),

$$\frac{di_{masw}}{dT_w} = \frac{i_{masw} - i_{maswo}}{T_{wi} - T_{wo}} = 5052.85\,\mathrm{J/kg\,K}$$

To find out what case this test falls under the following must be checked,

$$\frac{m_w c_{pwm}}{di_{masw}/dT_w} = \frac{13.241\ \ 4179.094}{5052.85} = 10.9513 < m_a = 8.860$$

Therefore this is a Case 2 (see Section 2.6) which follows that,

$$C_{emin} = m_a = 8.860$$

$$C_{emax} = \frac{m_w c_{pwm}}{di_{masw}/dT_w} = 10.9513$$

The capacity ratio is determined according to Eq. (2.55),

$$C = \frac{C_{emin}}{C_{emax}} = \frac{8.860}{10.9513} = 0.8090$$

To find Q_{max} evaluate the correction factor according Berman (1961) give in Eq. (2.57),

$$\lambda = \frac{i_{maswo} + i_{maswi} - 2i_{maswm}}{4} = \frac{76725.1 + 116390.0 - \ 2\ \ 94819.8}{4}$$
$$= 868.85\,\mathrm{J/kg}$$

With these values, Q_{max} can be determined

$$Q_{max} = C_{emin}\,(i_{maswi} - \lambda - i_{mai}) = 8.860\,(116390.0\ - 868.85 - 35271.6)$$
$$= 711011.1\,\mathrm{J/kg}$$

The effectiveness can then be determined

$$e = \frac{Q}{Q_{max}} = \frac{434382.7}{711011.1} = 0.61094$$

In a crossflow evaporative system the effectiveness can also be express in terms of NTU where both streams are unmixed, given in Eq. (2.59),

$$0.61094 = 1 - \exp(NTU^{0.22}(\exp(-C\ NTU^{0.78}) - 1)/C$$

Solve iteratively to find *NTU* = 1.5997. With the *NTU*, the Merkel number can be calculated from Eq. (2.60),

$$Me = \frac{C_{emin}}{m_w} NTU = 8.860 \frac{8.860}{13.241} 1.5997 = 1.0704$$

Merkel number per meter of fill can be written as,

$$\frac{Me}{L_{fi}} = \frac{h_d a_{fi}}{G_w} = \frac{1.0704}{2.0} = 0.5352\ m^{-1}$$

APPENDIX B – Fill performance tests

B.1 Introduction

To obtain Merkel numbers for a packing/fill material, performance tests are conducted in a specialized cooling tower test facility. To obtain a Merkel number, the outlet water temperature is measured along with all relevant inlet conditions. The following data was obtained by testing a trickle fill in the cross- and counterflow cooling tower test facility at the University of Stellenbosch. Crossflow tests were conducted by Grobbelaar (2012) and counterflow tests by Bertrand (2010).

B.2 Description of the test facility

In Figure B.1, a schematic representation of the wet-cooling tower test facility is given. Air mass flow rates are determined by measuring the average pressure difference over three flow nozzles.

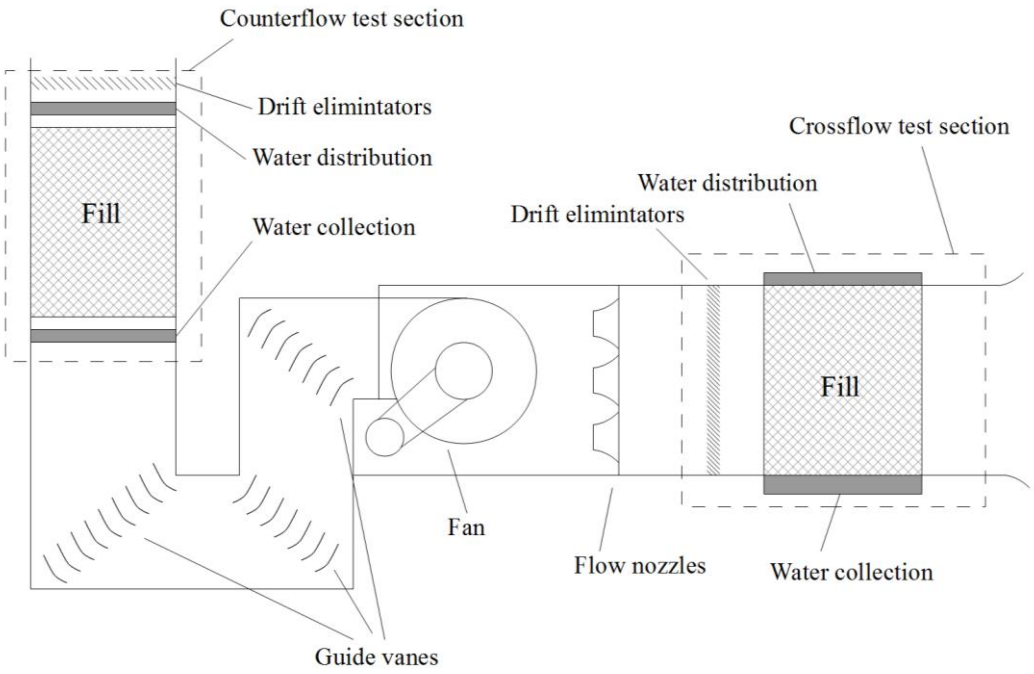

Figure B 1: Schematic of the wet-cooling tower fill performance test facility

In Figure B.2 a more detailed description of the counterflow test section is given,

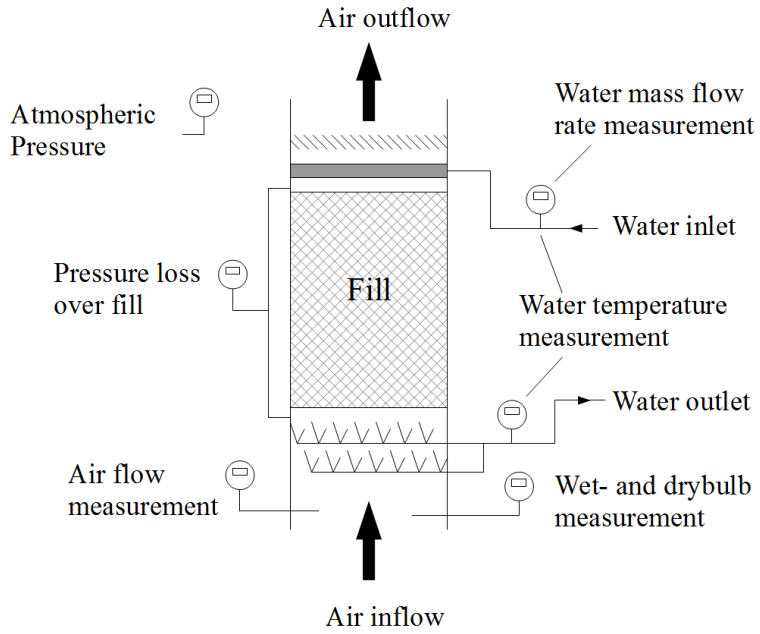

Figure B.2: Counterflow wet-cooling tower fill performance test section

The outlet water temperature is measured after the collection region. Cooling takes place as soon as the water comes in contact with the air and until it is isolated from the air within the outlet pipe. Therefore, the measured cooling does not all take place within the fill area. To get a more accurate Merkel number, empty test are conducted where the water distribution system is placed just above the collection region. Empirical relations are obtained for Merkel numbers from the empty test, which are subtracted from the Merkel number obtained in the fill test. Empirical relations for empty test Merkel numbers are given in Table B.1,

Table B.1: Empirical relation for empty test Merkel numbers obtained using the e-NTU, Merkel and Poppe methods

Model	Empirical equations (curve fit)	Correlation
e-NTU	$Me = 0.121\ G_{wi}^{-0.673}\ G_a^{0.750}\ T_{wi}^{0.043}$	0.988
Merkel	$Me = 0.122\ G_{wi}^{-0.678}\ G_a^{0.748}\ T_{wi}^{0.043}$	0.988
Poppe	$Me = 0.136\ G_{wi}^{-0.674}\ G_a^{0.748}\ T_{wi}^{0.035}$	0.988

In Figure B.3 a more detailed description of the crossflow test section is given,

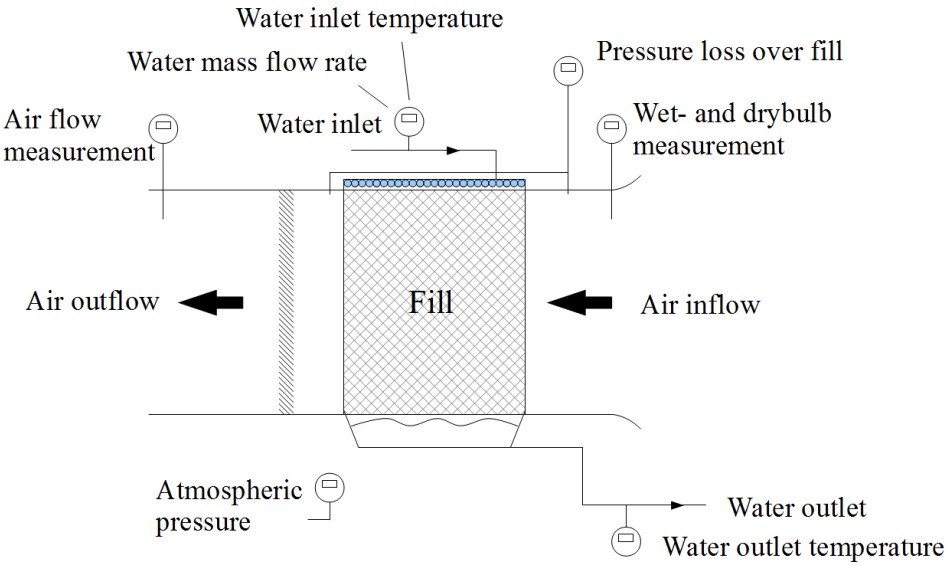

Figure B.3: Crossflow wet-cooling tower fill performance test section

B.3 Measured test data and fill performance

Performance data is presented for a trickle fill in cross- and counterflow.

B.3.1 Counterflow - 1.5 m fill height

The counterflow test facility is 1.5m x 1.5m at inlet and outlet.

Table B.2: Trickle fill counterflow experimental measurements

Nr.	T_{ai} °C	T_{wb} °C	T_{wi} °C	T_{wo} °C	m_a kg/s	m_w kg/s	dp_{fi} N/m^2	p_a N/m^2
1	18.23	15.04	48.75	29.06	2.29	3.35	9.45	100940
2	18.26	14.83	47.66	25.22	3.38	3.33	17.73	100940
3	18.31	14.75	46.67	22.79	4.54	3.38	29.48	100940
4	18.42	14.67	45.5	21.03	5.64	3.38	43.61	100940
5	18.66	14.71	44.61	19.96	6.77	3.38	60.88	100940
6	18.9	14.71	43.12	18.79	7.89	3.4	81.4	100940
7	19.25	14.77	40.19	17.85	9.01	3.38	104.48	100940
8	18.35	15.39	46.85	35.35	2.26	6.68	10.44	100940
9	18.04	15	45.92	31.61	3.39	6.7	19.7	100940

Nr.	T_{ai} °C	T_{wb} °C	T_{wi} °C	T_{wo} °C	m_a kg/s	m_w kg/s	dp_{fi} N/m^2	p_a N/m^2
10	18.21	14.81	45.11	28.84	4.5	6.72	31.79	100940
11	18.39	14.69	44.43	26.9	5.63	6.76	47.09	100940
12	18.55	14.57	43.71	25.05	6.76	6.72	65.57	100940
13	18.83	14.58	43.06	23.85	7.9	6.77	88.06	100940
14	19.03	14.7	42.21	22.66	9	6.74	114.6	100940
15	18.58	15.88	43.02	36.42	2.26	10.13	11.6	100940
16	18.47	15.46	42.39	33.5	3.37	10.15	21.4	100940
17	18.39	15.05	41.78	31.28	4.49	10.15	34.36	100940
18	18.35	14.89	41.1	29.28	5.64	10.12	50.97	100940
19	18.45	14.71	40.68	27.66	6.77	10.12	70.85	100940
20	18.85	14.62	40.13	26.31	7.86	10.1	94.5	100940
21	19.28	14.75	39.31	25.2	8.99	10.09	124.94	100940
22	18.9	16.13	39.09	34.93	2.24	12.58	12.24	100940
23	18.6	15.71	39.09	33.07	3.37	12.58	22.7	100940
24	18.72	15.21	38.72	31.24	4.47	12.55	36	100940
25	18.84	15.03	38.42	29.7	5.65	12.53	54.18	100940
26	19	14.85	38.13	28.59	6.7	12.6	73.96	100940
27	19.19	14.85	37.9	27.29	7.9	12.52	101.86	100940
28	19.46	14.98	37.52	26.27	9.02	12.57	135.47	100940
29	18.06	14.61	36.76	25.13	2.29	3.35	8.64	100860
30	18.05	14.36	36.21	22.35	3.36	3.35	16.56	100860
31	18.15	14.49	35.67	20.36	4.51	3.34	27.89	100860
32	18.24	14.52	35.18	19.1	5.67	3.38	42.15	100860
33	18.53	14.5	34.71	18.26	6.76	3.35	58.85	100860
34	18.8	14.55	34.06	17.44	7.91	3.37	79.47	100860
35	19.3	14.69	32.16	16.74	8.99	3.37	101.53	100860
36	18.21	15.13	35.82	29.79	2.25	6.76	9.37	100860
37	18.19	14.97	35.43	27.38	3.39	6.75	18.57	100860
38	18.14	14.81	35	25.49	4.52	6.71	30.47	100860
39	18.35	14.61	34.71	23.92	5.62	6.67	45.01	100860
40	18.65	14.68	34.43	22.8	6.79	6.7	63.94	100860
41	18.86	14.7	33.98	21.73	7.88	6.69	85.43	100860

Nr.	T_{ai} °C	T_{wb} °C	T_{wi} °C	T_{wo} °C	m_a kg/s	m_w kg/s	dp_{fi} N/m^2	p_a N/m^2
42	19.29	14.87	33.55	20.82	9.1	6.68	114.91	100860
43	18.55	15.44	34.33	30.53	2.27	10.13	10.71	100860
44	18.51	15.14	34.14	28.83	3.36	10.13	19.98	100860
45	18.54	14.92	33.86	27.31	4.54	10.12	33.3	100860
46	18.7	14.81	33.57	26.08	5.63	10.06	48.8	100860
47	18.9	14.72	33.32	24.99	6.72	10.08	67.72	100860
48	19.22	14.72	32.97	23.96	7.87	10.05	92.08	100860
49	19.65	14.8	32.6	23.09	9.01	10.05	122.78	100860
50	18.9	15.62	32.98	30.12	2.32	12.51	12.16	100860
51	18.86	15.33	33.04	29	3.41	12.51	22.05	100860
52	18.79	15.09	32.93	27.9	4.47	12.48	34.63	100860
53	18.86	15	32.81	26.82	5.62	12.43	51.89	100860
54	19.05	14.91	32.75	26.04	6.71	12.47	72.24	100860
55	19.29	14.9	32.74	25.21	7.87	12.46	98.89	100860
56	19.54	15.18	32.56	24.5	8.99	12.46	132.12	100860
57	18.05	14.82	32.3	23.82	2.24	3.4	8.01	100830
58	18.17	14.77	31.96	21.4	3.41	3.42	16.64	100830
59	18.36	14.75	31.72	19.79	4.49	3.4	27.33	100830
60	18.7	14.68	31.41	18.64	5.62	3.39	41.31	100830
61	19.02	14.75	31	17.93	6.71	3.39	57.54	100830
62	19.41	14.71	30.69	17.24	7.89	3.39	78.95	100830
63	20.12	14.66	29.11	16.51	8.97	3.38	100.8	100830
64	18.75	14.98	31.94	27.39	2.28	6.77	9.25	100830
65	18.76	14.85	31.93	25.75	3.35	6.77	17.76	100830
66	19.04	14.58	31.66	24.06	4.52	6.76	29.94	100830
67	19.2	14.62	31.39	22.83	5.63	6.73	44.59	100830
68	19.35	14.74	30.93	21.82	6.74	6.7	62.41	100830
69	19.67	14.71	30.69	20.87	7.84	6.7	83.83	100830
70	20.22	14.81	30.25	20.04	9.16	6.68	115.76	100830
71	19.02	15.37	30.8	27.97	2.29	10.14	10.5	100830
72	18.94	15.06	30.47	26.53	3.37	10.12	19.47	100830
73	19.02	14.8	30.1	25.22	4.52	10.1	32.27	100830

Nr.	T_{ai} °C	T_{wb} °C	T_{wi} °C	T_{wo} °C	m_a kg/s	m_w kg/s	dp_{fi} N/m^2	p_a N/m^2
74	19.09	14.67	29.92	24.27	5.6	10.11	47.48	100830
75	19.26	14.83	29.62	23.4	6.74	10.1	66.98	100830
76	19.48	15.03	29.39	22.61	7.88	10.1	91.15	100830
77	19.84	15.14	29.04	21.79	9.14	10.09	125.55	100830
78	18.9	15.5	28.98	27.09	2.27	12.43	11.31	100830
79	18.8	15.49	28.69	25.98	3.39	12.43	21.21	100830
80	18.87	15.27	28.11	24.84	4.48	12.42	33.75	100830
81	18.93	15.17	27.5	23.77	5.66	12.43	51.06	100830
82	19.2	15	27.1	22.94	6.73	12.46	70.48	100830
83	19.36	15.03	26.66	22.18	7.88	12.46	96.44	100830
84	19.72	15.08	26.22	21.5	8.99	12.44	128.46	100830

Table B.3: Trickle fill counterflow results

Nr.	G_w kg/sm^2	G_a kg/sm^2	Me/L_{fi} m^{-1} (e-NTU)	Me/L_{fi} m^{-1} (Merkel)	Me/L_{fi} m^{-1} (Reuter) w. Merkel assumptions	Me/L_{fi} m^{-1} (Reuter) w. Poppe assumptions	Me/L_{fi} m^{-1} (Poppe)
1	1.49	1.02	0.80	0.84	0.84	0.94	0.93
2	1.48	1.50	1.06	1.09	1.09	1.19	1.18
3	1.50	2.02	1.30	1.30	1.29	1.40	1.40
4	1.50	2.51	1.58	1.50	1.49	1.60	1.60
5	1.50	3.01	1.83	1.63	1.61	1.73	1.73
6	1.51	3.51	2.31	1.86	1.83	1.95	1.96
7	1.50	4.00	2.63	2.07	2.05	2.17	2.18
8	2.97	1.00	0.46	0.46	0.46	0.54	0.54
9	2.98	1.51	0.60	0.61	0.61	0.69	0.69
10	2.99	2.00	0.73	0.75	0.76	0.84	0.83
11	3.00	2.50	0.83	0.86	0.86	0.94	0.94
12	2.99	3.00	0.96	0.99	0.99	1.08	1.07
13	3.01	3.51	1.05	1.08	1.08	1.17	1.16
14	3.00	4.00	1.17	1.20	1.20	1.29	1.29
15	4.50	1.00	0.32	0.32	0.32	0.39	0.39
16	4.51	1.50	0.45	0.45	0.46	0.54	0.53
17	4.51	2.00	0.53	0.54	0.54	0.62	0.61

Nr.	G_w kg/sm^2	G_a kg/sm^2	Me/L_{fi} m^{-1} (e-NTU)	Me/L_{fi} m^{-1} (Merkel)	Me/L_{fi} m^{-1} (Reuter) w. Merkel assumptions	Me/L_{fi} m^{-1} (Reuter) w. Poppe assumptions	Me/L_{fi} m^{-1} (Poppe)
18	4.50	2.51	0.63	0.64	0.64	0.72	0.71
19	4.50	3.01	0.72	0.73	0.74	0.82	0.81
20	4.49	3.49	0.80	0.82	0.82	0.91	0.90
21	4.48	4.00	0.87	0.89	0.89	0.97	0.97
22	5.59	1.00	0.26	0.25	0.26	0.32	0.31
23	5.59	1.50	0.37	0.36	0.37	0.44	0.43
24	5.58	1.99	0.46	0.46	0.46	0.53	0.53
25	5.57	2.51	0.53	0.53	0.54	0.61	0.60
26	5.60	2.98	0.58	0.58	0.59	0.66	0.65
27	5.56	3.51	0.67	0.68	0.68	0.76	0.75
28	5.59	4.01	0.75	0.76	0.76	0.84	0.83
29	1.49	1.02	0.99	1.00	1.01	1.13	1.11
30	1.49	1.49	1.22	1.25	1.25	1.37	1.36
31	1.48	2.00	1.48	1.52	1.52	1.65	1.63
32	1.50	2.52	1.70	1.73	1.73	1.85	1.84
33	1.49	3.00	1.86	1.86	1.85	1.97	1.97
34	1.50	3.52	2.16	2.10	2.09	2.22	2.21
35	1.50	4.00	2.52	2.39	2.37	2.50	2.50
36	3.00	1.00	0.48	0.47	0.48	0.56	0.55
37	3.00	1.51	0.64	0.64	0.65	0.73	0.72
38	2.98	2.01	0.77	0.77	0.78	0.86	0.85
39	2.96	2.50	0.90	0.91	0.91	1.00	0.99
40	2.98	3.02	1.00	1.01	1.02	1.11	1.10
41	2.97	3.50	1.12	1.14	1.14	1.24	1.23
42	2.97	4.04	1.25	1.27	1.28	1.38	1.37
43	4.50	1.01	0.34	0.33	0.34	0.41	0.40
44	4.50	1.49	0.47	0.46	0.47	0.55	0.54
45	4.50	2.02	0.56	0.56	0.56	0.64	0.63
46	4.47	2.50	0.64	0.63	0.64	0.71	0.70
47	4.48	2.99	0.72	0.72	0.73	0.81	0.80
48	4.47	3.50	0.81	0.81	0.82	0.90	0.89
49	4.47	4.00	0.89	0.90	0.90	0.99	0.98
50	5.56	1.03	0.29	0.28	0.29	0.35	0.34
51	5.56	1.52	0.38	0.37	0.38	0.44	0.43
52	5.55	1.99	0.45	0.45	0.45	0.52	0.51

Nr.	G_w kg/sm^2	G_a kg/sm^2	Me/L_{fi} m^{-1} (e-NTU)	Me/L_{fi} m^{-1} (Merkel)	Me/L_{fi} m^{-1} (Reuter) w. Merkel assumptions	Me/L_{fi} m^{-1} (Reuter) w. Poppe assumptions	Me/L_{fi} m^{-1} (Poppe)
53	5.52	2.50	0.53	0.53	0.54	0.61	0.60
54	5.54	2.98	0.58	0.58	0.59	0.65	0.64
55	5.54	3.50	0.66	0.66	0.67	0.74	0.73
56	5.54	4.00	0.73	0.74	0.74	0.82	0.81
57	1.51	1.00	1.00	1.00	1.01	1.13	1.11
58	1.52	1.52	1.26	1.28	1.29	1.41	1.40
59	1.51	2.00	1.52	1.54	1.55	1.68	1.66
60	1.51	2.50	1.72	1.75	1.75	1.87	1.86
61	1.51	2.98	1.89	1.90	1.90	2.02	2.01
62	1.51	3.51	2.11	2.10	2.09	2.21	2.21
63	1.50	3.99	2.40	2.35	2.34	2.46	2.46
64	3.01	1.01	0.47	0.46	0.47	0.54	0.53
65	3.01	1.49	0.62	0.61	0.62	0.70	0.69
66	3.00	2.01	0.77	0.77	0.78	0.86	0.85
67	2.99	2.50	0.89	0.89	0.90	0.99	0.98
68	2.98	3.00	0.99	1.00	1.01	1.09	1.08
69	2.98	3.48	1.13	1.14	1.15	1.24	1.23
70	2.97	4.07	1.25	1.26	1.27	1.36	1.35
71	4.51	1.02	0.32	0.31	0.32	0.37	0.36
72	4.50	1.50	0.45	0.44	0.45	0.51	0.50
73	4.49	2.01	0.55	0.54	0.55	0.62	0.61
74	4.49	2.49	0.63	0.62	0.63	0.70	0.69
75	4.49	3.00	0.71	0.71	0.71	0.78	0.78
76	4.49	3.50	0.82	0.82	0.82	0.90	0.89
77	4.48	4.06	0.93	0.93	0.94	1.02	1.01
78	5.52	1.01	0.23	0.22	0.23	0.26	0.26
79	5.52	1.51	0.35	0.35	0.36	0.41	0.40
80	5.52	1.99	0.43	0.43	0.43	0.49	0.48
81	5.52	2.52	0.51	0.51	0.51	0.57	0.56
82	5.54	2.99	0.59	0.59	0.59	0.65	0.65
83	5.54	3.50	0.67	0.66	0.67	0.74	0.73
84	5.53	4.00	0.75	0.75	0.75	0.82	0.81

Table B.4: Empirical relation of counterflow trickle fill Merkel numbers (Performance curves)

Model	Empirical equations (curve fit)	Correlation
e-NTU	$\frac{Me}{L_{fi}} = 3.082\ G_{wi}^{-0.924}\ G_a^{0.672}\ T_{wi}^{-0.250}$	0.995
Crossflow Merkel	$\frac{Me}{L_{fi}} = 4.003\ G_{wi}^{-0.900}\ G_a^{0.627}\ T_{wi}^{-0.318}$	0.997
Reuter w. Merkel assumptions	$\frac{Me}{L_{fi}} = 4.384\ G_{wi}^{-0.889}\ G_a^{0.616}\ T_{wi}^{-0.343}$	0.996
Crossflow Poppe	$\frac{Me}{L_{fi}} = 4.204\ G_{wi}^{-0.860}\ G_a^{0.583}\ T_{wi}^{-0.307}$	0.997
Reuter w. Poppe assumptions	$\frac{Me}{L_{fi}} = 4.374\ G_{wi}^{-0.851}\ G_a^{0.570}\ T_{wi}^{-0.315}$	0.997

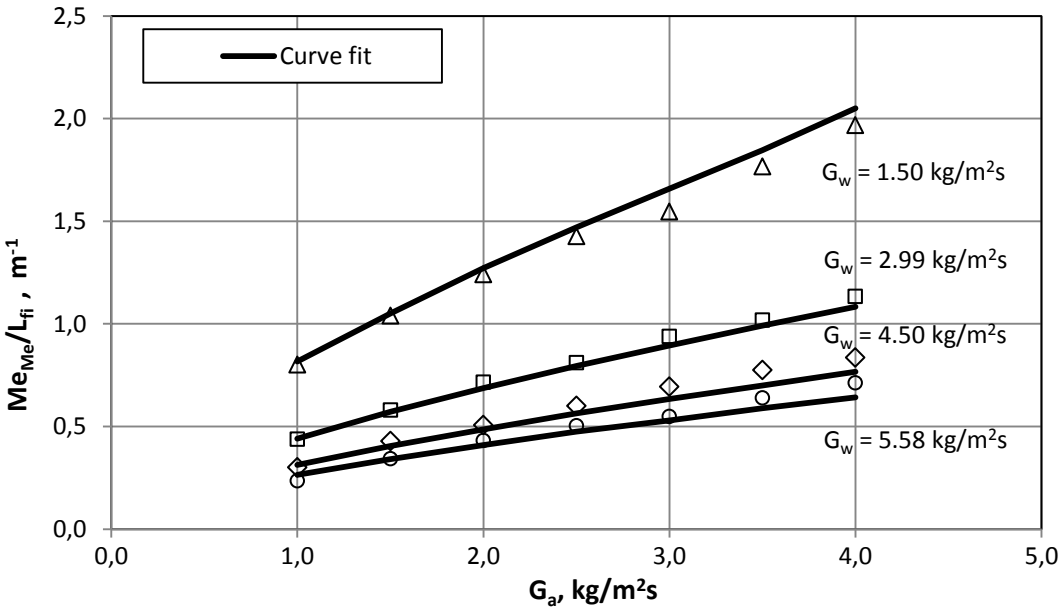

Figure B.4: Trickle fill counterflow Merkel method Performance curve with experimental data

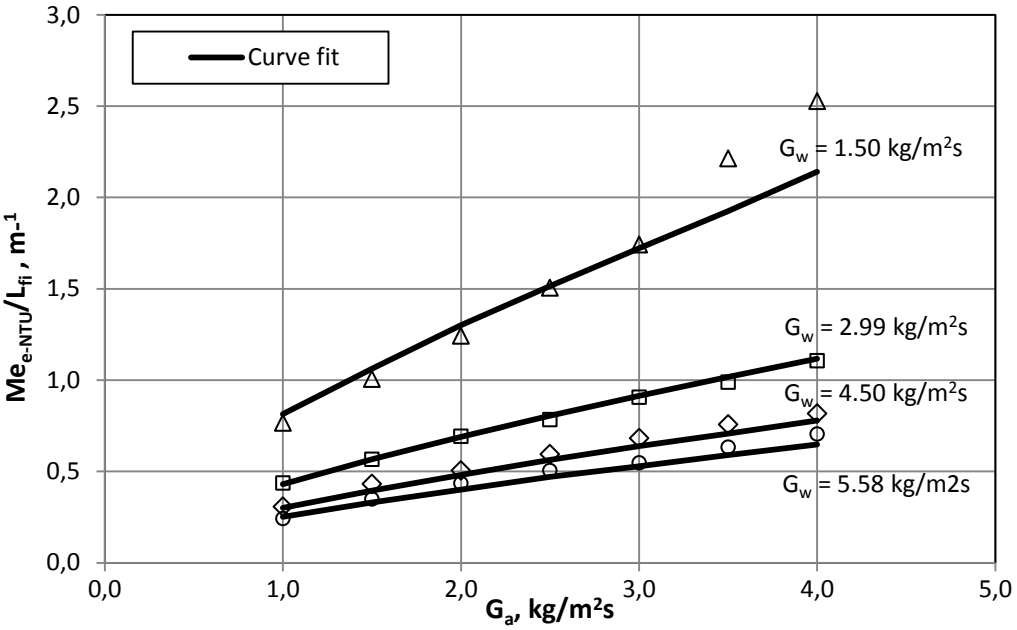

Figure B. 5: Trickle fill counterflow e-NTU method Performance curve with experimental data

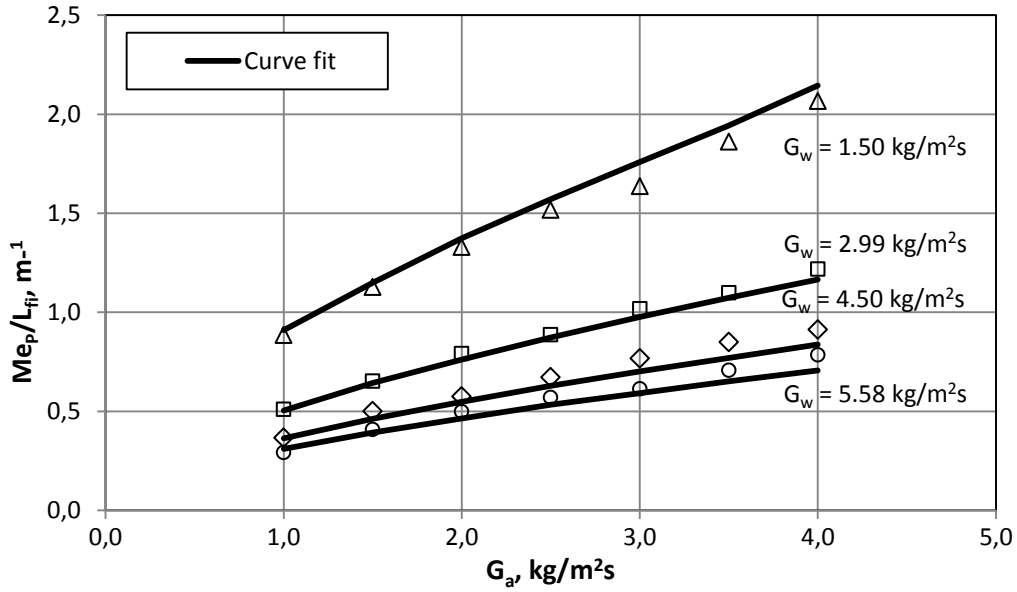

Figure B.6: Trickle fill counterflow Poppe method Performance curve with experimental data

Correlation between the Reuter method and Poppe method gives, 0.99998 and 0.99995 between Merkel equation and Reuter method with Merkel assumptions. Performance graphs for the Reuter method are therefore not displayed.

B.3.2 Crossflow test - 2.0 m fill height

The crossflow test facility is has and water inlet frame of 1.5 m x 2.0 m and air inlet of 2.0 m x 2.0 m.

Table B.5: Trickle fill crossflow experimental measurements

Nr.	T_{ai} °C	T_{wb} °C	T_{wi} °C	T_{wo} °C	m_a kg/s	m_w kg/s	dp_{fi} N/m^2	p_a N/m^2
1	17.05	13.78	52.16	26.62	4.98	4.45	19.0	100330
2	16.92	13.56	51.59	24.09	6.55	4.34	31.0	100330
3	16.67	13.37	49.71	21.15	9.06	3.99	57.0	100330
4	14.68	13.27	47.69	20.95	10.30	4.50	75.0	100330
5	14.89	13.44	47.30	32.46	4.45	8.50	18.5	100330
6	14.58	13.19	45.98	28.73	6.67	8.58	36.5	100330
7	14.50	13.10	45.03	26.83	8.93	9.05	66.0	100330
8	14.70	13.13	44.27	25.67	10.09	8.64	84.0	100330
9	14.91	13.36	41.90	33.22	4.72	13.26	20.0	100330
10	14.85	13.28	41.73	30.80	6.59	13.18	39.0	100380
11	14.89	13.19	41.67	29.16	8.80	13.16	74.5	100380
12	15.92	13.58	41.60	28.34	10.07	13.16	98.5	100380
13	16.40	13.99	41.61	33.75	4.46	14.20	0.0	100380
14	15.69	13.61	41.50	31.33	6.51	14.15	0.0	100380
15	15.43	13.47	40.37	29.09	9.11	14.16	83.5	100380
16	15.19	13.34	38.27	27.49	10.08	14.21	112.0	100380
17	14.64	12.78	35.83	25.86	10.10	13.13	99.0	100380
18	14.22	12.55	33.67	22.58	10.32	8.79	87.5	100380
19	14.22	12.39	32.85	18.35	10.51	4.46	76.0	100380
20	14.15	12.34	32.77	24.92	8.86	13.24	75.0	100380
21	14.34	12.62	32.11	22.59	9.00	8.77	64.5	100380
22	14.28	12.54	31.63	18.53	9.19	4.38	56.0	100380
23	14.01	12.53	30.97	25.34	6.56	13.40	38.5	100380
24	14.13	12.49	30.21	22.83	6.81	9.02	36.0	100380
25	13.33	11.89	29.45	18.34	6.99	4.21	32.0	100380
26	13.39	12.00	27.94	24.23	4.69	12.88	20.0	100380
27	13.20	11.96	26.47	21.86	4.74	8.96	18.0	100380
28	13.12	11.97	25.91	18.68	4.80	4.35	16.0	100380
29	13.39	12.05	25.79	20.59	10.46	13.98	103.0	100380
30	13.34	12.13	25.12	20.83	9.10	14.09	0.0	100380
31	13.36	12.08	24.70	21.29	6.74	14.04	40.0	100380

Nr.	T_{ai} °C	T_{wb} °C	T_{wi} °C	T_{wo} °C	m_a kg/s	m_w kg/s	dp_{fi} N/m^2	p_a N/m^2
32	13.13	12.04	24.69	22.05	4.90	14.11	22.0	100380
33	14.14	10.94	49.74	31.26	9.62	13.83	97.0	100900
34	14.17	10.93	47.47	31.26	8.93	13.88	84.0	100900
35	14.24	11.04	45.63	32.75	6.52	13.86	42.0	100900
36	14.30	11.01	44.47	34.85	4.46	13.87	20.5	100900
37	13.42	10.70	42.88	28.21	9.93	13.13	98.0	100900
38	13.26	10.54	39.95	27.79	8.98	12.95	78.0	100900
39	13.44	10.71	38.57	28.74	6.61	12.88	40.5	100900
40	13.47	10.60	37.64	30.18	4.60	12.87	21.0	100900
41	13.41	10.71	36.98	23.31	10.27	9.02	87.0	100900
42	13.35	10.56	36.27	23.81	8.80	9.01	63.5	100900
43	13.47	10.57	35.53	24.93	6.61	9.02	35.0	100900
44	13.42	10.57	34.53	26.15	4.82	9.04	20.0	100900
45	13.10	10.46	34.04	17.38	10.56	4.32	74.0	100900
46	13.43	10.69	33.17	17.88	8.87	4.31	51.0	100900
47	13.37	10.70	32.68	18.73	6.92	4.32	31.5	100900
48	13.35	10.68	32.20	20.16	4.97	4.27	16.5	100900

Table B.6: Trickle fill crossflow results

Nr.	G_w kg/sm^2	G_a kg/sm^2	Me/L_{fi} m^{-1} (e-NTU)	Me/L_{fi} m^{-1} (Merkel)	Me/L_{fi} m^{-1} (Reuter) w. Merkel assumptions	Me/L_{fi} m^{-1} (Reuter) w. Poppe assumptions	Me/L_{fi} m^{-1} (Poppe)
1	1.48	1.25	0.89	0.91	0.89	0.98	0.98
2	1.45	1.64	1.09	1.05	1.04	1.13	1.14
3	1.33	2.26	1.48	1.25	1.24	1.33	1.33
4	1.50	2.57	1.34	1.23	1.21	1.31	1.31
5	2.83	1.11	0.51	0.51	0.50	0.56	0.57
6	2.86	1.67	0.65	0.66	0.65	0.72	0.73
7	3.02	2.23	0.71	0.72	0.71	0.78	0.79
8	2.88	2.52	0.74	0.76	0.75	0.82	0.82
9	4.42	1.18	0.35	0.35	0.34	0.39	0.39
10	4.39	1.65	0.47	0.46	0.46	0.51	0.52
11	4.39	2.20	0.52	0.51	0.50	0.56	0.56
12	4.39	2.52	0.56	0.55	0.54	0.60	0.60
13	4.73	1.12	0.34	0.33	0.33	0.38	0.38

Nr.	G_w kg/sm^2	G_a kg/sm^2	Me/L_{fi} m^{-1} (e-NTU)	Me/L_{fi} m^{-1} (Merkel)	Me/L_{fi} m^{-1} (Reuter) w. Merkel assumptions	Me/L_{fi} m^{-1} (Reuter) w. Poppe assumptions	Me/L_{fi} m^{-1} (Poppe)
14	4.72	1.63	0.44	0.43	0.43	0.48	0.49
15	4.72	2.28	0.50	0.48	0.48	0.53	0.53
16	4.74	2.52	0.54	0.52	0.51	0.57	0.57
17	4.38	2.53	0.57	0.54	0.54	0.59	0.59
18	2.93	2.58	0.73	0.72	0.72	0.78	0.78
19	1.49	2.63	1.16	1.18	1.18	1.26	1.27
20	4.41	2.21	0.53	0.52	0.51	0.56	0.57
21	2.92	2.25	0.70	0.69	0.69	0.74	0.75
22	1.46	2.30	1.13	1.17	1.16	1.24	1.25
23	4.47	1.64	0.43	0.42	0.42	0.47	0.47
24	3.01	1.70	0.65	0.64	0.63	0.69	0.70
25	1.40	1.75	1.11	1.14	1.14	1.22	1.22
26	4.29	1.17	0.36	0.35	0.35	0.39	0.40
27	2.99	1.18	0.55	0.55	0.55	0.61	0.61
28	1.45	1.20	0.99	0.98	0.98	1.06	1.07
29	4.66	2.62	0.61	0.58	0.58	0.63	0.63
30	4.70	2.28	0.51	0.49	0.49	0.53	0.53
31	4.68	1.69	0.43	0.42	0.42	0.46	0.46
32	4.70	1.22	0.33	0.33	0.33	0.36	0.36
33	4.61	2.41	0.51	0.51	0.50	0.55	0.56
34	4.63	2.23	0.48	0.48	0.47	0.53	0.53
35	4.62	1.63	0.43	0.42	0.41	0.47	0.47
36	4.62	1.12	0.34	0.33	0.32	0.37	0.37
37	4.38	2.48	0.55	0.54	0.54	0.59	0.59
38	4.32	2.24	0.52	0.50	0.50	0.55	0.55
39	4.29	1.65	0.47	0.46	0.46	0.51	0.51
40	4.29	1.15	0.39	0.38	0.38	0.43	0.43
41	3.01	2.57	0.71	0.71	0.70	0.76	0.76
42	3.00	2.20	0.68	0.67	0.67	0.73	0.73
43	3.01	1.65	0.63	0.62	0.62	0.68	0.68
44	3.01	1.21	0.53	0.53	0.52	0.58	0.59
45	1.44	2.64	1.20	1.23	1.22	1.30	1.31
46	1.44	2.22	1.17	1.21	1.20	1.29	1.29
47	1.44	1.73	1.11	1.16	1.15	1.24	1.24
48	1.42	1.24	1.00	1.03	1.02	1.11	1.11

Table B.7: Empirical relation of crossflow trickle fill Merkel numbers (Performance curves)

Model	Empirical equations (curve fit)	Correlation
e-NTU	$\frac{Me}{L_{fi}} = 1.245\ G_{wi}^{-0.735}\ G_a^{-0.365}\ T_{wi}^{-0.024}$	0.992
Merkel eq.	$\frac{Me}{L_{fi}} = 1.280\ G_{wi}^{-0.748}\ G_a^{0.346}\ T_{wi}^{-0.028}$	0.995
Reuter w. Merkel assumptions	$\frac{Me}{L_{fi}} = 1.298\ G_{wi}^{-0.748}\ G_a^{0.346}\ T_{wi}^{-0.028}$	0.995
Poppe	$\frac{Me}{L_{fi}} = 1.407\ G_{wi}^{-0.748}\ G_a^{0.346}\ T_{wi}^{-0.028}$	0.995
Reuter w. Poppe assumptions	$\frac{Me}{L_{fi}} = 1.407\ G_{wi}^{-0.748}\ G_a^{0.350}\ T_{wi}^{-0.029}$	0.995

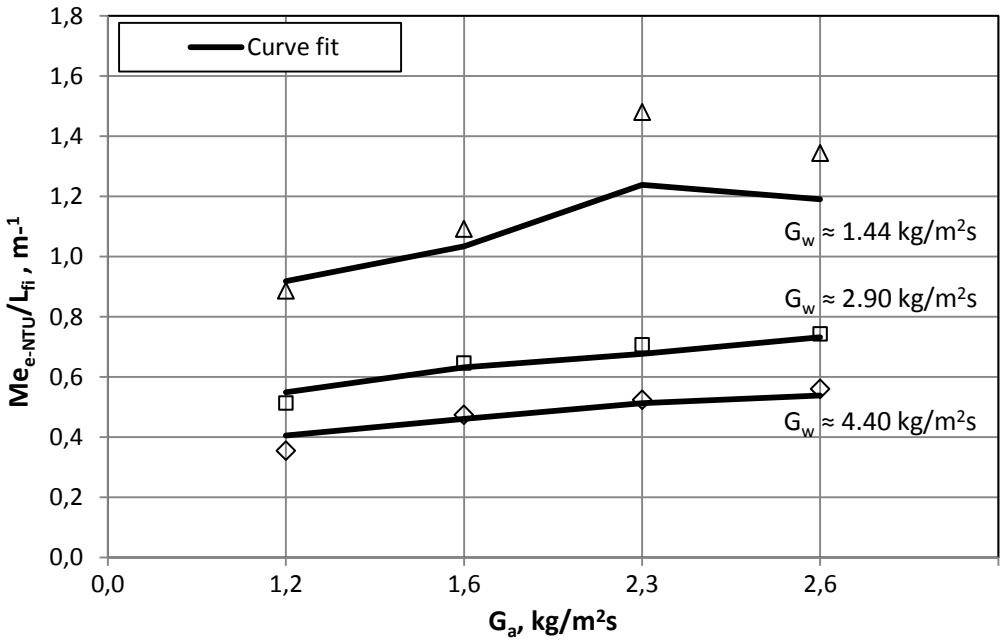

Figure B.7: Trickle fill crossflow e-NTU method performance curve with experimental test data

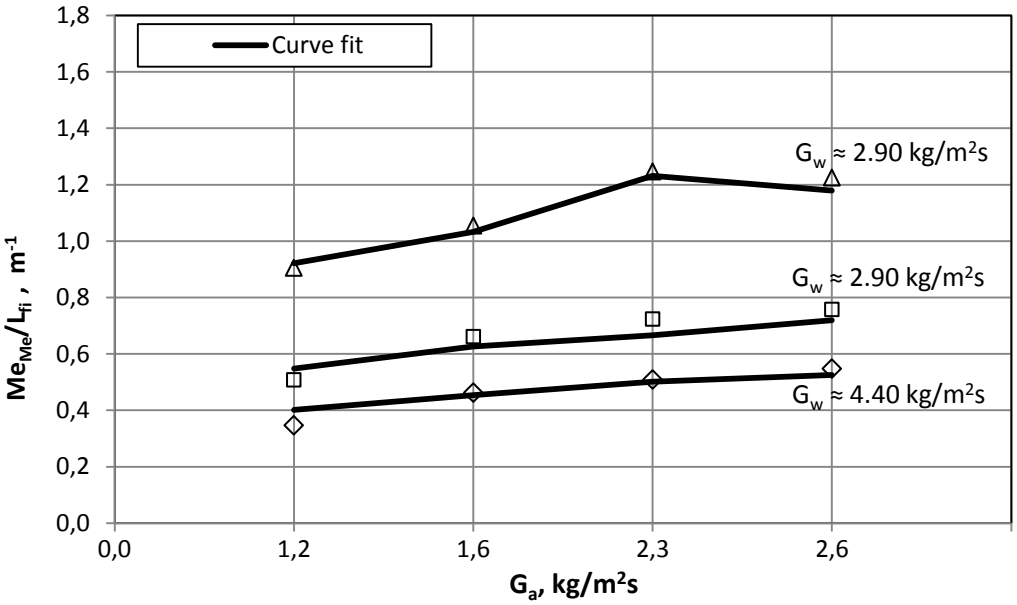

Figure B.8: Trickle fill crossflow Merkel method performance curve with experimental test data

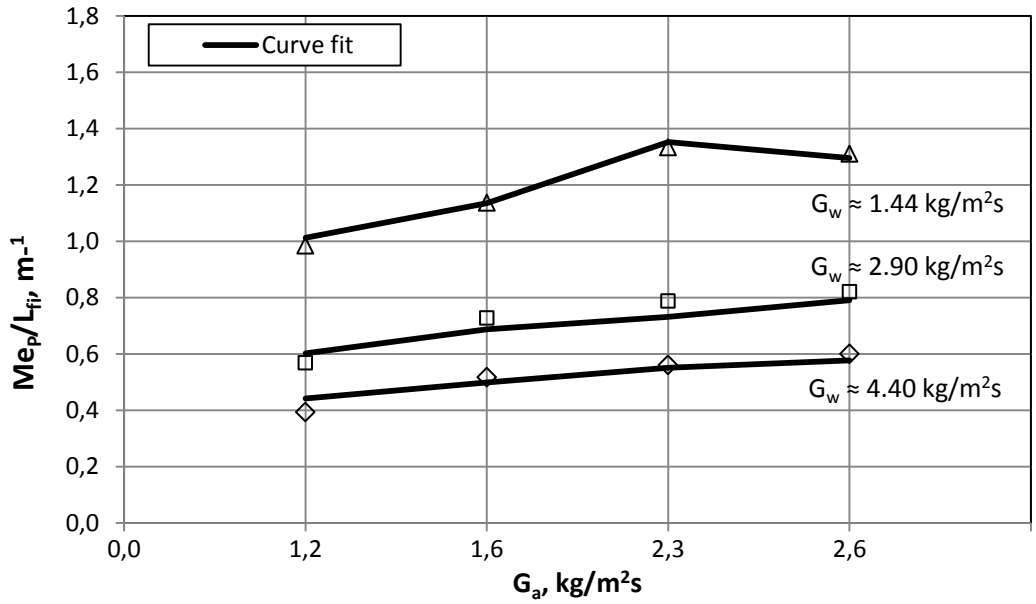

Figure B.9: Trickle fill crossflow Poppe method performance curve with experimental test data

APPENDIX C – User defined function for CFD model

C.1 Introduction

The following appendix provides snapshots from the UDF used in the ANSYS-*Fluent*® model for modelling heat and mass transfer in the fill area.

C.2 User defined function (UDF)

The user has to give all the necessary inputs.

```
/*******************************************************************************
*                                  USER INPUTS                                 *
*******************************************************************************/
static int  init_UDMI = 0;          /* If 1 saves constant values in the UDMIs      */
/* Total number of cells obtained from DEFINE_ON_DEMAND(store_cell_numbers) using
Fluent contour plot of UDM 0                                                     */
static int  ni = 1087;
static int  PACK_ID = 6;            /* Cell Zone cell ID of packing                 */
static real z_CW_in = 1.4;          /* Height of CW inlet                           */
static real p_ref = 101325.;        /* Reference air pressure                       */
static real T_ref = 288.15;         /* Reference air temperature in Kelvin          */
static real mv_ref = 0.0064232;     /* Air inlet vapour mass fraction               */
static real Tw_in = 40.0;           /* Inlet water temperature in degrees celcius   */
static real p_fill = 101325.;       /* Air pressure in fill                         */
static real G_wi = 3.0;             /* Water inlet mass velocity                    */
static real Relax = 0.1;            /* Relaxation for the fill source terms         */
static real Le_f = 1;               /* Lewis factor                                 */
static real B_Me = 0;               /* constant for Merkel assumptions              */
/*******************************************************************************/
```

When the user inputs have been given, variables are defined in the Execute and end function

```
DEFINE_EXECUTE_AT_END(calculate_source_terms)           /* USED TO RUN THE UDF
                                                        AFTER EACH CFD ITERATION    */
{
/*******************************************************************************
*                                DEFINE VARIABLES                              *
*******************************************************************************/

  int       i,n;                    /* Integers for determining cell ID             */
  Domain    *d;                     /* Domain pointer                               */
  Thread    *t,*cct,*ft     ;       /* Thread pointer                               */
  face_t    f;                      /* Face thread                                  */
  cell_t    c,cc,c1_star,c2_star,c3_star,c4_star,c5_star,c6_star;/* Cell threads    */
  Node      *node;                  /* Node pointer                                 */
  real      ni;                     /* Number of cells in the fill zone             */
  real      zmin,zmax,z_cc,deltaZ;  /* Variables for cell location and ID           */
  real      xmin,xmax,x_cc,deltaX;  /* Variables for cell location and ID           */
  real      ymin,ymax,y_cc,deltaY;  /* Variables for cell location and ID           */
  real      xc[ND_ND],z_bound,z_b2; /* Variables for cell location and ID           */
                                    /* Variables for cell properties                */
  real      T_a, p_a, T_w, G_w, m_v, w_a,w_sa; /* Variables for cell properties     */
  real      w_sw, cp_ma, cp_v, cp_w, i_fg;  /* Variables for cell properties        */
  real      k_av, rho_av, G_a, dwsa,dwsax;  /* Variables for cell properties        */
  real      i_fga,D_W,dGw,dwsay,dwsaz;      /* Variables for cell properties        */
  real      Me, Theta;              /* Performance characteristics                  */
  real      dTw, dm_v, dQ_a, dw;    /* Source terms                                 */
```

The user defined function searches the cell for max and min coordinates and compares them to coordinates of its neighbouring cell. The cell that has central

coordinates higher than the *zmax* of the current cell is identified as the upstream cell.

```
/*****************************************************************************
*   DEFINE THE CELL REFERENCE NUMBER AND DELTA_Z AND DELTA_R FOR EACH CELL          *
*****************************************************************************/
/*  GET THE DOMAIN */
    d = Get_Domain(1);
/*  LOOK UP THREAD FOR PACK_ID*/
    t = Lookup_Thread(d, PACK_ID);
    for (i = 0 ; i <= ni ; i++)
    {   c = i;  /* CELL NUMBER CALCULATED FOR PRINTING PURPOSES IS EQUAL TO CELL ID */
        zmax=-1000.;                /* Initializing */
        zmin=1000.;
        xmax=-1000.;
        xmin=1000.;
        ymax=-1000.;
        ymin=1000.;

        c_node_loop(c,t,n)/* NODE LOOP TO DETERMINE THE MAX AND MIN FACE COORDINATES */
        {
            node = C_NODE(c,t,n);
            if (NODE_X(node)>zmax)  zmax=NODE_X(node);
            if (NODE_X(node)<zmin)  zmin=NODE_X(node);
            if (NODE_Y(node)>rmax)  rmax=NODE_Y(node);
            if (NODE_Y(node)<rmin)  rmin=NODE_Y(node);
        }
        c_face_loop(c, t, n)            /* LOOPS OVER ALL THE FACES OF A CELL        */
        {
            ft = C_FACE_THREAD(c,t,n);
            f = C_FACE(c,t,n);

            cc = F_C1(f,ft);
            cct = THREAD_T1(ft);
            if (cc == c)
            {
                cc = F_C0(f,ft);
                cct = THREAD_T0(ft);
            }

           C_CENTROID(xc,cc,t)
           z_cc = xc[0];
           x_cc = xc[1];
           y_cc = xc[2];

           if (cct == t)
           {
               if (z_cc > zmax)
               {
                   c1_star = cc;
               }
               if (z_cc < zmin)
               {
                   c2_star = cc;
               }
               if (x_cc < xmin)
               {
                   c3_star = cc;
               }
```

```
            if (x_cc > xmax)
            {
                c4_star = cc;
            }
            if (y_cc > ymax)
            {
                c5_star = cc;
            }
            if (y_cc < ymin)
            {
                c6_star = cc;
            }
        }
    }
    C_UDMI(c,t,17) = zmax;
    z_bound = C_UDMI(c1_star,t,17);  /* UDM FOR BOUNDARY CELL IDENTIFICATION */
deltaZ = zmax - zmin;
deltaX = xmax - xmin;
deltaY = ymax - ymin;
```

With the coordinates of the cell determined thermophysical properties and fill performance characteristics can be calculated.

```
/*****************************************************************************************************************
*  CALCULATE THE WATER TEMPERATURE AND SOURCE TERMS FOR THE AIR TEMPERATURE AND AIR HUMIDITY
*****************************************************************************************************************


    T_a = C_T(c,t);                                     /* AIR TEMPERATURE OF CURRENT CELL
    p_a = C_P(c,t);                                     /* AIR PRESSURE OF CURRENT CELL
    T_w = C_UDMI(c,t,1) + 273.15;                       /* WATER TEMPERATURE OF CURRENT CELL
    G_w = C_UDMI(c,t,4);                                /* WATER MASS VELCOITY OF CURRENT CELL
    m_v = C_YI(c,t,0);                                  /* VAPOUR MASS FRACTION
    w_a = m_v / (1 - m_v);                              /* HUMIDITY RATIO OF AIR
    w_sa = WA(T_a, T_a, p_fill, PV(T_a));
    C_UDMI(c,t,12) = w_sa ;                             /* HUMIDITY RATIO OF SATURATED AIR
    w_sw = WA(T_w, T_w, p_fill, PV(T_w));               /* HUMIDITY RATIO OF SATURATED AIR AT Tw
    cp_ma = CPMA(T_a,w_a) ;                             /* SPECIFIC HEAT OF AIR-VAPOUR MIXTURE
    cp_v = CPV(T_a) ;                                   /* SPECIFIC HEAT OF VAPOUR
    cp_w = CPW(T_w) ;                                   /* SPECIFIC HEAT OF WATER
    i_fg = IFG(T_w) ;                                   /* LATENT HEAT
    i_fga = IFG(T_a) ;
    k_av = KAV(T_a, w_a) ;                              /* THERMAL CONDUCTIVITY OF AIR-VAPOUR MIXTURE
    rho_av = RHOAV(p_fill, T_a, w_a);                   /* DENSITY OF AIR-VAPOUR MIXTURE
    G_a = pow(C_U(c,t)*C_U(c,t)+C_V(c,t)*C_V(c,t)+C_W(c,t)*C_W(c,t),0.5) * rho_av/(1 + w_a); /* AIR MASS
                                                                                                VELOCITY
    if ( zmax >= z_CW_in)
    {
        Me = 0;
    }
    else
    {   /* Merkerl Number */
        Theta = atan2 (C_U(c,t),fabs(C_V(c,t))) / pi_1 * 180;                    /* AIR FLOW ANGLE
        Me_count = c1_count*pow(G_wi,c2_count)*pow(G_a,c3_count)*pow(Tw_in,c4_count); /* COUNTERFLOW
        Me_cross = c1_cross*pow(G_wi,c2_cross)*pow(G_a,c3_cross)*pow(Tw_in,c4_cross); /* CROSSFLOW
        Me = (Me_count + (Me_cross - Me_count)*((90-theta)/90));
    }
    if (B_Me < 1) /* LEWIS FACTOR FOR POPPE ASSUMPTIONS */
    {
    Le_f = pow(0.865, 0.666666667) * (( w_sw + 0.622)/(w_a+0.622)-1)/log((w_sw+0.622)/(w_a+0.622));
    }
```

With all the necessary information at hand, the UDF calculates source terms.

```
/* SATURATED HUMIDITY SOURCE TERM */
dwsaz = (C_U(c,t) * rho_av)/deltaZ * (C_UDMI(c,t,12) - C_UDMI(c2_star,t,12))
dwsax = (C_V(c,t) * rho_av)/deltaX * (C_UDMI(c,t,12) - C_UDMI(c4_star,t,12))
dwsay = (C_W(c,t) * rho_av)/deltaY * (C_UDMI(c,t,12) - C_UDMI(c6_star,t,12))
dwsa = dwsaz + dwsa + dwsax;

if (w_a <= w_sa) /* UNSATURATED AIR */
{
    dTw = cp_ma/cp_w*Me*(Le_f*( T_w - T_a )+(i_fg + B_Me*cp_w*(T_w-273.15))/cp_ma*(w_sw - w_a));
    dGw = Me * G_w * ( w_sw - w_a ) ;
    dw = Me * G_w * ( w_sw - w_a ) ;
    dQ_a = (Me * G_w) * ( T_w - T_a ) * ( Le_f * cp_ma + ( w_sw - w_a ) * cp_v);
    C_UDMI(c,t,9) = 0; /* SATURATION IDENTIFIER */
}
else /* SUPERSATURATED AIR */
{
    dTw = cp_ma/cp_w*Me*(Le_f*(T_w - T_a)+(i_fg + B_Me* cp_w*(T_w-273.15))/cp_ma*( w_sw - w_sa ));
    dGw = Me * G_w * ( w_sw - w_sa ) ;
    dw = Me * G_w * ( w_sw - w_sa ) ;
    D_W = C_UDMI(c2_star,t,9); /* D_W USED TO IDENTIFY WHETHER THE DOWNSTREAM CELL IS SUPERSATURATED */
    if (D_W < 1) /* TRANSITION COEFFICIANT APPLIED */
    {
    dQ_a = (Me*G_w)*(Le_f*cp_ma*(T_w - T_a)+(w_sw - w_sa)*(i_fg + cp_w*(T_w - T_a))) - 1.4*dwsa*i_fga;
    }
    else /* NORMAL SUPERSATURATED CELL */
    {
    dQ_a = (Me*G_w)*(Le_f*cp_ma*(T_w - T_a)+(w_sw - w_sa)*(i_fg + cp_w*( T_w - T_a ))) - dwsa*i_fga;
    }
    C_UDMI(c,t,9) = 1;  /* SATURATATION IDENTIFIER */
}

if (zmax > z_CW_in)
{
    C_UDMI(c,t,1)= Tw_in;
    C_UDMI(c,t,2) = 0.0;
    C_UDMI(c,t,3) = 0.0;
    C_UDMI(c,t,4)= G_wi;
}
```

When the source terms have been calculated, discretized equations for the water properties can solved.

```
/* DISRETIZATION OF WATER TEMPERATURE AND WATER MASS VELOCITY                                    */
C_UDMI(c,t,19) = 0;
if (zmax <= z_CW_in)    /* FILL ZONE                                                            */
{
    if (z_bound >= z_CW_in)
    {
    if (zmax <= z_CW_in) /* BOUNDARY DISCRETIZATION - CELL NEXT TO WATER INLET                   */
    {
        C_UDMI(c,t,1) = C_UDMI(c1_star,t,1) - 0.5 * dTw; /* WATER TEMPERATURE DICRETIZATION      */
        C_UDMI(c,t,4) = C_UDMI(c1_star,t,4) - 0.5 * dGw; /* WATER TEMPERATURE DICRETIZATION      */
        C_UDMI(c,t,19) = 2;                              /* BOUNDARY CELL IDENTIFIED             */
    }
    }
    z_b2 = C_UDMI(c1_star,t,19);
    if (z_b2 >= 1) /* BOUNDARY DISCRETIZATION - SECOND BOUNDARY CELL                            */
    {
        C_UDMI(c,t,1) = C_UDMI(c1_star,t,1) + 2.0*(0.3333 * C_UDMI(c1_star,t,7)) - 0.66667 * dTw;
        C_UDMI(c,t,4) = C_UDMI(c1_star,t,4) + 2.0*(0.3333 * C_UDMI(c1_star,t,15)) - 0.66667 * dGw;
        C_UDMI(c,t,19) = 0.5;                            /* BOUNDARY CELL IDENTIFIED             */
    }

    }
    else /* INTERNAL CELL DISCRETIZATION */
    {
    C_UDMI(c,t,1) = C_UDMI(c1_star,t,1) + 0.3333 * C_UDMI(c1_star,t,7) - 0.66667 * dTw;
    C_UDMI(c,t,4) = C_UDMI(c1_star,t,4) + 0.3333 * C_UDMI(c1_star,t,15) - 0.66667 * dGw;
    }
```

```
    C_UDMI(c,t,7) = C_UDMI(c,t,1) - C_UDMI(c1_star,t,1); /* WATER TEMPERATURE GRADIENT              */
    C_UDMI(c,t,8) = dTw ; /* WATER TEMPERATURE GRADIENT STORED IN UDM 7                           */
    C_UDMI(c,t,15) = C_UDMI(c,t,4) - C_UDMI(c1_star,t,4); /* WATER MASS VELOCITY GRADIENT          */
    C_UDMI(c,t,16) = dGw ; /* WATER MASS VELOCITY GRADIENT STORED IN UDM 16                       */
    C_UDMI(c,t,2) = C_UDMI(c,t,2) + (dQ_a - C_UDMI(c,t,2)) * Relax; /* STORE ENERGY SOURCE IN UDM 2 */
    C_UDMI(c,t,3) = C_UDMI(c,t,3) + (dw - C_UDMI(c,t,3)) * Relax;   /* STORE VAPOUR SOURCE IN UDM 3 */
    C_UDMI(c,t,13) = dwsa ; /* SATURATED HUMIDITY GRADIENT STORED IN UDM 13                       */
}
```

The energy and species sources are given to ANSYS-*Fluent*® by built-in commands.

```
/*****************************************************************************************
 *                        SOURCE TERM FOR ENERGY EQUATIONS                                *
 *****************************************************************************************/
DEFINE_SOURCE(energy_source,c,t,dS,eqn)
{
  real source;
     source = C_UDMI(c,t,2);
  return source;
}
/*****************************************************************************************
 *                        SOURCE TERM FOR HUMIDITY EQUATIONS                              *
 *****************************************************************************************/
DEFINE_SOURCE(w_source,c,t,dS,eqn)
{
  real source;
    source = C_UDMI(c,t,3);
  return source;
}
```

REFERENCES

Al-Waked, R and Behnia, M, 2006, CFD simulation of wet cooling towers, J. Applied Thermal Engineering, Vol. 26, pp. 382-395.

ANSYS-*Fluent*® *v13.0*: Theory Guide, ANSYS Inc. 2011

ANSYS-*Fluent*® *v13.0*: User's Guide, ANSYS Inc. 2011

Berman, L D, 1961, *Evaporative Cooling of Circulating Water*, 2nd Ed., Chapter 2, pp. 94-99, ed. Sawistowski, H, Translated from Russian by R. Hardbottle, Pergamon press, New York, USA.

Bertrand, T P, 2011, Evaluation of a 1.5 x 1.5 m^2 Counter-flow Fill Performance Test Facility with a View To Contributing To a Fill Performance Standard, MSc Thesis, Stellenbosch University.

Bosnjacovic, F, 1965, Technische Thermodinamik, Theodor Steinkopf, Dresden.

Grobbelaar, P, 2012, Performance Evaluation of Fill in Cross- and Counterflow, MSc Thesis, Stellenbosch University.

Häszler, R, 1999, Einflusz von Kondensation in der Grenzschicht auf die Wärme- und Stoffübertragung an einem Rieselfilm, Fortschritt-Berichte VDI 3 (615).

Jaber, H and Webb, R L, 1989, Design of Cooling Towers by the Effectiveness-NTU Method, J. Heat Transfer,Vol. 111, pp. 837–843.

Johnson, B M, 1989, Cooling Tower Performance Prediction and Improvement, Volume 1, Applications Guide, EPRI Report GS-6370, Volume 2, Knowledge Base, Palo Alto.

Klimanek A, Ryszard, A and Bialecki, Z O, 2010,CFD Two-Scale Model of a Wet Natural Draught Cooling Tower, Numerical Heat Transfer, Vol. 57, pp. 119–137.

Kloppers, J, 2003, A Critical Evaluation and Refinement of the Performance Prediction of Wet-Cooling Towers, PhD Thesis, Stellenbosch University, South Africa.

Kloppers, J C, Kröger, D G, 2004, A critical investigation into the heat and mass transfer analysis of crossflow wet-cooling towers, Numerical Heat Transfer, Vol. 46, pp. 785–806.

Kloppers, J C, Kröger, D G, 2005a, A critical investigation into the heat and mass transfer analysis of counterflow wet-cooling towers, International Journal of Heat and Mass Transfer, Vol. 48, pp. 765-777.

Kloppers, J C, Kröger, D G, 2005b, The Lewis factor and its influence on the performance prediction of wet-cooling towers, International Journal of Thermal Sciences, Vol. 44, pp. 879-884.

Kloppers, J C, Kröger, D G, 2005c, Cooling Tower Performance Evaluation: Merkel, Poppe, and e-NTU Method of Analysis, Journal of Engineering for Gas Turbine and Power, Vol. 127, pp. 1 – 7.

Kröger, D G, 2004, *Air-cooled Heat Exchangers and Cooling Towers*, University of Stellenbosch, U. (ed.), PennWell Corp. Tulsa, USA.

Merkel, F, 1925, Verdunstungskühlung, VDI-Zeitschrift, Vol. 70, pp. 123–128.

Poppe, M and Rögener, H, 1991, Berechnung von Rückkühlwerken, VDI-Wärmeatlas, pp. Mi 1–Mi 15.

Reuter, H C R, 2010, Performance Evaluation of Natural Draught Cooling Towers with Anisotropic Fills, PhD Thesis, Stellenbosch University, South Africa.

Roach, P, 1997, Quantification of Uncertainty in Computational Fluid Dynamics, Ann. Rev. Fluid Mech., Vol. 29, pp. 123-160.

Versteeg, H K and Malalasekera, W, 2007, *An Introduction to Computational Fluid Dynamics – The Finite Volume method*, 2nd Ed., Pearson Education Limited, Essex, England.

Williamson, N and Armfield, S, M B, 2008, Numerical simulation of flow in a natural draught wet cooling tower - The effect of radial thermofluid fields, Applied Thermal Engineering, Vol. 28, pp. 178–189.

Zivi, S M and Brand, B B, 1956, An analysis of the Crossflow Cooling Tower, Refrig. Eng., Vol. 64, pp. 31–34, 90–92.